

UNIVERSITÀ DEGLI STUDI DI MILANO



SCUOLA DI DOTTORATO

*Scienze endocrinologiche e metaboliche*

DIPARTIMENTO

*Dipartimento di Scienze Farmacologiche e Biomolecolari (DiSFeB)*

CORSO DI DOTTORATO

*XXVII ciclo*

TESI DI DOTTORATO DI RICERCA

***Different approaches to understand and counteract Spinal and  
Bulbar Muscular Disease (SBMA)***

Settore scientifico disciplinare BIO/13 - Biologia Applicata

NOME DEL DOTTORANDO

*Elisa Giorgetti  
Matr. R09576*

NOME E COGNOME DEL TUTOR

*Angelo Poletti*

NOME E COGNOME DEL COORDINATORE DEL DOTTORATO

*Angelo Poletti*

A.A. 2013/2014

## **Table of contents**

<b>Abstract</b> .....	1
<b>Chapter:</b>	
<b>1. Introduction</b> .....	3
<i>Polyglutamine (polyQ) diseases</i> .....	4
<i>Spinal and Bulbar Muscular Atrophy (SBMA)</i> .....	5
<i>Clinical features and disease pathogenesis</i> .....	5
<i>The Androgen Receptor (AR)</i> .....	8
<i>AR in SBMA</i> .....	11
<i>AR protein degradation processes: ubiquitin proteasome system (UPS) and autophagy</i> .....	17
<i>Current strategies to contrast polyQ AR toxicity</i> .....	23
<b>2. Synergic prodegradative activity of Bicalutamide and trehalose on the mutant androgen receptor responsible for spinal and bulbar muscular atrophy</b>	
<b>Introduction</b> .....	31
<b>Results</b> .....	35
<i>Bicalutamide and trehalose alone promotes ARQ46 clearance</i> .....	35
<i>Combined effect of Bicalutamide and trehalose on ARQ46</i> .....	37
<i>Autophagy activation is mediated by trehalose and not influenced by Bicalutamide</i> .....	39
<i>Combined effect of Bicalutamide and trehalose on ARQ112</i> .....	40
<b>Discussion</b> .....	47

### **3. The small molecule JG98 promotes polyQ AR ubiquitination and proteasomal degradation through the activation of Hsp70.**

<b>Introduction</b> .....	52
<b>Results</b> .....	57
<i>JG98 promotes polyQ AR degradation in a dose-dependent manner</i> .....	57
<i>Proteasomal degradation of polyQ AR</i> .....	58
<i>PolyQ AR ubiquitination is promoted by Hsp70 co-chaperones</i> .....	58
<b>Discussion</b> .....	64

### **4. Chronic exercise-induced muscle changes in AR113Q vs wild type mice.**

<b>Introduction</b> .....	68
<b>Results</b> .....	70
<i>Six-weeks training improves mice performance</i> .....	70
<i>Muscle analysis in AR113Q and wt mice</i> .....	71
<b>Discussion</b> .....	75

### **5. Conclusion**.....78

<b>UPS and autophagy in SBMA</b> .....	79
<i>Enhancing autophagic activity in SBMA</i> .....	80
<i>Promoting selective proteasomal degradation in SBMA</i> .....	81
<b>A non-pharmacological intervention in SBMA: chronic exercise</b> .....	82

### **6. Materials and Methods**.....85

### **References**.....97

## **Abstract**

Spinal and Bulbar Muscular Atrophy (SBMA), or Kennedy's disease, is a hereditary neuromuscular disorder that affect only men and is characterized by slowly progressive weakness and atrophy of bulbar, facial, and limb muscles, which are attributable to degeneration of lower motor neurons in the spinal cord and brainstem [1]. The disease is associated with an abnormally expanded CAG repeat in the androgen receptor (AR) gene which results in a longer polyglutamine tract (polyQ) at the N-terminus of the protein [2]. PolyQ tract triggers AR protein misfolding and aggregation and leads to nuclear toxicity and cell death. Many efforts have been done to examine in depth disease pathogenesis and to find strategies to counteract polyQ AR toxicity but many aspects remain incompletely understood. Here we propose three different approaches aimed to contrast the disease.

In the first chapter, the anti-androgen Bicalutamide is used in combination with the autophagy activator trehalose, in order to slowdown polyQ AR nuclear translocation and promote its clearance through the cytoplasmic autophagic machinery. The combined treatment strongly reduces polyQ AR protein levels more than the single treatment, thus suggesting an autophagy-mediated clearance as a potential therapeutic strategy [3].

The second chapter focuses on polyQ AR degradation via the ubiquitin-proteasome system (UPS), another major degradation process within the cell. We stabilized Hsp70 in its more active ADP-bound state with the small molecule JG98 and promoted a selective CHIP-mediated ubiquitination and proteasomal degradation of polyQ AR. This confirms the

involvement of UPS in SBMA pathogenesis and proposes UPS-mediated degradation of polyQ AR as a possible approach for the treatment of the disease.

The last chapter proposes exercise as a non-pharmacological intervention for the treatment of SBMA. Wild type (wt) and AR113Q knock-in mice followed a mild exercise regimen for six weeks, then mice were run to exhaustion and sacrificed. Muscle tissues analysis revealed a significant decrease in type I and II fiber size in the exercised cohort of AR113Q mice compared to control rest mice. These data suggested the existence of muscle abnormalities, possibly exacerbated by exercise, in AR113Q mice.

# **Chapter 1**

## ***Introduction***

## **Polyglutamine (polyQ) diseases**

Over the last two decades, nine different neurodegenerative disorders with a common trait have been identified [4]: all of them are characterized by the presence of an abnormally long polyglutamine (polyQ) tract in the protein responsible for disease pathogenesis. This type of mutation has been first identified in the androgen receptor (AR) and has been established to be the cause of disease onset in Spinal and Bulbar Muscular Atrophy (SBMA; Kennedy's disease) [2]. Then, the same mutation has been also found in huntingtin protein responsible for Huntington's disease (HD), in atrophin-1 protein in dentatorubral-pallidoluysian atrophy (DRPLA), in ataxin-1, -2 and -3, in the Ca<sub>v</sub>2.1 P/Q voltage-dependent calcium channel, in ataxin-7 and in TATA-binding protein (TBP), responsible for spinocerebellar ataxia (SCA) type 1, 2, 3, 6, 7 and 17, respectively. Since all are caused by an abnormal glutamine expansion and result in similar protein aggregates, toxicity of the polyQ tract has been hypothesized as a common mechanism of disease. Moreover, the number of glutamines in the expanded tract is negatively related to the age of disease onset and positively linked to the severity of the disease in all the polyQ diseases: a longer polyQ tract leads to an earlier onset and a greater severity. Similar to other repeat expansion disorders [4], polyQ diseases show the "genetic anticipation" phenomenon: the repeat inherited by the following generation is longer than the preceding one, resulting in increased severity and earlier onset of the disease.

Taken together, polyQ diseases represent the most common cause of inherited neurodegenerative disorders.

---

## **Spinal and Bulbar Muscular Atrophy (SBMA)**

### **Clinical features and disease pathogenesis**

SBMA was first described in 1897 by H. Kawahara [5] but the details of clinical, genetic and pathological features of this disorder were first documented by W. Kennedy [1] and since 1968 it has been known worldwide as Kennedy's disease.

The onset of the disease is usually between 30 and 60 years old but it is often preceded by nonspecific symptoms such as tremor and muscle cramps. The prevalence of the disease is 1-2 per 100,000 individuals, but SBMA patients may be misdiagnosed as other neuromuscular diseases, such as amyotrophic lateral sclerosis.

SBMA chiefly affects adult males; females show only subclinical disease manifestations when homozygous for the mutation [6]. This sex specificity seems to be related to testosterone levels and is well described in mice models of SBMA: surgical or chemical castration of male polyQ AR mice showed marked improvement of symptoms and ameliorated disease phenotype, whereas testosterone administration in female mutant mice markedly exacerbated symptoms and pathologic features [7-9].

The disease is characterized by the degeneration of lower motor neurons in the anterior horn of the spinal cord and in the brainstem [1, 10, 11]. As a consequence, muscle tissues innervated by these motor neurons, such as proximal limb, facial and bulbar muscles, are affected. In fact, the exordium of the disease usually manifests with cramps, hand tremor and fatigue, followed by progressive muscle weakness and atrophy. Distal muscles weakness and atrophy are observed in the arms more than the legs. In addition, patients show



fasciculation of muscles around the mouth and of the tongue, and in some cases dysarthria and dysphagia are observed. Degeneration of sensory neurons in the dorsal root ganglia has been also noticed to a lower extent [12]. It is noteworthy that AR toxicity specifically affects lower motor neuron function and maintenance, even though AR is expressed also in other areas of the central nervous system, including the olfactory bulb, hippocampus, cerebellum, cortex and hypothalamus [13-15]. In addition to the neuromuscular phenotype primarily caused by a toxic gain-of-function mechanism, SBMA patients show also endocrine signs [16, 17] like androgen insensitivity, gynecomastia, reduced fertility and testicular atrophy, due to a partial loss of function of the mutant AR.

Recent evidences challenge the traditional view of SBMA as a primary motor neuron disease and establish muscle as a site of mutant AR toxicity [18, 19]. Skeletal muscle is one of the major targets of androgens and it is possible that muscle deterioration is not only a consequence of chronic denervation due to motor neuron loss. Other previous studies support a primary contribution of skeletal muscle in the disease pathogenesis: muscle biopsies of patients showed both myogenic and myopathic features and demonstrated, in particular, fiber type grouping, atrophic fibers and angulated fibers [20]; knock-in mutant AR mice develop myopathy prior to the onset of spinal cord pathology [9]; genetic overexpression of muscle-specific insulin-like growth factor (IGF-1) or peripheral IGF-1 administration mitigates SBMA symptoms in transgenic mice [21, 22]. Supporting this hypothesis is the evidence of abnormally increased levels of creatine kinase in the serum of SBMA patients, usually not expected for a neurogenic-only disorder [23, 24]. Moreover, myogenin and acetylcholine receptor expression was up-regulated in the muscle of polyQ AR mice compared to controls, prior to spinal cord pathology [9]. These results suggest skeletal

muscle alterations as cell-autonomous and also propose that AR toxicity can occur in muscle prior to motor neurons. It has been demonstrated that AR toxicity in skeletal muscles is sufficient to cause motor neuron disease and lead to the denervation-induced atrophy [25]. Therefore, muscle defects in SBMA mouse models may be both intrinsic and motor neuron-dependent.

Damages to motor neurons depend not only on defects in skeletal muscle but also on alterations in other cell types, such as glia cells. Glia cells provide trophic support to motor neurons through the release of the neurotrophins, like the ciliary neurotrophic factor (CNTF) and the glial-cell derived neurotrophic factor (GDNF), that protect neurons by promoting the activation of pro-survival pathways. In mouse models of SBMA the expression of neurotrophins and growth factors is altered [9] and, as a consequence, the trophic support to motor neurons is also changed. In a similar way, brain-derived neurotrophic factor (BDNF) is secreted by muscle and promotes motor neuron survival and maintenance [26]. Among growth factors, vascular endothelial growth factor (VEGF) and IGF-1 have been shown to be protective for motor neurons but reduced in mouse models of SBMA. VEGF has direct and indirect beneficial effects on motor neurons: first, it has angiogenic and neuroprotective functions and, second, it activates the release of trophic factors from glial cells that in turn protect neurons from degeneration. IGF-1 promotes sprouting, axonal growth and survival of motor neurons and, in addition to a direct action on motor neurons, IGF-1 induces muscle hypertrophy and inhibits muscle atrophy through the activation of phosphoinositide 3-kinase/Akt pathway [21].

Taken together, these evidences suggest that motor neurons are not the only cell type affected in SBMA and that skeletal muscle cells may represent a primary target for polyQ AR toxicity.

### **The Androgen Receptor (AR)**

In 1986 the causative gene of SBMA pathogenesis was identified and located on the proximal arm of chromosome X [27] and in 1991 the trinucleotide CAG repeat abnormal expansion was found in the androgen receptor (AR) gene [2].

#### **AR structure and function**

AR protein is a well-described 110 kDa nuclear receptor that belongs to the steroid/thyroid hormone receptor family.

After the binding to its natural ligand, testosterone or dihydrotestosterone, AR translocates to cell nuclei and mediates the effects of androgens, by regulating the expression of target genes. AR is physiologically involved in functions related to male sexual differentiation and pubertal sexual development: its effects include the development of sex organs, the growth of pubic hair, the enlargement of vocal cords, the production of sperms, the increase in muscle strength and the development of masculine behavior. AR is not only expressed in sexual organs but it has been found also in skeletal muscle, kidney, adrenal gland, skin and central nervous system, suggesting that it may support the development and/or the maintenance of different tissues [28].

The AR gene is located on the proximal arm of chromosome X (Xq11-12) [27] and it is composed of 8 exons. The first one codes for the N-terminal transactivation domain and contains the CAG trinucleotide repeat. It has the major transactivation activity, since it contains the activation function 1 (AF-1) and the activation function 5 (AF-5), both required for the interaction with co-regulators of transcription. AF-1, in particular, interacts with transcriptional coactivators such as c-AMP responsive element binding protein (CBP) and steroid receptor coactivator-1. In addition to the polyQ tract, the N-terminus domain of AR protein contains also polyglycine (polyG) and polyproline (polyP) stretches but the functional role of these aminoacid sequences in AR is not known.

The DNA-binding domain (DBD) and the hinge region are encoded by exons 2 and 3. DBD is composed of two zinc fingers that allow specificity in DNA binding and stabilization of DNA-protein interaction whereas the hinge region contains a PEST sequence (P is proline, E glutamic acid, S serine, T threonine), which targets proteins for degradation through the proteasome [29]. In addition, DBD contains a nuclear localization signal which drives AR to the nucleus in response to ligand binding.

The ligand-binding domain (LBD) is encoded by exons 4-8 and upon ligand binding, this domain undergoes a conformational change that leads to the assembly of the less potent activation function 2 (AF-2) [30] (Figure 1).

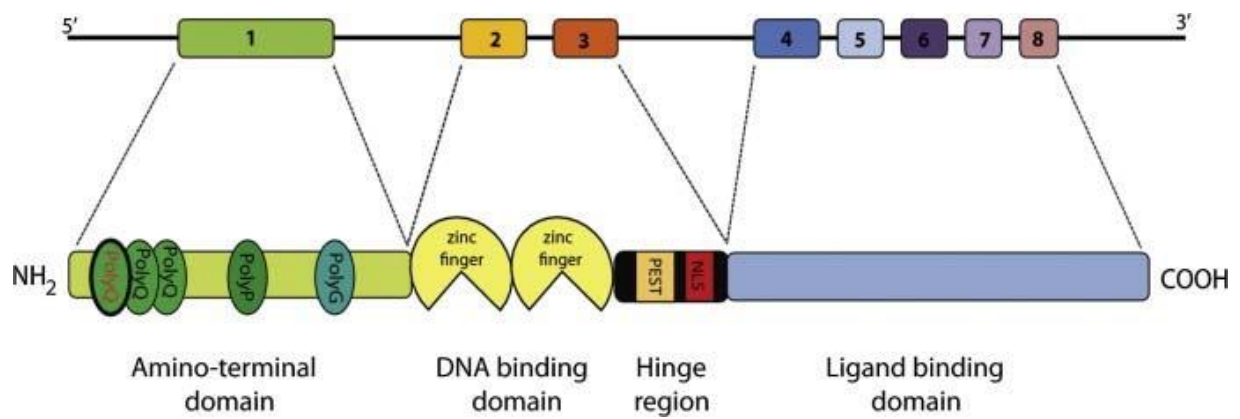


**Figure 1**

The androgen receptor is composed of 8 exons. PolyQ repeats are located at the N-terminus domain of the protein [31].

## **AR in SBMA**

The number of glutamines in the polyQ tract at the N-terminal domain of the AR protein determines AR toxicity. The polyQ tract ranges from 9 to 34 in normal individuals, whereas it becomes longer than 38 (up to 62) in SBMA patients. Although the abnormal elongation is causative of SBMA, a shorter polyQ tract is associated with increased prostate cancer risk, hirsutism, male infertility and cryptorchidism [32-34].

The expanded polyQ tract in the AR protein is responsible for both loss of AR normal function and gain of AR novel toxic properties [35] that damage motor neurons and, according to recent evidences, skeletal muscle cells [18, 19]. The loss of AR function could be linked to the expansion of the polyQ tract that seems to disrupt the interaction between the N-terminal transactivation domain and transcriptional co-activators [36] and, since AR has trophic effects, its reduced activity might be involved in SBMA pathogenesis. Despite this, a gain of toxic function of the polyQ AR has been established to be the main cause of cell degeneration in SBMA.

### ***Accumulation and nuclear toxicity***

The presence of the polyQ tract in AR protein alters its conformation from a regular random coil to a parallel helical  $\beta$ -sheet: these changes lead to the formation of AR oligomeric fibrils that are considered the rate-limiting step of aggregation [37]. The formation of toxic oligomers or intermediates of aggregates of mutant AR protein instigates a series of cellular events which lead to cell degeneration [38-40].

Therefore, the histopathological hallmark of SBMA is the presence of nuclear inclusions (NIs) containing polyQ AR in brainstem and spinal cord motor neurons, as well as in non-neuronal tissues such as prostate, testis, skin and skeletal muscle [9, 41]. However, several studies demonstrated that NIs have a protective role, since they sequester the mutant protein and prevent its toxicity [39, 42]. Instead, diffused accumulation of misfolded proteins seems to play a role in the initiation of neurodegeneration in polyglutamine diseases [42, 43]. Adachi et al. [44] demonstrated that diffuse nuclear accumulation of mutant AR is more frequent than the NIs in the anterior horn of the spinal cord and that is strictly correlated with the number of glutamines in the AR polyglutamine tract. It appears that the polyQ AR principally accumulates within the nuclei of motor neurons in a diffusible form, leading to neural dysfunction and eventual cell death (Reviewed in [30]).

Moreover, AR accumulation was also detected in the cytoplasm of certain types of cells [44]: sensory neurons in the dorsal root ganglion often show AR aggregates in the cytoplasm that seems to be associated with axonal degeneration [45]. However, nuclear localization of mutant AR is essential for triggering intracellular toxic events that induce cell dysfunction and lead to neurodegeneration. Indeed, it has been demonstrated that a mutation in AR nuclear localization signal or the addition of a nuclear export signal reduces polyQ AR toxicity [46, 47].

### ***Ligand-dependent toxicity***

In its inactive state, polyQ AR localizes in the cytoplasm and it is associated with heat shock proteins (Hsps) such as Hsp90, Hsp70 and Hsp40. Hsps maintain polyQ AR in its inactive and non-toxic status, by preventing its aggregation and regulating its turnover. After interaction

and binding of AR to its natural ligands, testosterone or dihydrotestosterone, the receptor dissociates from the Hsps [48]. Ligand binding also induces conformational changes and dimerization through the interaction between N-terminal and C-terminal domains (N/C interaction) of the mutant AR; this confers to AR the ability to move to the nucleus, bind to the DNA and interact with co-regulators (both co-activators and co-repressors) to modulate the expression of androgen-responsive genes [49]. Ligand-dependent AR nuclear translocation is required, but not sufficient for its toxicity. Once in the nucleus, AR must bind to DNA to exert its toxic activity. For instance, a mutation in the DNA binding domain that does not affect ligand-binding domain abolishes neurodegeneration, indicating that DNA binding is necessary for AR-mediated pathogenic mechanism [50]. Moreover, ligand-dependent interaction of the C-terminal AF-2 domain and co-regulators [50] and the N/C interaction [51] are both required for polyQ AR toxicity.

### ***Post-translational modification***

Phosphorylation, acetylation and sumoylation are common events following translation that modify AR activity and can occur through both androgen-independent and androgen-dependent mechanisms. Of note is the demonstration that wild type AR undergoes post-translation modifications only in the presence of ligand while mutant AR can be acetylated and phosphorylated even in the absence of the ligand [52]. Therefore, these modifications may be involved in AR-mediated toxic pathways. AR **phosphorylation** on Ser 215 and Ser 792 induced by Akt inhibits ligand binding and mitigates toxicity in cultured motor neurons [53]. Insulin-growth factor 1 (IGF-1) increases this effect: in fact, muscle-specific IGF-1 overexpression attenuates both muscle and spinal cord pathology in SBMA mice through



phosphorylation and inactivation of AR by Akt [21]. On the other hand, phosphorylation at Ser 516 enhances the ability of caspase-3 to cleave the polyQ AR and generate cytotoxic polyQ fragments [54]. **Acetylation** at Lys 630, 632 and 633 is also known to increase AR cytotoxicity. PolyQ AR nuclear hyper-acetylation is suppressed by sirtuin 1 (SIRT1, a nicotinamide adenine dinucleotide-dependent histone deacetylase): it reduces AR nuclear accumulation and toxicity in primary motor neurons [55]. However, mutation at the same lysines induces the formation of cytoplasmic AR aggregates in non-neuronal cells [56]. **Sumoylation** inhibits the formation of AR insoluble aggregates and soluble oligomers by increasing the solubility of the polyglutamine protein [57]. On the other hand, the disruption of sumoylation at Lys 385 and 518 enhances mutant AR activity as a hormone-dependent transcriptional regulator and increases its trophic support: in a knock-in mutant AR mice model, the disruption of AR sumoylation rescues exercise endurance, type I muscle fiber atrophy, and early death ([58] *submitted*).

### ***Altered transcriptional activity***

Transcriptional dysregulation is considered to be a major molecular mechanism through which the polyQ AR contributes to the development of SBMA. The pathogenic polyQ AR accumulates in the cell nucleus in a ligand-dependent manner and may inhibit transcription by interfering with the function of essential transcriptional factors and co-activators [59]. For example, in animal models of SBMA and HD the expression levels of different Hsps are notably decreased [59, 60]. Moreover, many transcriptional co-activators are sequestered in polyQ AR inclusions and are not able to exert their physiological function. For example, the c-AMP response element binding protein (CBP) has a reduced histone acetyltransferase

(HAT) activity in cellular models of polyglutamine diseases [61]: the decrease in histone acetylation leads to chromatin structure changes and transcription dysregulation that in turn leads to a decreased expression of several genes (e.g. vascular endothelial factor VEGF and type II transforming growth factor-beta receptor) that are required for neuronal survival [62, 63]. On the other hand, polyQ expansion causes partial loss of AR trophic function by promoting AR proteasomal degradation and by altering post-translational modifications and activity as a ligand-activated transcription factor. In this context, AR fails to regulate a subset of genes whose expression is normally affected by ligand activation of the wild type receptor [52].

### ***Impaired axonal transport and mitochondrial dysfunction***

Another aspect of mutant AR toxicity is the inhibition of axonal transport. PolyQ AR has been shown to disrupt anterograde axonal transport through the activation of the c-Jun N-terminal kinase (JNK) that leads to the inhibition of the motor protein kinesin-1 microtubule-binding activity [64]. Moreover, cytoplasmic inclusions of the polyglutamine expanded AR, when localized in the axons, alter the distribution of kinesin and influence the transport of intracellular organelles [65]. However, it has been noticed that the pathogenic AR may inhibit fast axonal transport in both anterograde and retrograde directions, even without any visible aggregate formation [66]. Mutations in different genes involved in the retrograde axonal transport, such as dynein and dynactin 1, seem to be also involved in SBMA pathogenesis. In the AR97Q transgenic mouse model of SBMA [67], mRNA levels of dynactin 1 are substantially reduced while an AR113Q knock-in mouse model show deficits in retrograde axonal transport and blockade of endosomal trafficking, conditions that are

partially rescued by the local administration of VEGF [68]. Also, over-expression of wild type AR in muscle has been shown to alter the retrograde axonal transport and mimic SBMA phenotype [25, 68].

Mitochondrial impairment is also known to be involved in disease pathogenesis. Mutant AR activates JNK-mediated apoptotic pathway in primary cortical neurons and this activation depends on Bax, a factor that plays an important role in apoptosis by stimulating cytochrome c release from mitochondria [69]. It has also been shown that polyQ AR expression in the presence of the ligand results in membrane depolarization and release of reactive oxygen species. Moreover, polyQ AR reduces the expression levels of mitochondria-related genes, such as the peroxisome proliferator-activated receptor gamma coactivator-1 (PGC-1), responsible for mitochondria biogenesis and functions [70].

## **AR protein degradation processes**

### **Ubiquitin-proteasome system (UPS)**

The ubiquitin-proteasome pathway (UPS) is the principal system for degradation of short-lived proteins in mammalian cells [71]. In this pathway, proteins are targeted for degradation by covalent ligation to ubiquitin, a highly conserved small protein. In the first step, a ubiquitin-activating enzyme (E1) adenylates an ubiquitin molecule by ATP hydrolysis and binds to “activated” ubiquitin through a cysteine residue. Then, acetylated ubiquitin is transferred to a cysteine of a second enzyme named ubiquitin-conjugating enzyme (E2) and, finally, the ubiquitin-ligase enzyme (E3) recognizes specific substrates to be ubiquitinated and catalyzes the transfer of ubiquitin from the E2 enzyme to the target protein [72, 73]. The ubiquitin ligases that are known to ubiquitinate AR include MDM2 [74], C-terminus of heat-shock cognate protein 70 (Hsc70)-interacting protein (CHIP) [75] and RNF6 [76]; while MDM2 and CHIP ubiquitination translates into AR proteasomal degradation, RNF6 ubiquitination promotes AR-dependent transcription [76]. Other UPS proteins interact with AR, such as an E2 enzyme (UbcH7), several E3 enzymes, a deubiquitinating enzyme (USP10) and a proteasomal subunit (Rpt5/PSMC3) [77].

Each ubiquitin molecule contains seven lysine residues that can be bound by other ubiquitins to form various types of polyubiquitin chains. When the additional ubiquitin is linked to the lysine 48 of the previous one, proteins with this kind of polyubiquitin chain will be targeted to the proteasome for degradation, while other types of chains may be involved in other processes [78]. It was suggested that a chain should contain at least four ubiquitin moieties to be recognized by the proteasome but recent investigations show that the proteasomal

proteolytic signal is more complex and diverse and the link between ubiquitination and proteasomal processing is subject to numerous regulatory steps [78]. The 26S proteasome is a large, multicatalytic protease that degrades polyubiquitinated proteins to small peptides and it is composed of two sub-complexes: a barrel-shape 20S core particle that has the catalytic activity, and a regulatory 19S regulatory particle that is able to recognize ubiquitinated proteins and other potential substrates of the proteasome. Since a folded protein would not be able to fit through the narrow proteasomal channel, it is assumed that the 19S particle unfolds substrates and inserts them into the 20S [73].

In this process of recognition, ubiquitination and degradation through the proteasome of unfolded or damaged proteins, chaperones are involved as major players. The two most relevant chaperones in this protein quality control system are the heat shock proteins 90 (Hsp90) and 70 (Hsp70) that act together in a multi-chaperone machinery to regulate folding, trafficking and clearance of various substrates [79]. Hsp90 and Hsp70 have opposite roles in the machinery, since Hsp90 stabilizes proteins in their native conformation and inhibits their ubiquitination while Hsp70 promotes protein ubiquitination and following degradation by the proteasome. Both Hsp90 and Hsp70 have ATP binding sites and intrinsic ATP activity. These chaperones have low affinity for the substrates in their ATP-bound status but the hydrolysis of ATP changes their conformation and increases their binding affinity [79]. Hsp90 binds to pre-folded proteins and assists them in the opening and stabilization of their ligand binding cleft. When the continued opening of the cleft leads to the exposure of hydrophobic residues to the solvent, the protein may start to unfold and Hsp90 can no longer interact. At this point, Hsp70 binds to the unfolded substrates and the C-terminus of Hsp70-interacting protein (CHIP) E3 ligase promotes their ubiquitination and following

degradation through the proteasome [80]. The assembly of Hsp90/Hsp70 heterocomplexes requires the intervention of other molecules such as the Hsp organizer protein (Hop) that bring together Hsp90 and Hsp70 in the machinery, the Hsp70 co-chaperones Hsp40 and the Hsp90 co-chaperone p23 that interact, respectively, during or at the end of the assembly process [81, 82].

## **Autophagy**

By contrast with the UPS, autophagy is a less selective, bulk degradation process that is largely responsible for the turnover of longer-lived proteins. The term autophagy describes a catabolic process in which cytoplasmic components such as organelles and proteins are delivered to the lysosomal compartment, that is ultimately responsible for substrates degradation and subunits recycling [83, 84]. This highly conserved pathway can be distinguished in three major subcategories: macro-autophagy, micro-autophagy and chaperone-mediated autophagy (CMA). In micro-autophagy and CMA cytosolic components are directly incorporated into the lysosome and degraded. In contrast, macro-autophagy, that is here referred as autophagy, consists in subsequent steps starting with the formation of a lunate-shaped double-membrane structure, the phagophore, that evolves into a double-membrane vacuole, the autophagosome, which contains the membrane-anchored and lipidated form of the microtubule-associated protein-light chain 3 (LC3-II). The autophagosome then fuses with the lysosome to form the autophagolysosome and the acidic proteases content of this ultimate structure is responsible for protein degradation [85]. Autophagosome formation requires the intervention of various autophagy-related proteins. During autophagy activation, for example, LC3-I is cleaved to generate LC3-II that is

further conjugated to the lipid phosphatidylethanolamine (PE) and inserted in the phagophore [86]. LC3-II remains associated with the completed autophagosome and its accumulation is considered as an index of autophagic activity and/or flux [87]. Under normal conditions, autophagy functions as an intracellular protein quality control system and needs to distinguish between normal and unfolded or damaged substrates. The exact mechanism by which autophagy recognizes a potential substrate in a selective way is not completely understood. However, ubiquitination seems to be involved. Similarly to the proteasome system, where ubiquitinated cargoes are delivered by ubiquitin receptors, the ubiquitin binding proteins, like SQSTM1/p62, are responsible for substrate specificity in the autophagic machinery. These receptors, also known as autophagic adaptor proteins, recognize and deliver the ubiquitinated substrates to the nascent autophagosome where they function as scaffold proteins between ubiquitinated substrates and the autophagosome membrane-associated LC3-II protein. In fact, SQSTM1/p62 possesses a C-terminal ubiquitin-binding domain (UBA) and a short LIR (LC3-interacting region) sequence responsible for LC3 interaction [88].

Induction of autophagy leads to the degradation of nonessential cytoplasmic constituents into basic materials that can be reused for anabolism or energy production. For this reason, autophagy is tightly regulated by the nutrient content. Signals that indicates decreased nutrients such as serum starvation or growth factors removal strongly promote autophagic activation [84]. By contrast, phosphatidylinositol 3-kinase (PI3K) has been shown to be a nutrient sensor, and its downstream effector Akt controls the activity of the mammalian target of rapamycin (mTOR), a negative regulator of autophagy [89]. Thus, activation of

insulin-like receptors and PI3K leads to stimulation of mTOR activity and suppression of autophagy.

### ***A crosstalk between proteasome and autophagy***

The choice between the UPS and autophagic machinery for the removal of an ubiquitinated substrate seems to be dependent on how ubiquitin molecules are attached: monoubiquitination (conjugation of a single ubiquitin monomer) or polyubiquitination (several ubiquitin moieties). Another discriminating factor is the lysine (K) residue that undergoes ubiquitination: seven different lysines (K6, K11, K27, K29, K33, K48 and K63) may be conjugated to the ubiquitin monomer and subsequently form a chain. As mentioned above, K48 chains seem to be involved in proteasomal degradation while K63 chains target substrates for degradation via autophagy [90, 91]. Therefore, under certain conditions, such as UPS overloading and inability to remove all the ubiquitinated substrates, protein aggregation occurs and autophagy is activated: ubiquitin chains on misfolded proteins can be remodeled by the combined activity of deubiquitinating enzymes (DUBs) and E3 ligases, such as CHIP and Parkin. Newly formed ubiquitin chains, i.e. K63 chains, can be recognized by the ubiquitin binding domain (UBL) of SQSTM1/p62, to form inclusion bodies removed via autophagy, or by the corresponding UBL domain of HDAC6, to trigger aggresome formation and subsequent degradation through the proteasome or autophagy pathways [85] (Figure 2).



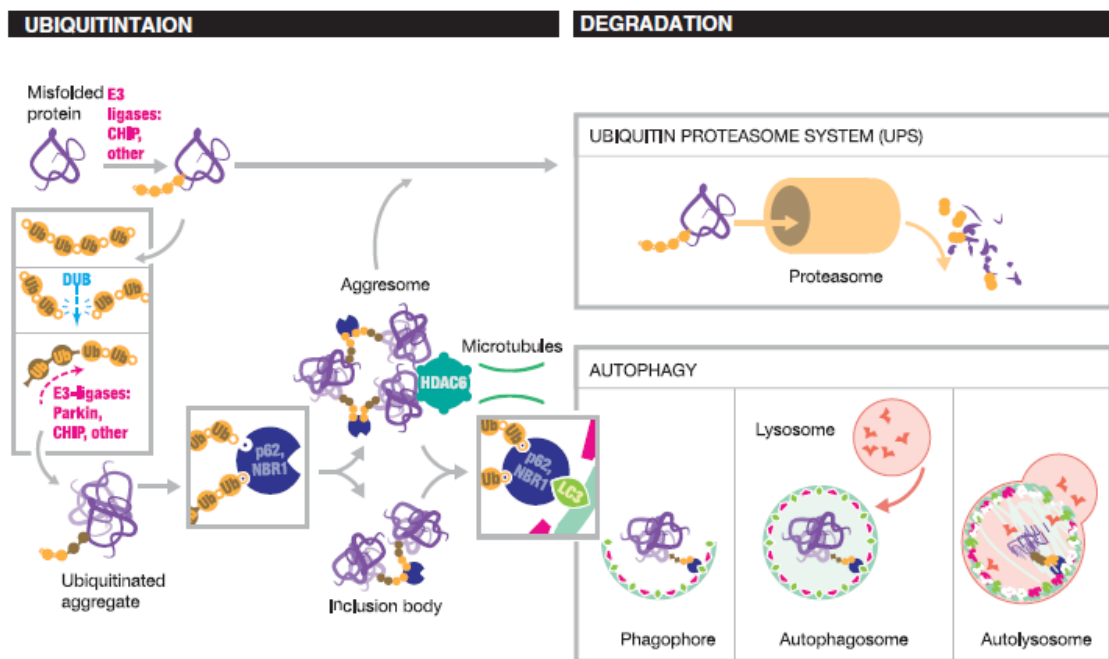


**Figure 2**

Schematic description of proteasomal and lysosomal degradation processes and the involvement of ubiquitin in the two machineries [85].

## **Current strategies to contrast polyQ AR toxicity**

### **Enhancing proteasomal and autophagic polyQ AR degradation**

UPS is responsible for wt and mutant AR degradation and various molecular chaperones are involved in this process. Different studies reported that increased proteasome activity due to heat shock proteins (Hsps) over-expression [92-95] or increased Hsp function [96] is able to reduce polyQ AR toxicity in cell and mouse models of SBMA. Moreover, overexpression of the E3 ubiquitin ligase CHIP promotes polyQ AR ubiquitination and following proteasomal degradation [97, 98]. Another way to modulate Hsps expression is pharmacological and consist in the use Hsp90 inhibitors to contrast mutant client proteins stabilization and favor their degradation: geranylgeranylacetone (GGA) is orally administrated in SBMA mice and upregulates the expression of Hsps that, in turn, attenuates disease symptoms [59]; geldanamycin reduces polyQ AR aggregation and promotes its degradation [99]; the less toxic GGA-derivatives 17-allylamino-17-demethoxygeldanamycin (17-AAG) [100, 101] and 17-dimethylaminoethylamino-17-demethoxygeldanamycin (17-DMAG) [102] has also been proven effective in SBMA cell and mouse models.

UPS and autophagy machineries are functionally linked: for example, the cellular response to impaired proteasome function is an increased HDAC6-mediated autophagic activity [103] and the 17-AAG effect is associated with enhanced autophagic degradation of polyQ AR [100]. Other studies propose the modulation of the autophagic process as a possible target to contrast the disease: for example, the autophagy activator rapamycin, that inhibits the activity of the autophagy inhibitor mTOR, counteracts polyQ AR toxicity in the eye of a *Drosophila* model of SBMA [103] and the mTOR-independent autophagy activator trehalose

promotes polyQ AR degradation and rescues its toxicity in motoneuronal cell models of SBMA [46, 104, 105]. A recent study demonstrated that polyQ AR interferes with the transactivation of the transcription factor EB (TFEB), a master regulator of lysosomal biogenesis and function, and accounts for autophagic flux defects in SBMA cell models, suggesting TFEB as a target for therapeutic intervention [106]. Moreover, paeoniflorin, a major component of *Paeonia* plants, promotes the degradation of polyQ AR by activating both the lysosomal biogenesis via TFEB pathway and the molecular chaperone-UPS system [107]. By contrast, autophagy has been shown to be abnormally activated in the skeletal muscle of SBMA mice and genetic ablation of autophagy-related gene Beclin-1 resulted to be beneficial in disease pathogenesis [108]. In addition, upregulation of TFEB target genes in skeletal muscle from AR113Q male mice and SBMA patients has been demonstrated, therefore underlying aberrant upregulation of autophagy in SBMA [109].

### **Hormonal therapies**

Testosterone has been found elevated in the serum of SBMA patients and the reduction of its levels can be considered a potential therapy. Two pharmacological approaches have been tested and translated in phase-II of clinical studies. Leuprorelin is an analog of the gonadotropin-releasing hormone (GnRH) and reduces the release of testosterone by inhibiting the production of luteinizing hormone (LH) in the anterior pituitary gland. Unfortunately, leuprorelin alters hormones balance and worsens the quality of life in patients [12]. With a different mechanism of action, dutasteride reduces the levels of the more active form of testosterone, the dihydrotestosterone, by inhibiting the activity of 5 $\alpha$ -

reductase but no significant effects of dutasteride on the progression of muscle weakness in SBMA were reported [110].

### **Modulation of polyQ AR expression**

The effect of surgical or chemical castration in alleviating the symptoms in mouse models of SBMA reveals that the reduction of the toxic protein might be beneficial. Various approaches have been tested to decrease polyQ AR expression: one strategy aims to reduce protein expression through post-transcriptional gene silencing while the second technology proposes to modulate gene expression at transcriptional levels.

As an example of the first strategy, a recent paper shows that anti-sense oligonucleotides (ASOs) targeting AR transcript in skeletal muscle of mutant AR mice suppressed polyQ AR toxicity and rescued weight loss, muscle weakness, abnormal gene expression, and lethality in mice [18]. Another approach to modulate polyQ AR mRNA levels is the use of adeno-associated virus to deliver the microRNA miR-196a to motor neurons: it results with reduction of polyQ AR levels and attenuation of symptoms in SBMA mouse models [111]. Moreover, RNAi targeting the polyQ AR transcript reduces polyQ AR expression and toxicity in a *Drosophila* model of SBMA [112].

Gene transcription is altered by polyQ AR expression [50, 52] and regulated by histone acetylation and the expression of polyQ proteins has been shown to sequester the histone acetylases CREB-binding protein (CBP) into inclusions. Therefore, targeting the histone deacetylases activity to contrast the loss in histone acetylation might be beneficial. To this purpose, the histone deacetylase (HDAC) inhibitor sodium butyrate has been tested and shown to ameliorate the SBMA phenotype [113]. An alternative approach is to restore

normal gene expression and the regular interaction of AR with co-regulators of the transcription: both the curcumin-derived compound 5-hydroxy-1,7-bis[3,4-dimethoxyphenyl]-1,4,6-heptatrien-3-one (ASC-J9) [114] and the soybean-derived isoflavone genistein [115] reduce the interaction of polyQ AR with the AR-associated coregulator 70 (ARA70) and ameliorate disease manifestations in SBMA mice.

### **Regulation of polyQ AR aggregation and toxicity**

After ligand binding, AR undergoes conformational changes and two molecules dimerize through N/C interactions before moving to the cell nucleus. Prevention of this interaction has been suggested to reduce polyQ AR toxicity [50, 51]. Other drugs act in a similar way by preventing N/C interaction: the nonsteroidal AR antagonist flutamide reverses or prevents motor dysfunction and extends the lifespan of three different mouse models of SBMA [116]; the antiandrogen bicalutamide slows down AR activation and toxicity by targeting the N/C interaction in cells and primary motor neurons from SBMA mice [42, 51]; then, selective AR modulators (SARMs) inhibit N/C interaction and, again, reduce polyQ AR aggregation and toxicity [51].

Other two compounds modulate polyQ AR aggregation process but they have different mechanisms of action: melatonin is able to shift AR aggregates structure from oligomeric fibrils, typical of mutant AR, to annular oligomers, the species formed by wt AR [38]; the compound B2 promotes inclusion formation and reduces polyQ AR toxicity in cell and fly models of SBMA by increasing AR accumulation into the inclusions [117].

## Targeting mitochondrial dysfunction

Mitochondrial dysfunction has been linked to SBMA pathogenesis. Neurons, in particular, continuously require high amount of energy to support their activity and they rely on mitochondria for energy production. Any mitochondrial dysfunction or oxidative stress may damage neurons and this could be related to SBMA pathogenesis. In fact, altered distribution and membrane potential of mitochondria has been found in cell models of SBMA, together with elevated levels of reactive oxygen species [65]. In addition, the transcription of mitochondria-related genes, such as the peroxisome proliferator-activated receptor gamma co-activator-1 (PGC-1 $\alpha$  and  $\beta$ ), the nuclear factor (erythroid-derived 2)-like 2 (Nrf2) and the superoxide dismutase 1 and 2 (SOD1 and 2), resulted changed in muscle of AR113Q mice compared to controls [70]. A recent paper addresses the involvement of the peroxisome proliferator-activated receptor  $\gamma$  (PPAR $\gamma$ ) in the pathogenesis of SBMA and found that its levels are reduced in skeletal muscle and spinal cord of SBMA mouse models; in addition, the oral administration of the synthetic PPAR $\gamma$  ligand pioglitazone mitigates the neurodegeneration induced by the polyQ AR [118]. The involvement of mitochondria is also supported by the fact that antioxidant agents such as coenzyme Q10 and idebenone are able to rescue cells from the toxicity induced by mutant AR [70]. Moreover, it has been shown that polyQ AR induces Bax-dependent cytochrome-c release and apoptosis [69]. All together, these studies suggest that mitochondrial dysfunction can be at least in part responsible for the toxicity of mutant AR in SBMA.

### Restoration of trophic support

Growth factors and neurotrophins are released from surrounding tissues such as glia and provide trophic support to neurons and peripheral tissues. In mouse models of SBMA, the expression of neurotrophins has been found altered [9, 62]. In example, vascular endothelial growth factor (VEGF) expression is decreased in SBMA mice and VEGF overexpression ameliorates disease manifestations [62]; the up-regulation of the muscle-specific isoform of insulin-like growth factor-1 (IGF-1) is able to reduce polyQ AR toxicity and ameliorates symptoms in mouse models of SBMA [21, 22]. Impaired levels of growth factor translate into reduced trophic support to neurons and, in turn, lead to neuron degeneration and death: for this reason, the restoration of growth factor levels may be of therapeutic value in SBMA [22].

### Use of triptans

A transcriptional profiling study revealed that the mRNA levels of calcitonin gene-related peptide  $\alpha$  *Calca* are upregulated by the presence of polyQ AR in pre-symptomatic, early and late disease stages in a transgenic mouse model of SBMA [119]. *Calca* encodes the small secreted peptide ligand CGRP1 that cause neuronal damage through activation of the c-Jun N-terminal kinase (JNK) and CGRP1 knockout partially ameliorated disease in SBMA mouse model. A class of migraine medications, the triptans, improved disease phenotype in a SBMA mouse model and naratriptan, in particular, reduces JNK activation through the induction of mitogen-activated protein kinase phosphatase 1 (MKP1) [119].

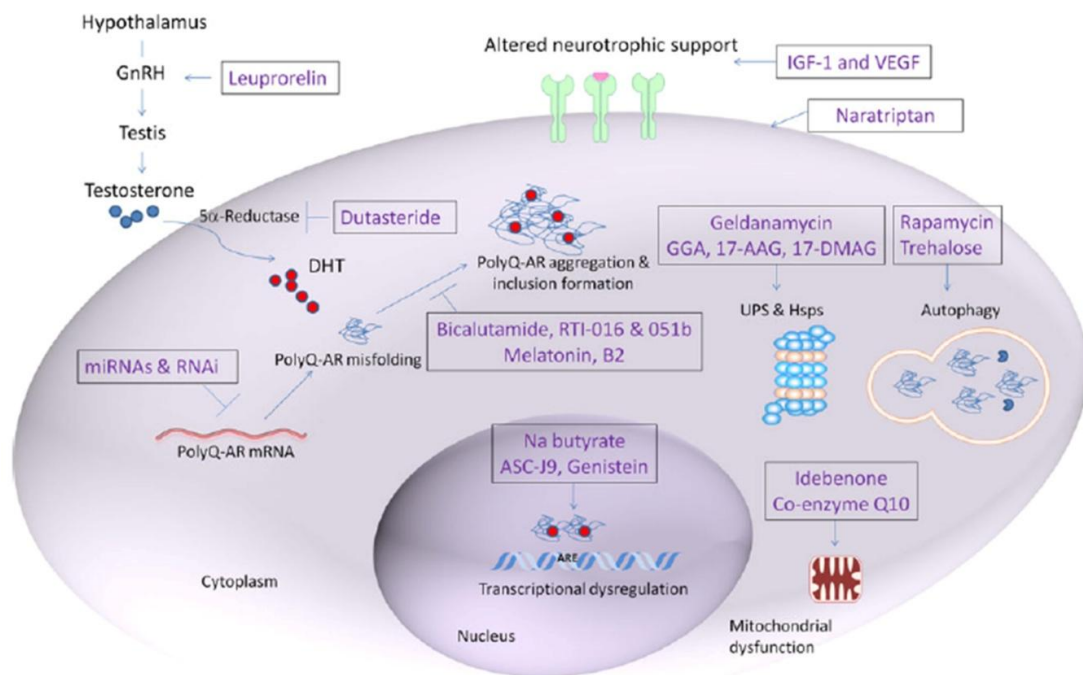


**Figure 3**

Current therapeutic strategies for SBMA and pathways involved [15].



## **Chapter 2**

***Synergic prodegradative activity of Bicalutamide  
and trehalose on the mutant androgen receptor  
responsible for SBMA.***

## ***Synergic prodegradative activity of Bicalutamide and trehalose on the mutant androgen receptor responsible for SBMA.***

### **Introduction**

In the absence of the natural ligand testosterone or dihydrotestosterone (DHT), polyQ AR localizes in the cytoplasm where it forms a multi-heteromeric complex with chaperones, such as Hsp90, Hsp70, Hsp40. Within these complexes, AR is not active and its polyQ tract is not exposed thanks to the interaction with other proteins. This binding prevents protein misfolding, aggregation and cytotoxicity. After the binding to testosterone, AR undergoes a conformational change that promotes heat-shock proteins dissociation, and exposes its nuclear localization signal (NLS), DNA-binding, and dimerization domains; however, the polyQ tract in AR may lead to an abnormal folding of the mutant protein, and in turn, to the formation of oligomeric and aggregated species of AR. Although the aggregation process may be initially protective to cells because neurotoxic misfolded species are sequestered into defined subcellular compartments, indeed referred as aggregates [36, 48, 105], later they may affect essential neuronal processes and become neurotoxic. Several evidences [46, 52, 55] suggest that misfolded polyQ AR exerts most of its toxicity into the nucleus, first because it may inhibit transcription by interfering with the function of essential transcriptional factors and co-activators [59] and, second, because transcriptional co-activators such as CREB-binding protein (CBP) can be sequestered into nuclear inclusions formed by the polyQ AR [61].

Nuclear or cytoplasmic polyQ AR aggregates are an indicator of protein accumulation, and resulting cell toxicity, and represent a valuable marker to monitor the formation/reduction

of toxic misfolded species in affected cells. In addition, if not removed by cytoplasmic autophagy, a large amount of misfolded polyQ AR goes into the nucleus where it can exert its toxicity. In fact, Montie et al [46, 55], already demonstrated that cytoplasmic polyQ AR retention correlates with increased neuronal survival in cells and improves motor functions in SBMA mice model. Thus, prevention of polyQ AR misfolding and nuclear translocation may counteract its toxicity.

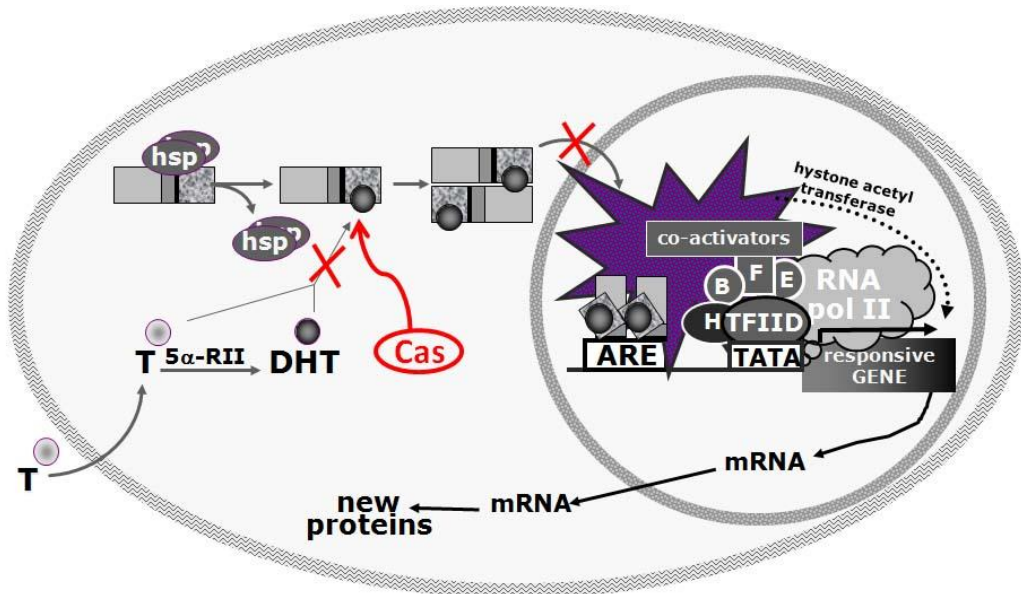
We [42, 105] and others [120] already showed that testosterone-induced polyQ AR misfolding and aggregation can be prevented/counteracted by some antiandrogens, like Bicalutamide, an FDA approved antiandrogen commercialized as Casodex® (Cas). Bicalutamide reduces the rate of polyQ AR nuclear translocation, allowing its more efficient cytoplasmic degradation via autophagy.

The disaccharide trehalose is an MTOR-independent autophagic inducer that is able to enhance polyQ AR (and other misfolded proteins) degradation [105, 121], extending lifespan of different mouse models of ND [121-127]. In particular, recent evidences suggest that autophagy induction mitigates neurodegeneration in ALS cell models [128] and that specifically trehalose delays disease onset, prolongs life span, and reduces motor neuron loss in the spinal cord of SOD1(G93A) mice [127]. The neuroprotective mechanisms of trehalose in neurodegenerative diseases are largely unknown. It is speculated that the neuroprotective effect of trehalose might be associated with the promotion of aggregated protein degradation. According to Zhang X. *et al.* trehalose might lead to motor neuron protection by activating the autophagic machinery at two different points: by promoting autophagosome formation but also by inducing autolysosome formation and degradation [127].

Since cytoplasmic polyQ AR retention is beneficial in SBMA models because it increases autophagic clearance of the misfolded polyQ AR [[46](#), [55](#), [104](#), [105](#), [129](#)], in this study, we tested a combination of Bicalutamide (which retains polyQ AR into the cytoplasm, by slowing down its nuclear translocation rate) [[42](#), [105](#), [120](#), [129](#)] and trehalose (which stimulates HSPB8 expression and enhances autophagy) (Figure 4).

In this study we decided to focus our attention on the polyQ AR alteration which are induced in motoneuronal cells. Our data demonstrated that the combinatory use of Bicalutamide and trehalose has a potent synergic activity against polyQ AR accumulation in neuronal models of SBMA: it efficiently decreases the number of aggregates and accelerates polyQ AR clearance; thus, this combined treatment could provide a novel valuable approach to counteract polyQ AR toxicity in SBMA.

**Bicalutamide (Casodex®, Cas):**



**Trehalose:**

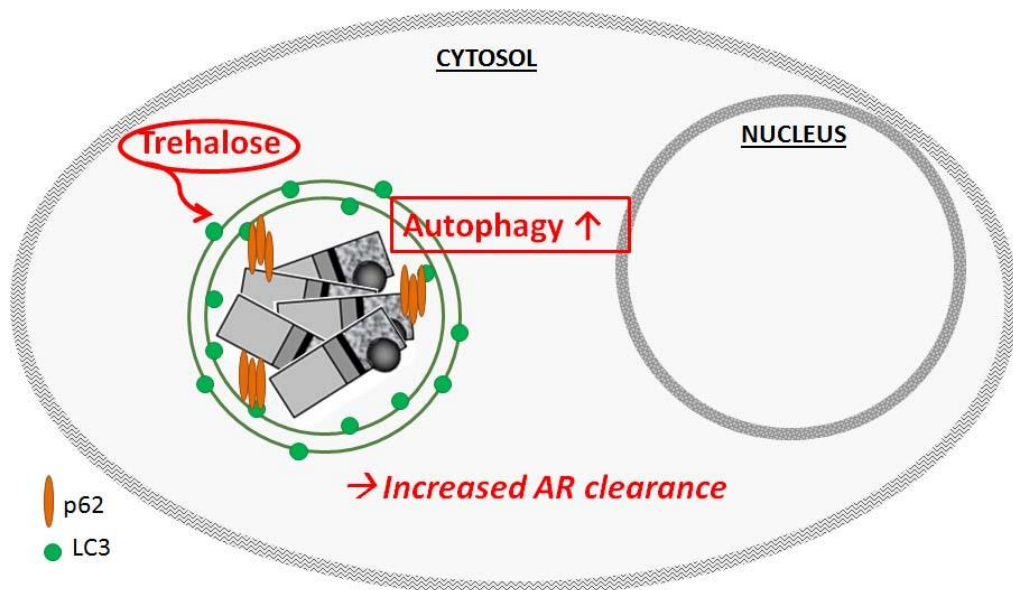


**Figure 4**

Schematic representation of Bicalutamide (Casodex®, Cas) and trehalose mechanisms of action. Bicalutamide competes with testosterone (T/DHT) in AR binding and slows down AR nuclear translocation, therefore AR remains longer in the cytosol. Trehalose promotes the autophagy-mediated cytoplasmic degradation of AR protein. Modified from Poletti A, *Front Neuroendocrinol*, 2004 [36].

## **Results**

### ***Bicalutamide and trehalose alone promotes ARQ46 clearance.***

In the first set of experiments performed using filter retardation assay (FRA), western blot (WB) and high-resolution fluorescence microscopy (HRFM) analysis, we compared the effects of single treatments with Bicalutamide or trehalose on polyQ AR aggregation and clearance in the absence of or in the presence of testosterone (to trigger the formation of polyQ AR toxic species) in NSC34 cells. The doses of trehalose have been selected by performing preliminary studies of dose-dependent response (Fig. 5A), while for Bicalutamide, a drug with a well-known pharmacokinetics and widely used in clinics against prostate cancer, we used the doses classically adopted to counteract testosterone activity in all transcriptional and binding assays, as well as against polyQ AR in SBMA. The results clearly demonstrated that Bicalutamide (Cas) reduces the accumulation of polyQ AR insoluble species induced by testosterone (Fig. 5B, lower panel and relative quantification, FRA), and to a lesser extent the total levels of the monomeric polyQ AR protein evaluated in western blot (Fig. 5B, upper panel, WB). This suggests that the misfolded polyQ AR fraction, in particular, is targeted by the Bicalutamide prodegradative activity. Trehalose also significantly reduces the accumulation of mutant polyQ AR insoluble species in FRA (Fig. 5C, lower panel and relative quantification), and reduces the monomeric polyQ AR levels both in the absence of and in the presence of testosterone, as show in WB analysis (Fig. 5C, upper panel). The presence of testosterone-induced polyQ AR aggregates was analyzed both after Bicalutamide (Cas, Fig. 5D) and trehalose (Fig. 5E) treatment in HRFM analysis. It clearly appears that whereas large cytoplasmic aggregates of polyQ AR are present in cells treated

with testosterone, few and very small polyQ AR aggregates are detectable in cells treated with either Bicalutamide (Cas) (no aggregates in Bicalutamide-treated cells in the absence of testosterone, approximately a 30% reduction induced by Bicalutamide on testosterone-induced polyQ AR aggregates) or trehalose (no aggregates in trehalose-treated cells in the absence of testosterone, approximately a 50% reduction induced by trehalose on testosterone-induced polyQ AR aggregates in the presence of testosterone). In addition, Bicalutamide (Cas) greatly reduces nuclear translocation and accumulation of polyQ AR, even in the presence of testosterone, retaining a large fraction of polyQ AR in the cytoplasm. This effect is not present in trehalose-treated cells expressing polyQ AR.

We next analyzed the effects of Bicalutamide and trehalose on two well-known autophagic markers, SQSTM1/p62 and LC3. The first, SQSTM1/p62, is upregulated during autophagy activation in our cell models and is responsible for insertion of polyubiquitinated misfolded protein species into autophagosomes. When autophagy is normally executed in cells, SQSTM1/p62 is continuously degraded via autophagy, together with the polyubiquitinated cargoes. Conversely, when autophagy flux is blocked (i.e. by polyQ AR), SQSTM1/p62 typically accumulates forming SQSTM1/p62 bodies that can be easily visualized in immunofluorescence (IF) microscopy. The second, LC3, is normally diffuse in cells as LC3-I in basal condition, but it is overexpressed during autophagy activation and converted into a lipidated autophagosome-anchored LC3-II protein showing a typical punctate distribution.

WB analysis in Figure 6A shows that SQSTM1/p62 levels remain unchanged after Bicalutamide treatment, but are increased by trehalose both in wild-type (wt; AR.Q23) and in polyQ AR (AR.Q46) expressing cells. Similarly, Bicalutamide has no effect on LC3-I to LC3-II

conversion, whereas trehalose stimulates the formation of large amounts of LC3-II form. These data were confirmed in IF microscopy (Fig. 6B), where it is noteworthy that SQSTM1/p62 and LC3 protein expression levels were greatly increased after trehalose treatment, but not by Bicalutamide.

#### ***Combined effect of Bicalutamide and trehalose on ARQ46.***

We next analyzed the possible synergic effect of the combinatory use of Bicalutamide and trehalose on the polyQ AR solubility in immortalized motoneuronal cells, both in the absence of and in the presence of testosterone. FRA analysis (Fig. 7A) clearly demonstrated that the levels of testosterone-induced polyQ AR insoluble species detected in cells simultaneously treated with Bicalutamide (Cas) and trehalose are significantly lower than that found in Bicalutamide (Cas)-treated cells ( $p < 0.001$ ) or in trehalose-treated cells ( $p < 0.05$ ). A similar effect is also present in polyQ AR insoluble species accumulating in the absence of testosterone, but in this case, the total insoluble material found in FRA is much lower than that found in testosterone-treated cells. We also analyzed the effect of the combined treatment with Bicalutamide and trehalose on monomeric polyQ AR in WB. Figure 7B shows that, in this case, the combined treatment with Bicalutamide (Cas) and trehalose results in a mild reduction of polyQ AR monomeric species, which is not significantly different from that observed after the separate treatments with the two compounds. Thus, the combinatory use of Bicalutamide and trehalose mainly affects the insoluble aggregated fraction derived from the misfolded polyQ AR and not the monomeric, possibly normally folded, polyQ AR present in immortalized motoneuronal cells. The presence of testosterone-induced aggregates of polyQ AR was evaluated in HRFM analysis (Fig. 7C). We found that the combined treatment



with Bicalutamide (Cas) and trehalose completely prevents the formation of polyQ AR aggregates (no aggregates in trehalose-treated or Bicalutamide-treated cells in the absence of testosterone, approximately a 80% reduction induced by Bicalutamide and trehalose co-treatment on testosterone-induced polyQ AR aggregates).

Since the UPS, together with autophagy, is involved in the removal of polyQ AR misfolded species, we analyzed whether UPS inhibition prevents the prodegradative activity of the combined treatment with Bicalutamide and trehalose. The FRA data reported in Figure 7D confirm the efficacy of the two drugs used in combination in the absence of MG132, which inhibits the chymotryptic activity of the proteasome. In addition, the data suggest that the prodegradative activity exerted by Bicalutamide on polyQ AR mainly requires a robust proteasomal activity; in fact, a large fraction of misfolded polyQ AR appears when the UPS is inhibited with MG132, even in the presence of Bicalutamide (Cas). Trehalose, which is an autophagy inducer, tends to increase insoluble polyQ AR clearance also in the presence of MG132, but not in a significant manner. The combined treatment with Bicalutamide (Cas) and trehalose further increases the clearance of insoluble polyQ AR, even in the presence of MG132. The role of the autophagic pathway was analyzed by blocking the autophagic flux with 3-methyladenine (3-MA), which prevents the assembly of mature autophagosomes. The data shown in Figure 7E clearly indicated that autophagy inhibition results in a complete loss of the prodegradative synergistic activity of Bicalutamide (Cas) and trehalose on polyQ AR insoluble species. Moreover, with Bicalutamide or trehalose alone, autophagy blockage by 3-MA resulted in a mild accumulation of mutant AR species, but not statistically relevant. Both the effects of single and double treatments are counteracted by autophagy inhibition, indicating that autophagy is active together with the ubiquitin–proteasome degradative

system. Therefore, although the UPS is largely involved in the removal of misfolded insoluble polyQ AR, cytoplasmic retention of the polyQ AR, combined with the activation of the cytoplasmic autophagic process, efficiently prevents its accumulation in cells.

***Autophagy activation is mediated by trehalose and not influenced by Bicalutamide.***

Based on these data we wished to evaluate the involvement of the autophagic process in the combined activity of Bicalutamide (Cas) and trehalose. Thus, we analyzed SQSTM1/p62 and LC3 expression and processing. As shown in Figure 8A, trehalose, alone or in combination with Bicalutamide (Cas), significantly increases SQSTM1/p62 mRNA expression levels in our cells expressing polyQ AR; Bicalutamide (Cas) is unable to enhance SQSTM1/p62 mRNA expression levels and does not amplify the trehalose-stimulated SQSTM1/p62 expression, both in the absence and presence of testosterone. Overlapping results were obtained when, in the same conditions, we analyzed the LC3 mRNA expression levels (Fig. 8B). In addition, the levels of the SQSTM1/p62 protein and the conversion of LC3-I to its lipidated and autophagosome-associated form, LC3-II, were increased after trehalose treatment but not influenced by the co-treatment with Bicalutamide (Fig. 8C and relative quantifications for SQSTM1/p62 in D and for LC3-II/LC3-I ratio in E). These results were further supported by the data obtained in IF microscopy analysis (Fig. 9) When cells were not treated with trehalose, SQSTM1/p62 shows an irregular and disorganized distribution, as shown in Figure 9A. In the presence of trehalose, SQSTM1/p62 protein levels notably increase and SQSTM1/p62 is homogeneously distributed into the entire cell cytoplasm. No changes in SQSTM1/p62 expression and distribution are induced by Bicalutamide (Cas) treatment. In the case of LC3 distribution analyzed in IF (Fig. 9B), we found that Bicalutamide (Cas) does

not influence the levels or the overall punctate distribution of LC3-II induced by mutant polyQ AR (both in the absence and presence of testosterone); conversely, trehalose treatment, which stimulates autophagy, enhances LC3-II levels which become exclusively present in its punctate distribution. As expected, similar levels and distribution of LC3-II are present in immortalized motoneurons expressing polyQ AR and simultaneously treated with Bicalutamide (Cas) and trehalose (both in the absence and presence of testosterone). In all cases, Bicalutamide and trehalose alone or in combination are all capable to reduce the number of polyQ AR aggregates formed after testosterone treatment. All together, the data strongly suggest the presence of active autophagy capable to remove the cytoplasmically retained polyQ AR.

***Combined effect of Bicalutamide and trehalose on ARQ112.***

To further characterize the effects of the combinatory use of Bicalutamide and trehalose, their activity was also tested on a form of AR containing a very long polyQ (Q112) tract, which has a different kinetic of aggregation and generates nuclear inclusions. To accomplish this, we used the PC12/AR.Q112 TET-On inducible cell model of SBMA. We demonstrated in FRA (Fig. 10A) that both Bicalutamide (Cas) and trehalose decrease the polyQ AR (112Q) aggregation, but the combinatory use of the two compounds is far more efficient than the two compounds used singularly. A similar effect was observed on the insoluble fraction (pellet) recovered after high-speed centrifugation of cell lysates of PC12/AR.Q112 cells (Fig. 6B). These results demonstrate a reduction in the amount of polyQ AR (112) present in the pellet fraction from cells treated simultaneously with Bicalutamide and trehalose (in the presence of testosterone). We also observed a trend toward a reduction in the levels of the

monomeric form of polyQ AR in the supernatant fractions, but these data did not reach statistical significance (Fig. 10B). This may reflect the possibility that the insoluble aggregated forms of polyQ AR (more than the soluble monomeric forms of polyQ AR) are preferentially degraded after the combinatory use of Bicalutamide and trehalose. Moreover, it is noteworthy that there is a reduction in the amount of polyQ AR oligomers, observed in the stacking gel, due to the combined treatment.

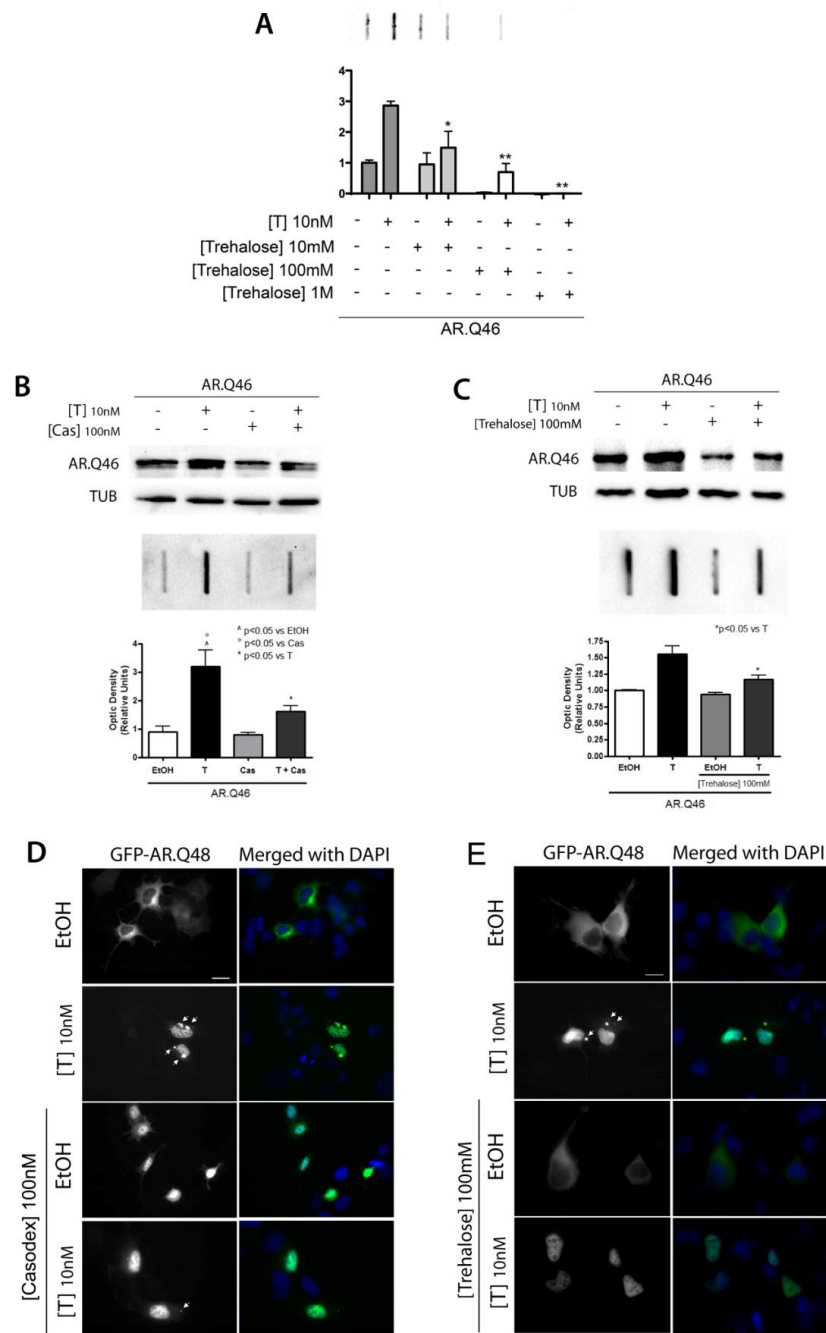


**Figure 5**

Effect of Bicalutamide or trehalose on testosterone-induced polyQ AR accumulation. (A) NSC34 cells expressing AR.Q46 treated with ethanol (EtOH) as a vehicle control, 10 nM testosterone (T) in the absence of or in the presence of different doses of trehalose (10 mM/100 mM/1 M) for 48 h. FRA shows AR.Q46 insoluble species accumulation after T treatment, and the dose-dependent effects of trehalose (\* $p < 0.05$  versus +T; \*\* $p < 0.001$  versus +T). (B) NSC34 cells expressing AR.Q46 treated with ethanol (EtOH) as a vehicle control, 10 nM testosterone (T) and/or 100 nM Bicalutamide (Cas) for 48 h. (C) NSC34 cells expressing AR.Q46 treated with ethanol (EtOH) as a vehicle control or 10 nM testosterone (T), in the absence of or in the presence of 100 mM trehalose for 48 h. Western blot analysis (B and C, upper panels) shows soluble AR.Q46 protein levels following different treatments. Alpha-tubulin was used to normalize protein loading. FRA in B, lower panel, illustrates the different accumulation of insoluble species of AR.Q46 after T or/and Cas treatments ( $^{\wedge}p < 0.05$  versus EtOH;  $^{\circ}p < 0.05$  versus +Cas;  $^{\ast}p < 0.05$  versus +T). FRA in C, lower panel, shows AR.Q46 insoluble species accumulation after T treatment, in the absence of or in the presence of trehalose ( $^{\ast}p < 0.05$  versus +T). (D) HRFM analysis (63 $\times$ magnification) on NSC34 cells expressing GFP-AR.Q48 in the absence of (EtOH) or in the presence of 10 nM testosterone (T) and/or 100 nM Bicalutamide (Cas) for 48 h. Nuclei were stained with DAPI (blue). Scale bar = 10  $\mu$ m. (E) HRFM analysis (63 $\times$ magnification) on NSC34 cells expressing GFP-AR.Q48 in the absence of (EtOH) or in the presence of 10 nM testosterone (T), with or without 100 mM trehalose treatment for 48 h. Nuclei were stained with DAPI (blue). Scale bar = 10  $\mu$ m.

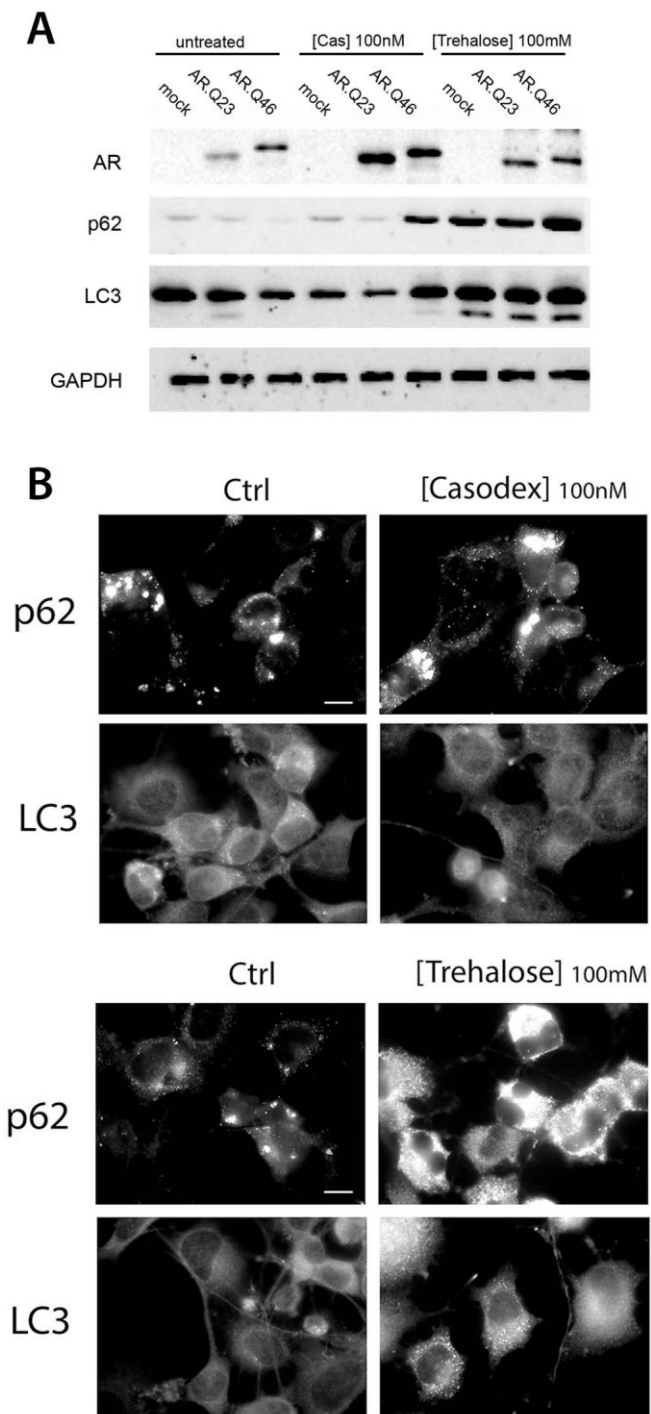


**Figure 6**

Autophagy activation is mediated by trehalose but not by Bicalutamide. (A) Western blot analysis on mock-transfected NSC34 cells and NSC34 cells transiently transfected with plasmids encoding AR.Q23 or AR.Q46 treated with 10 nM trehalose or 100 nM Bicalutamide (Cas) for 48 h. Two well-known markers of the autophagic pathway (SQSTM1/p62 and LC3-II) were used to compare the activation of autophagy mediated by trehalose or Bicalutamide. GAPDH was used to normalize protein loading. (B) HRFM analysis ( $63\times$  magnification) on NSC34 cells shows the subcellular distribution and the endogenous expression levels of LC3 and SQSTM1/p62 after 100 nM Bicalutamide (upper panel) or 100 mM trehalose (lower panel) treatments for 48 h, in the presence of mutant AR. Scale bar = 10  $\mu$ m.

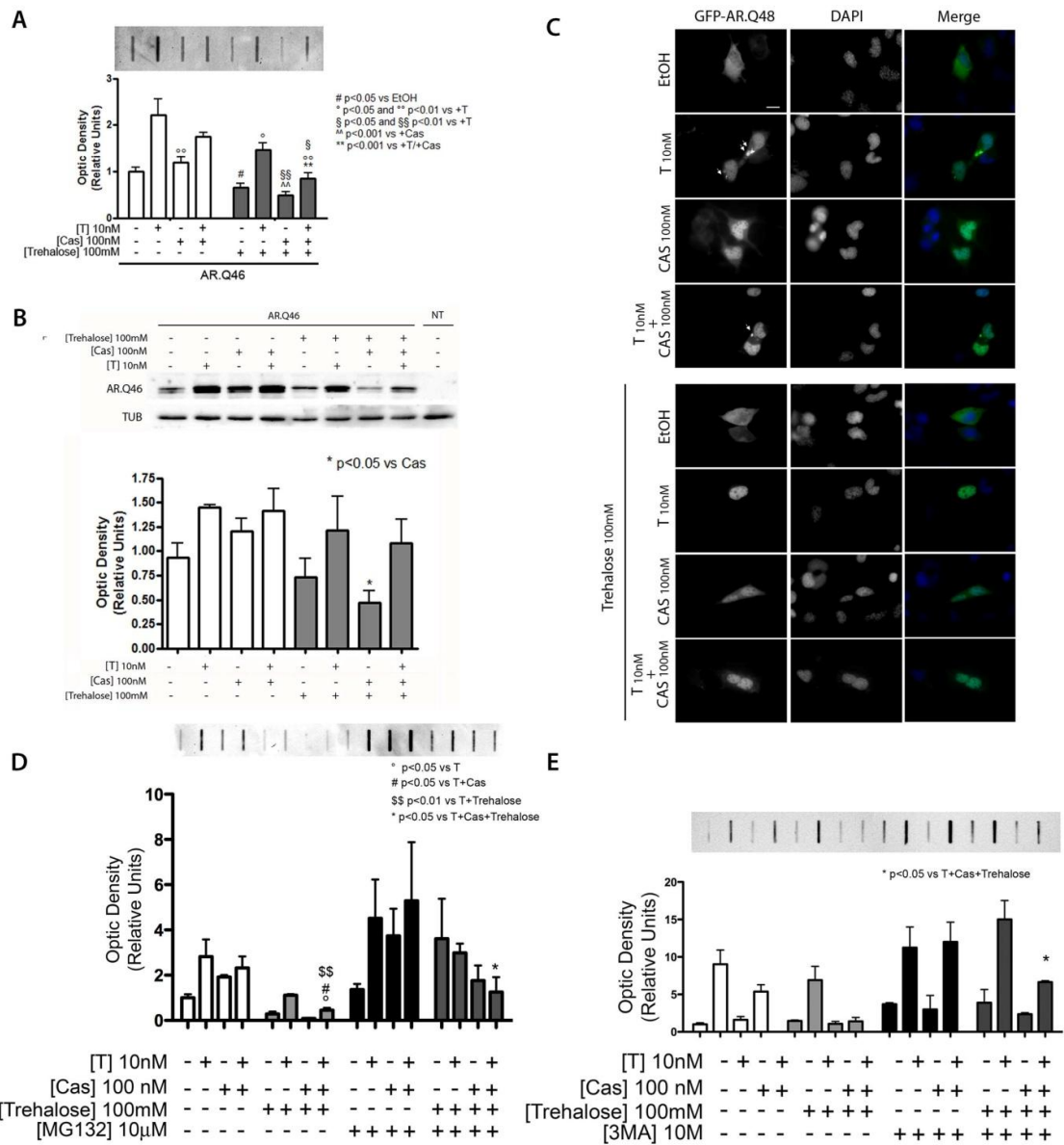


**Figure 7**

Combined effect of Bicalutamide and trehalose on AR.Q46 accumulation. (A and B) NSC34 cells expressing AR.Q46 treated with ethanol (EtOH) as a vehicle control, 10 nM testosterone (T) and/or 100 nM Bicalutamide (Cas) and/or 100 mM trehalose for 48 h. FRA (A) shows the synergic effect of Bicalutamide and trehalose on the accumulation of insoluble species of AR.Q46. The histogram represents a quantitative evaluation of AR.Q46 protein level carried out by densitometric scanning of the blots (#p<0.05 versus EtOH; °p<0.05 and °p<0.01 versus +T; §p<0.05 and §§p<0.01 versus +T; ^^p<0.001 versus +Cas; \*\*p<0.001 versus +T/+Cas). Western blot analysis (B) displays soluble AR.Q46 expression levels after single or combined treatments. The histogram represents a quantitative evaluation of AR.Q46 protein level normalized on alpha-tubulin carried out by densitometric scanning of the blots (\*p<0.05 versus +Cas). (C) HRFM analysis (63× magnification) on NSC34 cells expressing GFP-AR.Q48 in the absence of (EtOH) or in the presence of 10 nM testosterone (T) and/or 100 nM Bicalutamide (Cas), with or without 100 mM trehalose treatment for 48 h. Nuclei were stained with DAPI (blue). Scale bar = 10 mm. (D) FRA on NSC34 cells expressing AR.Q46 treated with ethanol (EtOH) as a vehicle control, 10 nM testosterone (T) and/or 100 nM Bicalutamide (Cas) and/or 100 mM trehalose for 48 h. AR.Q46 protein accumulation was analyzed in the condition described above or after treatment with 10 mM of MG132 for 16 h to inhibit the proteasome. The histogram represents a quantitative evaluation of AR.Q46 protein level carried out by densitometric scanning of the blots (°p<0.05 versus T; #p<0.05 versus T + Cas; §§p<0.01 versus T + trehalose; \*p<0.05 versus T + Cas + trehalose). (E) FRA on NSC34 cells expressing AR.Q46 treated with ethanol (EtOH) as a vehicle control, 10 nM testosterone (T) and/or 100 nM Bicalutamide (Cas) and/or 100 mM trehalose for 48 h. AR.Q46 protein accumulation was analyzed in the condition described above or after treatment with 10 mM of 3-MA for 48 h to block the autophagosome formation. The histogram represents a quantitative evaluation of AR.Q46 protein level carried out by densitometric scanning of the blots (\*p<0.05 versus T + Cas + trehalose).

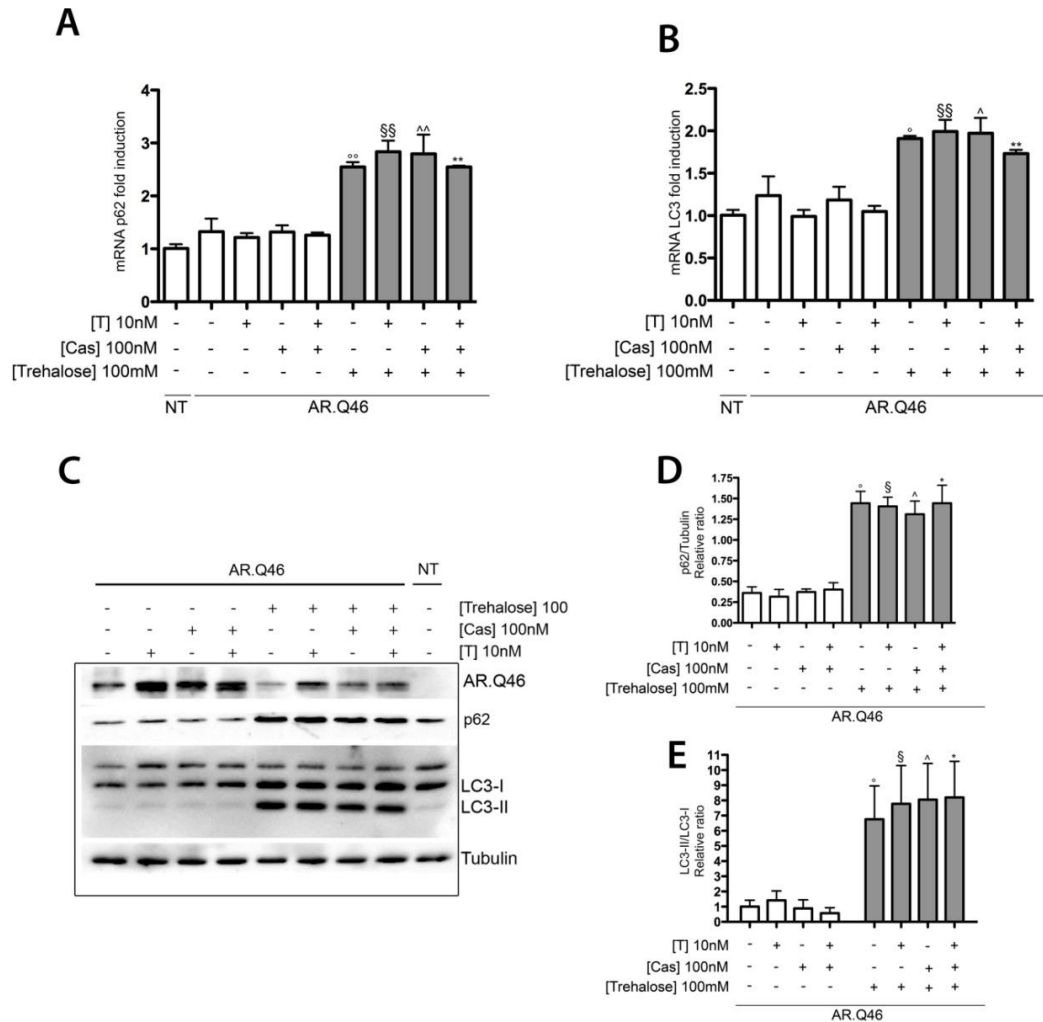


**Figure 8**

The autophagy activation is mediated by trehalose and not influenced by Bicalutamide. (A and B) Real-time PCR on SQSTM1/p62 (A) and on LC3 (B) mRNA expression levels on NSC34 cells expressing AR.Q46, in the absence of (ethanol as a vehicle control) or in the presence of 10 nM testosterone (T) and/or 100 nM Bicalutamide (Cas) and/or 100 mM trehalose for 48 h ( $^{**}p < 0.01$  versus EtOH;  $^{\$}p < 0.01$  versus +T;  $^{\wedge}p < 0.01$  versus +Cas;  $^{**}p < 0.01$  versus +T/+Cas). Not transfected cells (NT) show that AR.Q46 transfection does not alter SQSTM1/p62 and LC3 mRNA expression levels. (C) Western blot analysis on NSC34 cells expressing AR.Q46 treated with ethanol (EtOH) as a vehicle control, 10 nM testosterone (T) and/or 100 nM Bicalutamide (Cas) and/or 100 mM trehalose for 48 h. Two well-known markers of the autophagic pathway (SQSTM1/p62 and LC3-II) were used to show that the activation of autophagy is mediated by trehalose and not influenced by Bicalutamide. NT demonstrates that AR.Q46 transfection does not influence SQSTM1/p62 and LC3-II protein expression levels. Alpha-tubulin was used to normalize protein loading. (D and E) The two histograms, relative to western blot analysis in (C), represent a quantitative evaluation of SQSTM1/p62 protein level normalized on alpha-tubulin (D) ( $^{*}p < 0.05$  versus EtOH;  $^{\$}p < 0.05$  versus +T;  $^{\wedge}p < 0.05$  versus +Cas;  $^{*}p < 0.05$  versus +T/+Cas) and a quantitative evaluation of LC3-II/LC3-I ratio protein level (E) ( $^{8P} , 0.05$  versus EtOH;  $^{\$}P , 0.05$  versus +T;  $^{\wedge}P , 0.05$  versus +Cas;  $^{*}p < 0.05$  versus +T/+Cas), carried out by densitometric scanning of the blots.



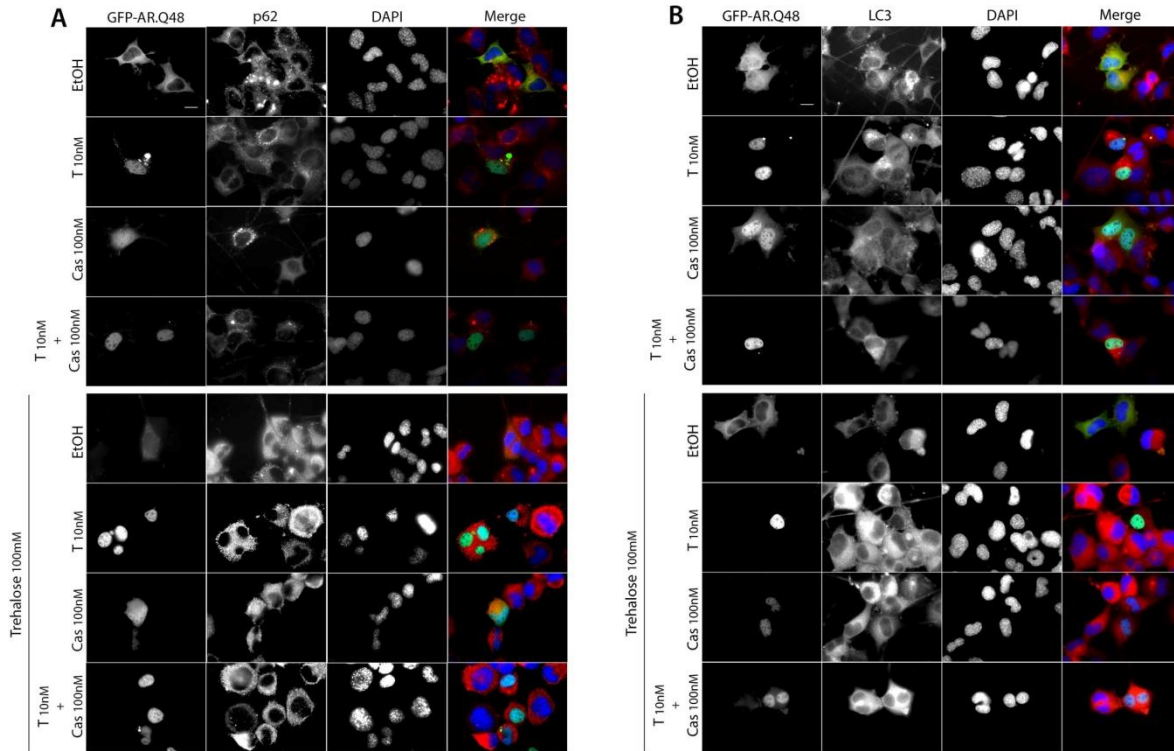


**Figure 9**

SQSTM1/p62 and LC3distribution. (A and B) HRFM analysis ( $63\times$  magnification) on NSC34 cells expressing GFP-AR.Q48 in the absence of (EtOH) or in the presence of 10 nM testosterone (T) and/or 100 nM Bicalutamide (Cas), with or without 100 mM trehalose treatment for 48 h. Endogenous SQSTM1/p62 (A) and LC3 (B) protein distribution and expression levels are shown in red. Nuclei were stained with DAPI (blue). Scale bar = 10  $\mu$ m.

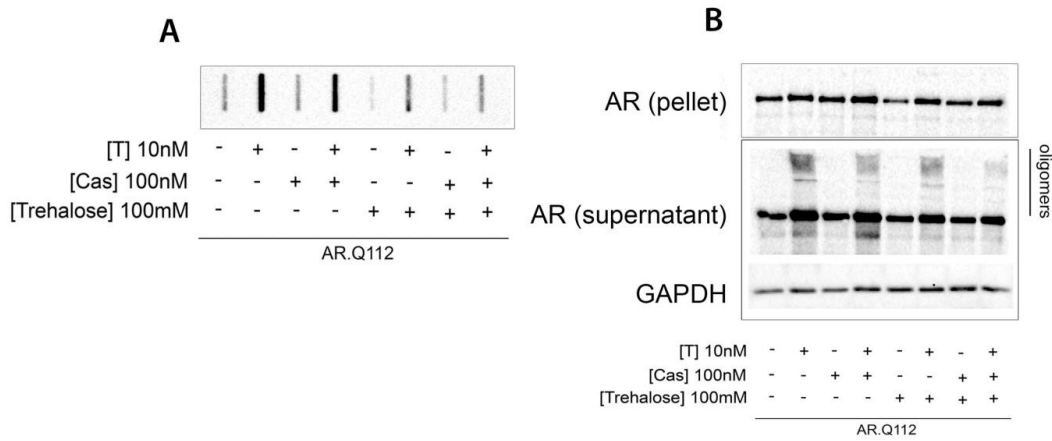


**Figure 10**

Combined effect of Bicalutamide and trehalose on PC12 cells expressing AR.Q112. (A and B) AR.Q112 protein expression in PC12 stable transfected cell line was induced by 1 mg/ml of doxycycline; after 12 h the cells were treated with ethanol (EtOH) as a vehicle control, 10 nM testosterone (T) and/or 100 nM Bicalutamide (Cas) and/or 100 mM trehalose for 48 h. The cells were re-suspended in RIPA buffer and centrifuged to separate the pellet and the supernatant fractions. The supernatant fraction was loaded in FRA (A). Both the supernatant and the pellet fractions were analyzed by western blot (B). GAPDH was used to normalize protein loading.

## **Discussion**

In this study, we evaluated whether a combined pharmacological treatment, aimed both to reduce the nuclear toxicity exerted by mutant AR and to enhance its autophagic clearance, may be of use as a novel therapeutic approach in SBMA. Our data clearly demonstrate that the simultaneous use of Bicalutamide (which reduces the rate of AR nuclear translocation) [[42](#), [46](#), [104](#), [120](#), [129](#)] and trehalose (an autophagy activator and HSPB8 stimulator) [[105](#), [122](#), [123](#), [125](#), [127](#)] results in an increase in the clearance of insoluble polyQ AR species induced by testosterone treatment in immortalized motoneuronal cells. Here, we decided to focus our attention only on motoneuronal cells, since the molecular events at the basis of polyQ AR neurotoxicity are quite well studied, while the muscle-related toxicity, which is clearly exerted by the SBMA polyQ AR, is still poorly understood. In any case, aberrations in both cell types participate to the onset and progression of the disease, even if it is still debated the relative contribution of each cell type to SBMA. It remains to be determined whether the therapeutic approach here postulated may have beneficial effects also in muscle, in which the toxicity exerted by polyQ AR may be due to different causes. We believe that further studies on muscle cell models and a trial on SBMA mice models may provide the answer to this question.

In general, the combined treatment has no relevant effects on the levels of monomeric soluble polyQ AR, both in the absence and presence of testosterone; in fact, the prodegradative effect of the two compounds acting in an additive manner is mainly exerted on the polyQ AR misfolded fraction. This fraction is capable of generating insoluble species and forming intracellular aggregates. Our data suggest that, at least in their earlier formation

stages, aggregates may protect against polyQ AR toxicity [48, 129] by confining neurotoxic species into a physically defined subcellular compartment. However, they may become toxic at later stages by altering essential neuronal processes [36, 65]. In any case, aggregates represent a valuable marker to follow protein misfolding, and the reduction in their number is indicative of a beneficial effect of the combinatory treatment against misfolded species in affected cells. Indeed, in this study, we show that polyQ AR aggregates were more efficiently reduced by the combined action of Bicalutamide and trehalose than when the same compounds were used separately. Therefore, the longer cytoplasmic retention of the Bicalutamide-bound polyQ AR facilitates a better cytoplasmic autophagic recognition of the misfolded species prior to its migration into the nucleus; at the same time, the trehalose-enhanced autophagy improves the capability of this proteolytic system to clear the excess of misfolded polyQ AR released from accessory chaperones after ligand interaction, also preventing any possible autophagic flux blockage. This can be also achieved by trehalose induction of the small HSPB8 [105], which we have previously shown to be a facilitator of autophagy. In fact, the response of cells to protein misfolding requires different HSPs [46, 97, 98, 100]. HSPB8 dramatically increases solubility and clearance of polyQ AR (and other misfolded proteins), decreasing their aggregation rate [105, 130-132]. HSPB8 acts via both the UPS and autophagy [105, 131, 132]; HSPB8 facilitation of autophagy requires the formation of a complex with BAG3/HSC70/CHIP, in which CHIP ubiquitinates HSPB8-associated substrates, allowing SQSTM1/p62 recognition for insertion into autophagosomes [131]. With this mechanism, HSPB8 facilitates polyQ AR autophagic clearance and relieves the blockage of autophagic flux [105].

Several advantages may arise from the use of these two active compounds in SBMA. First, the antiandrogen Bicalutamide is an FDA-approved and commercially available drug (Casodex), already widely used in prostate cancer therapy. It can be administered for chronic treatment and is relatively well tolerated by patients. Secondly, trehalose is a natural disaccharide widely present in microorganisms, plants and invertebrates, and used in several nutrients to preserve aliments. It is a nontoxic and very well-tolerated molecule consisting of two D-glucoses connected by an  $\alpha,\alpha$ -1,1-linkage. Trehalose is not considered a drug, but a nutrient supplement, with no particular restriction for its oral intake. Trehalose is hydrolyzed to glucose within the gastrointestinal tract, but the fraction adsorbed can reach the brain (see below). Trehalose was initially found active in a screening designed to find inhibitors of polyQ-mediated protein aggregation and was tested with various disaccharides because of the lack of toxicity and the possibility of safe, oral administration [122]. Trehalose has been proved active against aggregation of polyQ-expanded huntingtin [122, 123], beta-amyloid [133], polyA-binding protein nuclear 1 (PABPN1) [124], the pathological prion protein [125], the amyotrophic lateral sclerosis (ALS) and frontotemporal lobar degeneration (FTLD)-associated protein TDP-43 [134], mutant synuclein [126] and also on the polyQ AR [105]. Interestingly, tested in animal models, trehalose alone has been found useful in several mouse models of NDs. For example, the oral administration of trehalose counteracted polyQ toxicity and ameliorated the phenotype, improving motor dysfunction and extended life span in a mouse model of Huntington disease (HD) [122]; trehalose administration resulted in a decrease of aggregation of huntingtin mutant protein in several brain areas (but also in liver), thus even when administered orally, it can be adsorbed and a fraction non metabolized in the gastrointestinal tract, can cross the brain blood barrier reaching the

neuronal cells affected in HD [122]. In mouse models of oculo pharyngeal muscular dystrophy (OPMD), linked to an abnormal expansion of a polyalanine tract in PABPN1, oral administration of trehalose attenuated muscle weakness and reduced mutant PABPN1 aggregation in skeletal muscle [124]. Two recent reports have demonstrated that trehalose also improves motor function and extends survival of mouse models of ALS [121, 127]. These data together demonstrate that trehalose is a good candidate molecule to be used in future therapeutic approaches in human NDs. Unfortunately, even if trehalose has been found active in cellular models of SBMA [104, 105], no studies have been conducted in mouse models of SBMA. Similarly, several studies performed in cellular models of SBMA have demonstrated that Bicalutamide alone counteracts polyQ AR aggregation [42, 105, 120] possibly facilitating autophagic removal of polyQ AR misfolded species, thus preventing its neurotoxicity. Even in this case, no data are yet available in mouse models of SBMA. In this study, we tested the combinatory use of Bicalutamide and trehalose on cellmodels of SBMA, demonstrating a synergistic effect of the two compounds on polyQ AR removal. The slowed kinetics of polyQ AR nuclear translocation induced by Bicalutamide allows for an increased clearance of misfolded polyQ AR species via the cytoplasmic autophagic machinery, rendered more efficient and active by trehalose treatment. It is worth noting that the autophagic process is induced by trehalose but not influenced by Bicalutamide, as shown by the two well-known autophagic markers, SQSTM1/p62 and LC3-II. Collectively, the data here reported lay the foundation for preclinical trials in mouse models of SBMA to test the therapeutic potential of Bicalutamide and trehalose in single and combined administration.

## **Chapter 3**

***The small molecule JG98 promotes polyQ AR ubiquitination and proteasomal degradation through the activation of Hsp70.***

---

## ***The small molecule JG98 promotes polyQ AR ubiquitination and proteasomal degradation through the activation of Hsp70.***

### **Introduction**

The ubiquitin-proteasome system (UPS) is one of the main degradative machineries in the cell that regulates protein homeostasis [135]. During this process, ubiquitination occurs on unfolded or damaged substrates in order to target them for proteasomal degradation.

The two principal chaperones involved in making triage decisions for protein degradation are the heat shock proteins 70 (Hsp70) and 90 (Hsp90) [79, 81, 82]. Heat shock proteins are molecular chaperones that facilitate the folding, assembly and intercellular transport of proteins and the Hsp90/Hsp70-based chaperone machinery, in particular, stabilizes and maintains AR in a conformation that allows ligand binding [136] (Fig. 11). Hsp90 and Hsp70 have opposite roles in the chaperone-based machinery for proteasomal degradation of client proteins: Hsp90 inhibits and Hsp70 promotes substrates ubiquitination. This means that favoring Hsp90 activity results in client protein stability and increasing Hsp70 expression levels causes protein degradation.

As shown in many studies, the manipulation of Hsp90 activity can influence polyQ AR stability and degradation. When Hsp90 heterocomplex assembly is blocked by specific inhibitors like geldanamycin, polyQ AR undergoes rapid degradation through the UPS. Two less toxic derivatives of geldanamycin, 17-AAG [100, 101] and 17-DMAG [102], have been also demonstrated to increase polyQ AR degradation in cellular and mouse models of SBMA. The enhanced UPS degradation of Hsp90 client proteins is assisted by E3 ligases such as

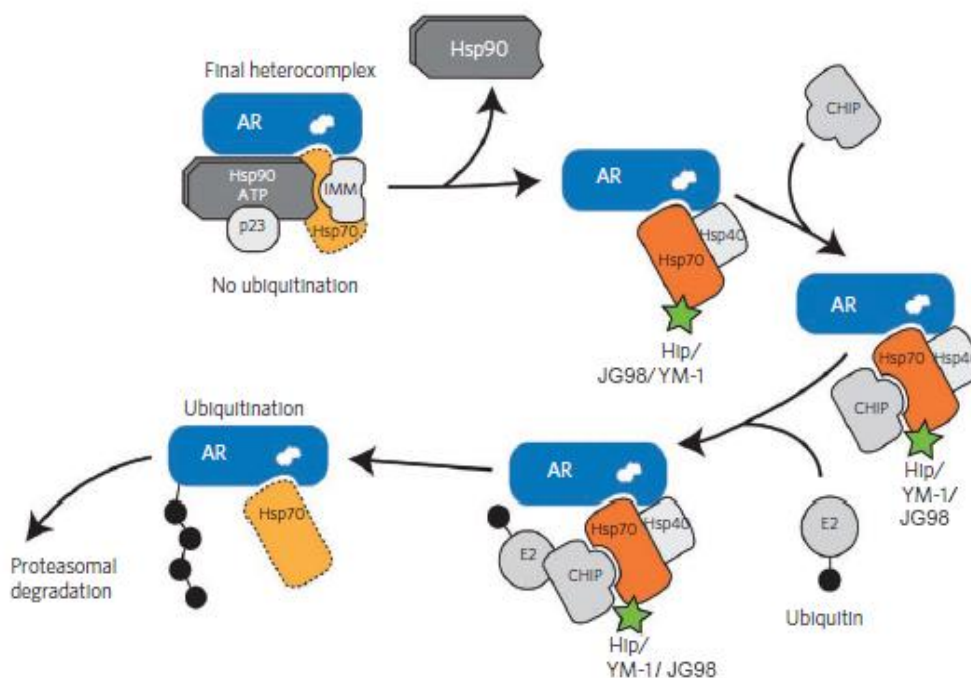
CHIP. In fact, increasing levels of CHIP promote polyQ AR ubiquitination and degradation in SH-SY5Y cells and overexpression of CHIP in AR97Q mice inhibits polyQ AR neuronal nuclear accumulation and ameliorates motor symptoms [98]. Moreover, increasing Hsp levels has proven effective in preventing toxic protein aggregation in SBMA models. Geranylgeranylacetone (GGA) treatment, which induces Hsp70, Hsp90 and Hsp105 expression, inhibited nuclear accumulation of the polyQ AR and ameliorated the neuromuscular phenotype in AR97Q mice [59] while AR100Q mice treated with arimoclomol, a co-inducer of the heat-shock stress response, displayed improved neuromuscular function and motor neuron survival, and delayed disease progression [137]. In particular, the role of Hsp70 in polyQ AR degradation has been extensively demonstrated. Inhibition of Hsp70 by methylene blue impaired degradation and enhanced aggregation of AR112Q in HeLa cells [136]. In contrast, overexpression of Hsp70-interacting protein (Hip) [138] or treatment with the small molecule YM-1 stabilized Hsp70 in its ADP-bound conformation, therefore increasing its affinity for the substrates, enhancing ubiquitination and degradation of AR112Q in a PC12 cells model [96]. Moreover, both Hip and YM-1 alleviate DHT-dependent toxicity in a *Drosophila* model of SBMA by stimulating polyQ AR ubiquitination and clearance through the UPS [96].

Although YM-1 was found to be effective in cell models of SBMA, it did not completely rescue the DHT-dependent rough eye phenotype in UAS-AR52Q flies [96]. This might be due to the extremely short half-life of the small molecule and the lack of in vivo bioavailability. Further studies led to the identification of a small molecule with the same chemical backbone as YM-1 but with different side groups that made the compound more stable with



improved in vivo bioavailability. The new compound, named JG98, has a phenyl ring and a chlorine as lateral groups that make it more hydrophilic (Table 1).

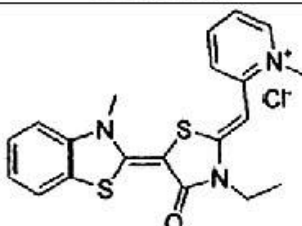
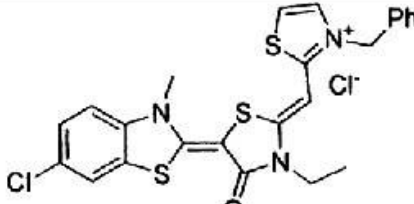
Here we show efficacy of JG98 in promoting polyQ AR clearance in a tetracycline-inducible PC12 cell model and demonstrate that JG98's pro-degradative activity is UPS-mediated. Like YM-1, JG98 favors the accumulation of the ADP-bound active form of Hsp70 that leads to substrate ubiquitination and proteasomal degradation. We also show that the JG98 mechanism of action does not alter the expression of other Hsps and does not influence the steady-state levels of other client proteins in their native conformations but can work synergistically with Hsp90 inhibitors. This new compound acts through the activation of Hsp70 and provides an alternative to Hsp90 inhibitors. As Hsp90 is responsible for maintaining many client proteins in their native conformation and managing their triage in the chaperone machinery, inhibition of Hsp90 may cause side effects and induce a stress response. In addition, the increased in vivo bioavailability of JG98 allows further studies in animal models that were not feasible with YM-1.



**Figure 11**

PolyQ AR degradation is regulated by the Hsp90/Hsp70-based chaperone machinery described here. Hsp90, Hsp70 and other co-chaperones bind to and stabilize polyQ AR to enable ligand binding (depicted as white steroid within AR) and subsequent nuclear translocation (top left). The presence of the polyQ tract in the AR promotes protein unfolding after dissociation from Hsp90 and ligand-binding. Misfolded polyQ AR is recognized and bound by Hsp70 that recruits chaperone-dependent ubiquitin ligases such as CHIP (or other chaperone-dependent ubiquitin ligases) to promote degradation through the proteasome. As shown in this model, allosteric Hsp70 co-chaperones, including Hip, YM-1 and JG98 (green), increase substrate binding affinity, facilitate client protein ubiquitination and promote polyQ AR clearance by the proteasome. This strategy alleviates polyglutamine toxicity by facilitating degradation of the mutant protein. The broken line for Hsp70 in the final heterocomplex indicates that it is present in substoichiometric amounts with respect to the receptor.

*Modified from Wang et al., 2013, Nature Chemical Biology*

<i>Compound</i>	<i>Structure</i>	<i>M.W.</i>
<b>YM-1</b>		417.98
<b>JG98</b>		534.54

**Table 1**

Chemical structure of the small molecules YM-1 and JG98 and relative molecular weight (M. W.).

## **Results**

### ***JG98 promotes polyQ AR degradation in a dose-dependent manner.***

The Hsp90/Hsp70-based chaperone machinery has a central role in the triage of unfolded proteins. It decides whether client substrates will be assisted in the refolding process or will be ubiquitinated and degraded by the proteasome. Similarly to Hip and to the small molecule YM-1, JG98 stabilizes Hsp70 in its ADP-bound. In this conformation Hsp70 recognizes with higher affinity unfolded or damaged substrates and facilitates their removal. Here we show in Western Blotting analysis (WB) and Filter Retardation Assay (FRA) that polyQ AR degradation is induced by JG98 treatment in a dose-dependent manner in a tetracycline-inducible PC12 cell model. We induced AR112Q expression with doxycycline in the presence of R1881 to activate the AR and to promote ligand-dependent misfolding. After 48 hrs, JG98 was able to reduce aggregated polyQ AR levels in the pellet fraction (Fig 12A) and in FRA (Fig. 12C left panel) more effectively than the monomeric AR present in the supernatant (Fig 12A). This indicates that JG98 preferentially promotes clearance of the misfolded and high-molecular weight species of mutant AR, like the oligomeric and aggregated forms. In a second set of experiments in PC12 cells, doxycycline was washed out after 48 hrs of transgene expression and the degradation rate of already synthesized polyQ AR was analyzed following a prolonged (72 hrs) treatment with JG98. The effect of JG98 in the absence of transgene expression is shown both in the supernatant, pellet fraction and FRA, even at lower doses of the compound (Fig. 12B and 12C right panel). The dose-dependent response analysis allowed us to select 0.5  $\mu$ M (half dose compared to 1  $\mu$ M used for YM-1) as the lower effective dose of JG98 that will be used in the following studies. We

also performed an immunofluorescence (IF) analysis to confirm the robust effect of JG98 in diminishing the accumulation of AR112Q nuclear inclusions in PC12 cells (Fig. 12D).

### ***Proteasomal degradation of polyQ AR***

According to our model of the role of the Hsp90/Hsp70-based machinery in protein triage, JG98 binds and activates Hsp70, then the E3 ubiquitin ligase CHIP is required for client proteins ubiquitination and degradation through the UPS. To prove the involvement of the proteasome in the JG98-mediated polyQ AR clearance, we used lactacystin to inhibit the proteasome activity in PC12 cells expressing AR112Q. We observed that the effects of JG98 on polyQ AR degradation were completely blocked (Fig. 13A). In contrast to chemical inhibitors of Hsp90 like geldanamycin and its derivatives that might alter the Hsp90-mediated stability of many other client proteins besides polyQ AR, JG98 does not alter the amount of Akt and ERK 1/2 proteins and does not increase the levels of the molecular chaperones Hsp70, Hsp40 and Hsp25 in PC12 cell lysates (Fig. 13B). To support our hypothesis that JG98 has an alternative mechanism of action to promote polyQ AR degradation compared to the Hsp90 inhibitors, we wondered if the combined treatment with JG98 and 17-AAG might have an additive and synergistic effect on polyQ AR proteasomal removal. As shown in FRA and relative quantification, the simultaneous treatment with the Hsp70 activator and the Hsp90 inhibitor in PC12 cells expressing AR112Q significantly increased polyQ AR degradation compared to JG98 treatment alone (Fig. 13C).

### ***PolyQ AR ubiquitination is promoted by Hsp70 co-chaperones***

We next analyzed AR protein ubiquitination by co-immunoprecipitating (co-IP) polyQ AR and HA-ubiquitin in PC12 cells expressing AR112Q. Cells were treated with JG98 for 24 hrs in the

presence of doxycyclin and R1881, and the proteasome activity was blocked by MG132 for the last 16 hrs to prevent the degradation of the ubiquitinated AR. As shown in Fig. 14A and relative quantification, the small molecule JG98 is able to significantly stimulate polyQ AR ubiquitination. YM-1 similarly increases polyQ AR ubiquitination (Fig. 14B). Moreover, we overexpressed Hip protein and found enhanced polyQ AR ubiquitination, comparable to that noticed after JG98 or YM-1 treatment (Fig. 14C). The AR/ubiquitin co-IP studies are accompanied by the relative input controls to prove plasmid transfection efficiency and show that monomeric AR112Q levels do not change in the presence of Hsp70 co-chaperones (Fig. 14, left panels). These data proved that JG98 and YM-1 acts similarly to Hip favoring Hsp70 activation and client proteins ubiquitination in the same way. In addition, the similar effect of these Hsp70 co-chaperones on AR112Q ubiquitination supports the idea that natural and synthetic molecules have similar actions on Hsp70 [96].

We later transfected HeLa cells with human CHIP-myc-His expressing plasmid and co-IP CHIP and Hsp70 proteins to verify their interaction during the protein degradation process and in the presence of JG98 or YM-1. Both compounds do not alter or increase CHIP/Hsp70 interaction. This likely reflects the fact that their mechanism of action is to stabilize the ADP-bound state of Hsp70 rather than to include the binding of Hsp70 to CHIP (Fig.15).

In its entirety, this study provides a detailed insight of the mechanisms by which the Hip protein and the small molecules JG98 and YM-1 promote polyQ AR ubiquitination and degradation through the proteasome, thus confirming our hypothesis of their activity is mediated through Hsp70.

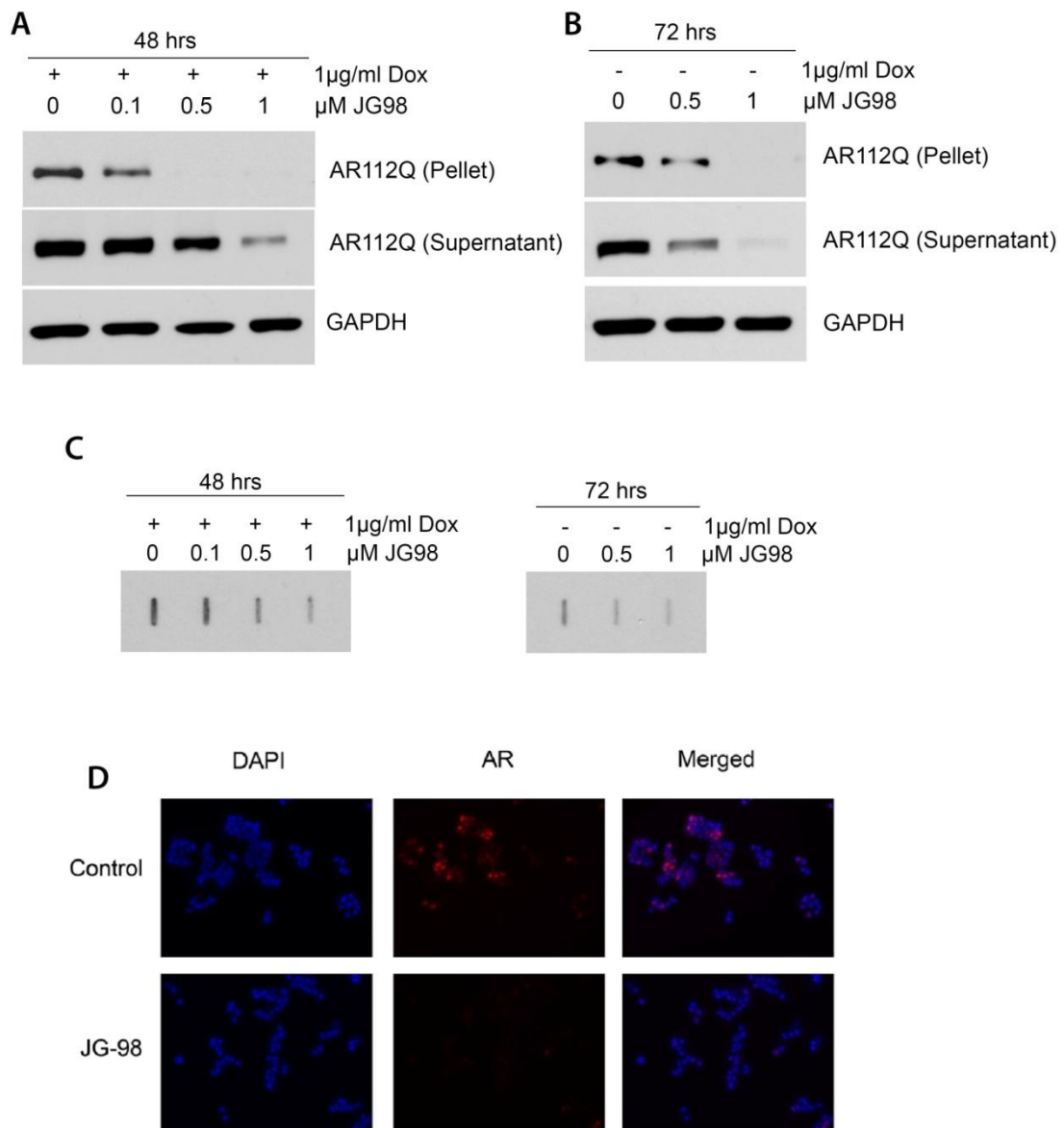


**Figure 12**

Dose-dependent degradation of polyQ AR mediated by JG98. (A) PC12 cells expressing AR112Q were treated with increasing amounts of JG98 (0.1, 0.5 and 1 µM) for 48 hours in the presence of doxycycline and 10 nM R1881. Monomeric (supernatant fraction) and aggregated (pellet fraction) species of polyQ AR were analyzed by Western Blotting. (B) 48 hours of transgene expression was switched off by washing out doxycycline and effects on AR112Q degradation were analyzed by Western Blotting following 72 hours of treatment with JG98 (0.5 and 1 µM) in the absence of newly synthesized polyQ AR. (C) AR112Q aggregation was also analyzed in Filter Retardation Assay, both in the presence (48 hrs experiment, upper panel) and the absence (72 hrs experiment, lower panel) of transgene expression. (D) Immunofluorescence analysis in PC12 cells expressing AR112Q and treated with JG98 (0.1, 0.5 and 1 µM) to analyze nuclear accumulation and aggregation of the polyQ AR. Nuclei stained with DAPI.

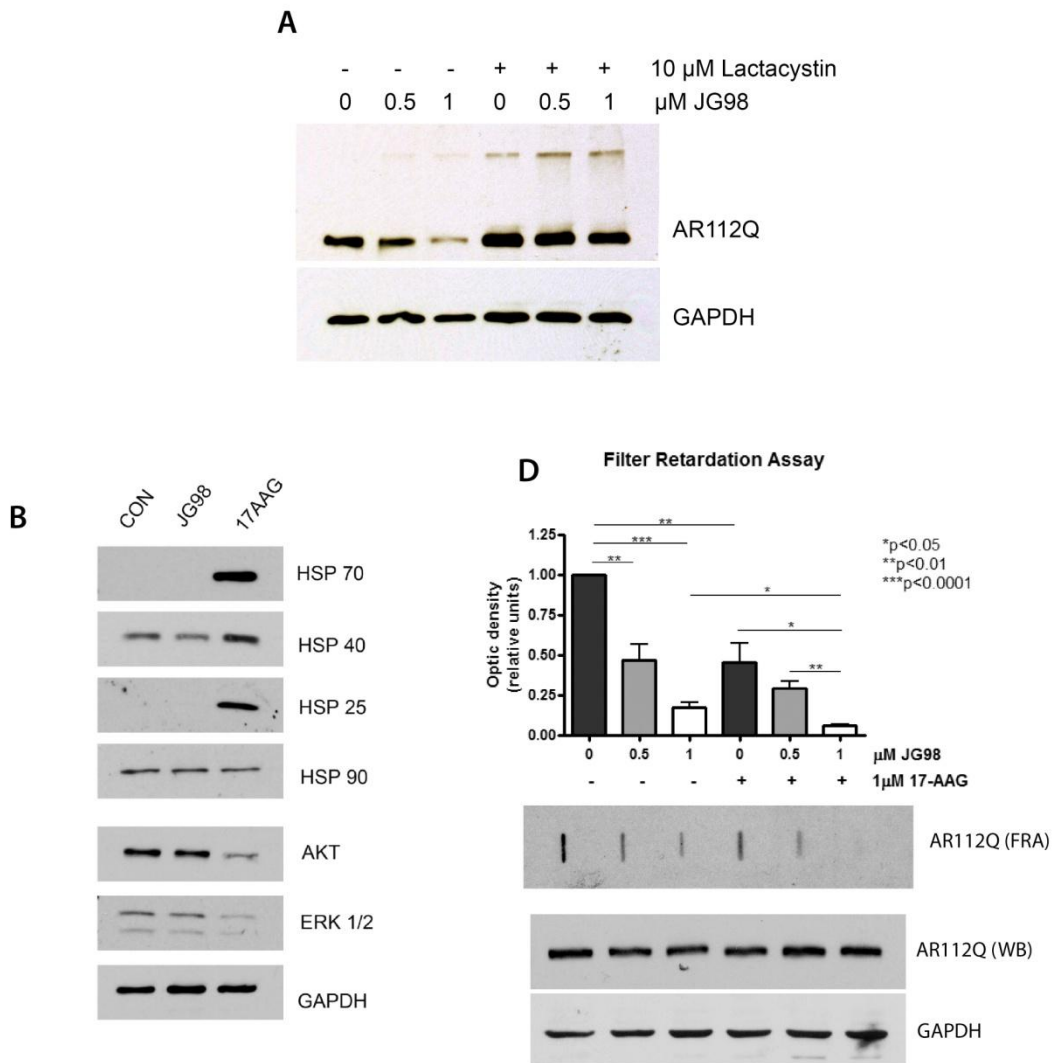


**Figure 13**

JG98 promotes proteasomal degradation of polyQ AR. (A) PC12 cells expressing AR112Q were treated with JG98 (0.5 and 1  $\mu$ M) for 48 hours and with the proteasome inhibitor lactacystin for the last 26 hours in the presence of doxycycline and the synthetic AR ligand R1881. AR112Q levels were analyzed by Western Blotting. (B) HeLa cells were treated with 0.5  $\mu$ M JG98 or 1  $\mu$ M 17-AAG and the levels of Hsps and Hsp90 clients Akt and Erk 1/2 were analyzed in Western Blotting. (C) Filter Retardation Assay and Western Blotting analysis on PC12 lysates following the combined treatment with JG98 (0.5 and 1  $\mu$ M) and 1  $\mu$ M 17-AAG for the last 24 hours in the presence of doxycycline and R1881. Quantification is from three independent experiments. Data are mean  $\pm$  SEM. \*P<0.05; \*\*P<0.01; \*\*\*P<0.001 by ANOVA.



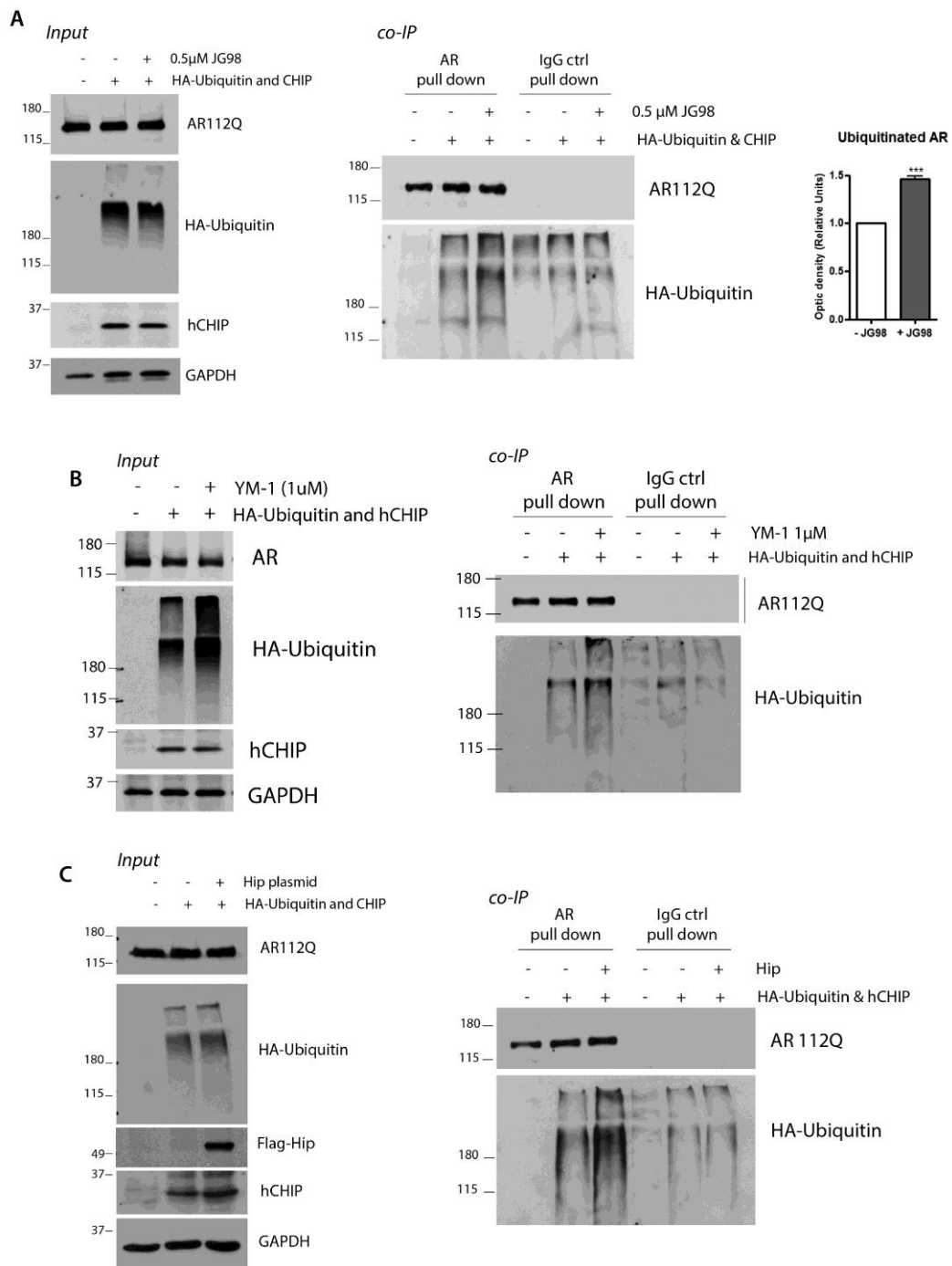


**Figure 14**

PolyQ AR ubiquitination is enhanced by Hsp70 co-chaperones. (A and B) PC12 cells were transiently transfected with plasmids coding for HA-ubiquitin and CHIP, transgene expression was induced by doxycycline for 48 hours, cells were treated with 0.5 μM JG98 or 1 μM YM-1 for the last 24 hours and with 10 μM MG132 for the last 16 hours. AR112Q and ubiquitin were co-immunoprecipitated (co-IP) and the amount of ubiquitinated AR was analyzed by Western Blotting. In JG98 co-IP experiment, quantification was from three independent experiments and data are mean ± SEM. \*\*\*P<0.001 by Student's t-test. (C) Similar to co-IP studies in panels A and B but Hip plasmid was co-transfected with CHIP and HA-ubiquitin plasmids. Left panels (A, B and C) represent input controls of the relative co-IP.

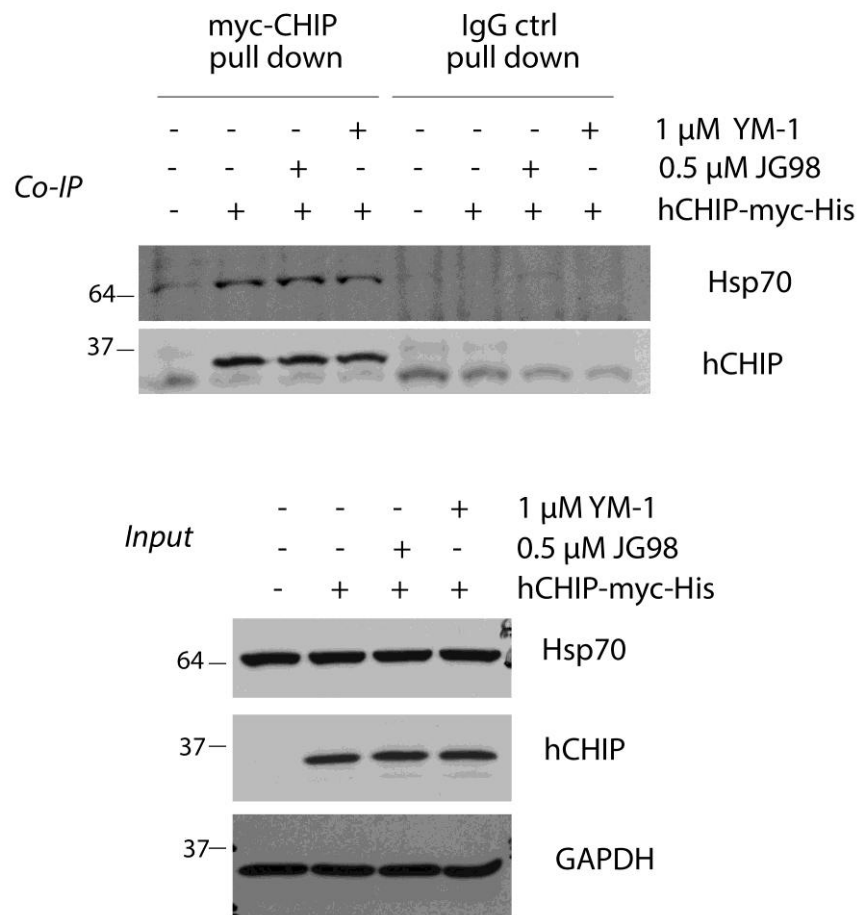


**Figure 15**

Hsp70/CHIP interaction is not modulated by JG98. HeLa cells were transiently transfected with plasmid coding for CHIP and then treated with 0.5  $\mu$ M JG98 or 1  $\mu$ M YM-1 for 24 hours. CHIP and Hsp70 were co-immunoprecipitated and their interaction was analyzed by Western Blotting.

## **Discussion**

In this analysis, we focused our attention on the Hsp90/Hsp70 chaperone machinery with the aim of increasing Hsp70 affinity for unfolded and damaged substrates, rather than to inhibit the stabilizing activity of Hsp90. Hsp90 and Hsp70 have opposite roles in this machinery, since Hsp90 inhibits protein ubiquitination while Hsp70 promotes the ubiquitination and subsequent degradation through the proteasome of the client proteins. Both inhibiting Hsp90 activity and promoting Hsp70 function might result in increased polyQ AR degradation.

Hsp90 regulates a wide variety of proteins in terms of function, trafficking, and turnover [81]. In some circumstances, a newly synthesized protein needs to be stabilized by Hsp90 and other co-chaperones designed to maintain the protein in its native conformation and to assist the protein folding. In this model, Hsp90 has a kind of “protective” role towards client proteins, both wild types and mutants, preventing their recognition by other chaperones like Hsp70 that trigger their ubiquitination and degradation through the proteasome. Even in the case of polyQ AR, Hsp90 stabilizes the mutant protein and prevents its degradation. Different studies support the evidence of positive effects of Hsp90 inhibitors, like radicicol or geldanamycin and the less toxic derivatives 17-AAG and 17-DMAG [100-102, 139], in promoting polyQ AR degradation through the proteasome. Moreover, many efforts have been made to reduce the hepatotoxicity caused by these compounds [140]. Nonetheless, the attempt to inhibit Hsp90 activity may affect different clients proteins and activate various intracellular pathways that may result in a stress response.

For this reason we propose to target Hsp70, instead of Hsp90, given that it preferentially recognizes and promotes the degradation of already misfolded or damaged substrates that Hsp90 was not able to fold correctly, without influencing the homeostasis of proteins in their native conformation. Previous studies demonstrated that the overexpression of Hsp70 reduces aggregate formation and suppress apoptosis in a cultured neuronal cell model of SBMA [93] and markedly ameliorates the motor function in a mouse model of SBMA [92], by enhanced polyQ AR degradation. Similarly, the Hsp70-interacting protein, Hip, cooperates with the chaperone Hsp70 in protein folding and prevention of aggregation. Hsp70 interacts with non-native protein substrates in an ATP-dependent reaction cycle and Hip is thought to delay substrate release by slowing ADP dissociation from Hsp70 [138]. In fact, Hip overexpression significantly reduces inclusion formation in both an in vitro model of SBMA and a primary neuronal model of polyglutamine disease [141] and, moreover, Hip stimulates the degradation of the polyQ AR by enhancing its ubiquitination in PC12 cells expressing AR112Q and rescues toxicity in a *Drosophila* model of SBMA [96]. These data strongly suggest that Hip may have a significant role in enhancing Hsp70 activity and for this reason, two small molecules that act similarly to Hip have been generated. The efficacy of YM-1 in promoting polyQ AR degradation has been recently demonstrated [96]. Here we tested a novel compound, named JG98, that is a derivative of YM-1 and has a common chemical structure (Table 1) but different side groups that enhance its in vivo bioavailability.

We first confirmed its efficacy in the proteasome-mediated clearance of the polyQ AR (Fig. 12 and 13). We also verified that JG98 enhances polyQ AR ubiquitination, similar to YM-1 and Hip, and thereby promotes its degradation (Fig. 14). This study demonstrates that JG98 has a mechanism of action similar to Hip and YM-1, thus favoring the ADP-bound state of

Hsp70 and then prolonging its interaction with the unfolded or damaged client proteins that need to be removed. Thus, JG98 prevents polyQ AR aggregation and facilitates its degradation through the UPS.

Hip displays broad anti-aggregation functions and has a critical function in preventing a wide range of protein misfolding pathologies. For example, Roodveldt and colleagues [142] demonstrated that Hip can prevent the co-aggregation of Hsp70 with alpha-synuclein resulting in an increase in available Hsp70 to carry out chaperone functions. Likewise, the small molecules YM-1 and JG98 might be effective in promoting the degradation of various disease-causative proteins, not only polyQ AR, by driving the Hsp90/Hsp70 cycling machinery towards the proteasome-mediated clearance of the mutant proteins.

Even though this analysis supplies evidence of the efficacy of this new compound and examines in depth its mechanism of action through polyQ AR ubiquitination and proteasomal degradation in a PC12 cellular model of SBMA, future studies are required to investigate the effect of JG98 in animal models of SBMA.

## **Chapter 4**

***Chronic exercise-induced muscle changes in  
AR113Q versus wild type mice.***

## ***Chronic exercise-induced muscle changes in AR113Q versus wild type mice.***

### **Introduction**

Several studies have reported benefits of exercise in learning and memory, protection from neurodegeneration, diminished age-related cognitive decline and alleviation of depression [143]. Focusing on neurodegeneration, exercise delays onset and reduces risk for Alzheimer disease (AD) [144, 145], Huntington's disease (HD) [146] and Parkinson's disease (PD) [147, 148] in clinical studies. Moreover, chronic exercise has been demonstrated to improve motor and cognitive function in the R6/1 mouse model of HD [149] and significantly extends the life span of Atxn1-154Q mouse model of spinocerebellar ataxia type I (SCA1), despite a lack of significant improvements in motor performance [150].

One of the central mechanisms in exercise-dependent beneficial effects is the regulation of growth factors. As a result, all the mechanisms that interfere with growth factor signaling, i.e. inflammation, might be modulated by exercise both in the periphery and in the central nervous system [143]. Several growth factors have been implicated in mediating the beneficial effects of exercise. For example, the levels of insulin-like growth factor- 1 (IGF-1) [151] and brain-derived neurotrophic factor (BDNF) [152], reduced by the presence of pro-inflammatory cytokines, are restored after exercise, while the pro-inflammatory cytokine IL-1 $\beta$  is reduced in the brain of a mouse model of AD following exercise [153]. It is likely that exercise improves growth factor signaling by both reducing pro-inflammatory conditions and directly increasing growth factors levels. Moreover, Fryer and colleagues [150] found

increased levels of the epidermal growth factor (EGF) in the brainstem of SCA1 mice that inversely correlates with the levels of the Ataxin-1 interactor Capicua. In addition to the regulation of growth factors, other mechanisms mediate the effects of exercise. In a clinical study, resistance training restores muscle sex steroid hormone levels in older subjects via enhancement of steroidogenesis-related enzymes and this results in increased IGF-1 gene expression and Akt signaling pathway [154, 155]. Moreover, aerobic exercise ameliorates the loss of skeletal muscle mitochondrial content [156] and strongly induces PPAR $\gamma$ -binding protein (PGC-1 $\alpha$ ) expression in human and rodent skeletal muscle. This, in turn, increases mitochondrial biogenesis and reverses sarcopenia but also has systemic benefits [157-159]. In addition, PGC-1 $\alpha$ , in part, is also required for the exercise training-induced anti-inflammatory effects since it reduces the levels of pro-inflammatory cytokines [160]. It is likely that many factors co-participate in exercise-related benefits and different aspects must be taken into account to have a wider and complete framework.

SBMA is characterized by muscle weakness and atrophy and recent papers elegantly established muscle as a site of mutant AR toxicity in the pathogenesis of the disease. These studies suggested that mutant protein expression in this tissue is a new target for treating the disorder [18, 19, 161]. Moreover, the overexpression of IGF-1 in muscle extends the life span and reduces both muscle and spinal cord pathology of SBMA mice through Akt signaling activation [21]. Skeletal muscle is the main engine of exercise and exercise is one of the most efficacious non-pharmacological interventions for the treatment of a wide variety of diseases. In this study we focused our attention on SBMA and exercise to analyze whether chronic exercise might be beneficial in our AR113Q knock-in mouse model, thus providing a better knowledge of exercise-dependent muscular changes in wild type and mutant mice.



## **Results**

### ***Six-weeks training improves mice performance.***

To determine the effect of exercise in SBMA mice, we enrolled wild-type (wt) mice and mutant androgen receptor (AR113Q) knock-in mice [9, 162]. A total of 18 AR113Q mice (10 mice in the exercised cohort and 8 mice in the control rest cohort) and 9 wt mice (5 exercised and 4 rest mice) were included in the study. Animals were randomly assigned to the exercise or rest cohorts.

The wt and mutant exercised mice cohorts followed a mild exercise regimen from 8 to 14 weeks of age. The mice were trained 5 days/week on a treadmill apparatus for 30 minutes at 10 meters/minute speed, whereas control mice were placed on the turned off apparatus for the same duration to control for confounding effects from environmental enrichment. All the wt mice completed the six-weeks training. In the case of mutant mice, only 7/10 mice in the exercised cohort (70%) and 6/8 mice in the rest cohort (75%) survived until the end of the study. This is consistent with previous analysis of lifespan in AR113Q mice. Given that the percentage of mutant mice that completed the study was similar in the rest and exercised cohorts, it seems that exercise does not increase the survival in our mouse models of SBMA.

Body weight and grip strength were monitored every other week during the training (Fig. 16A and B). During and at the end of the study (Fig. 16A, graph on the right), the exercised cohort showed a similar gain in body weight compared to the corresponding rest cohort, both in wt and mutant mice. Moreover, the measurements of grip strength in AR113Q mice did not significantly change during all the six weeks of training. In contrast, the exercised wt

mice showed a mild increase in grip strength at the end of the study (Fig. 16B, graph on the right).

At the end of the six-weeks training, the mice were exercised on the treadmill for two additional days prior. On the third day, mice were run at increasing speeds starting from 10 meters/minute until exhaustion and time and distance run were recorded (Fig. 16C and D). Both wt and AR113Q exercised mice were able to run longer compared to the corresponding rest cohorts. In addition, wt mice ran a greater distance compared to AR113Q mice, as expected.

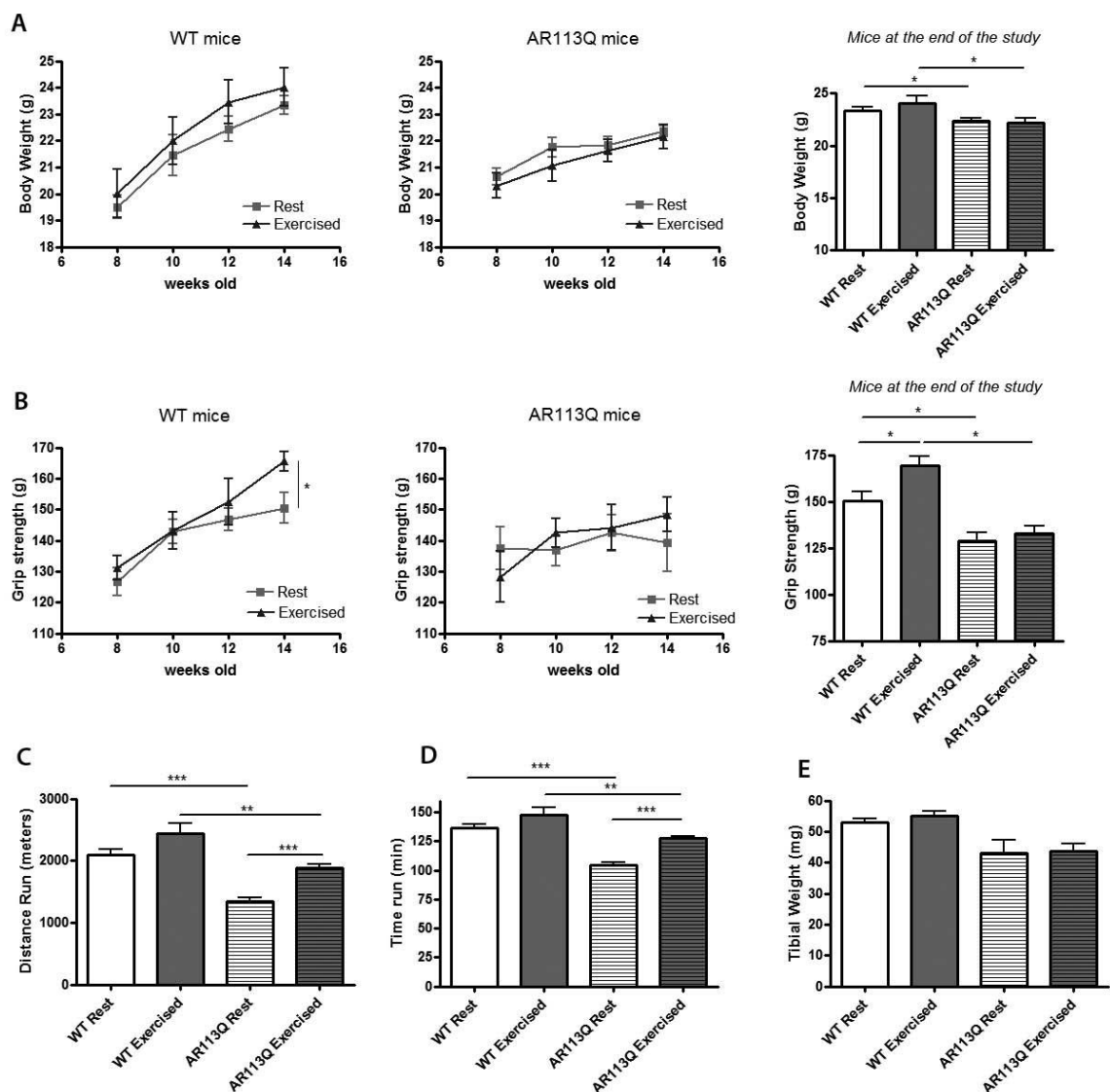
After two days of recovery following the exhaustion exercise, mice were sacrificed and tibialis anterior (TA) muscles were weighed. TA muscle weight higher in wt mice compared to AR113Q mice and these data reflect the muscle atrophy observed in the mutant mice [9]. No differences between rest and exercised mice in each group were noticed (Fig. 16E).

#### ***Muscle analysis in AR113Q and wt mice***

We next analyzed AR expression levels in the quadriceps muscles by immunoprecipitating (IP) AR113Q and noticed similar levels of the mutant protein in the two cohorts, thus indicating that exercise does not modulate AR protein levels (Fig. 17A). Likewise, immunofluorescence analysis performed on quadriceps muscles showed a comparable nuclear AR staining in the rest and exercised cohorts (Fig. 17B).

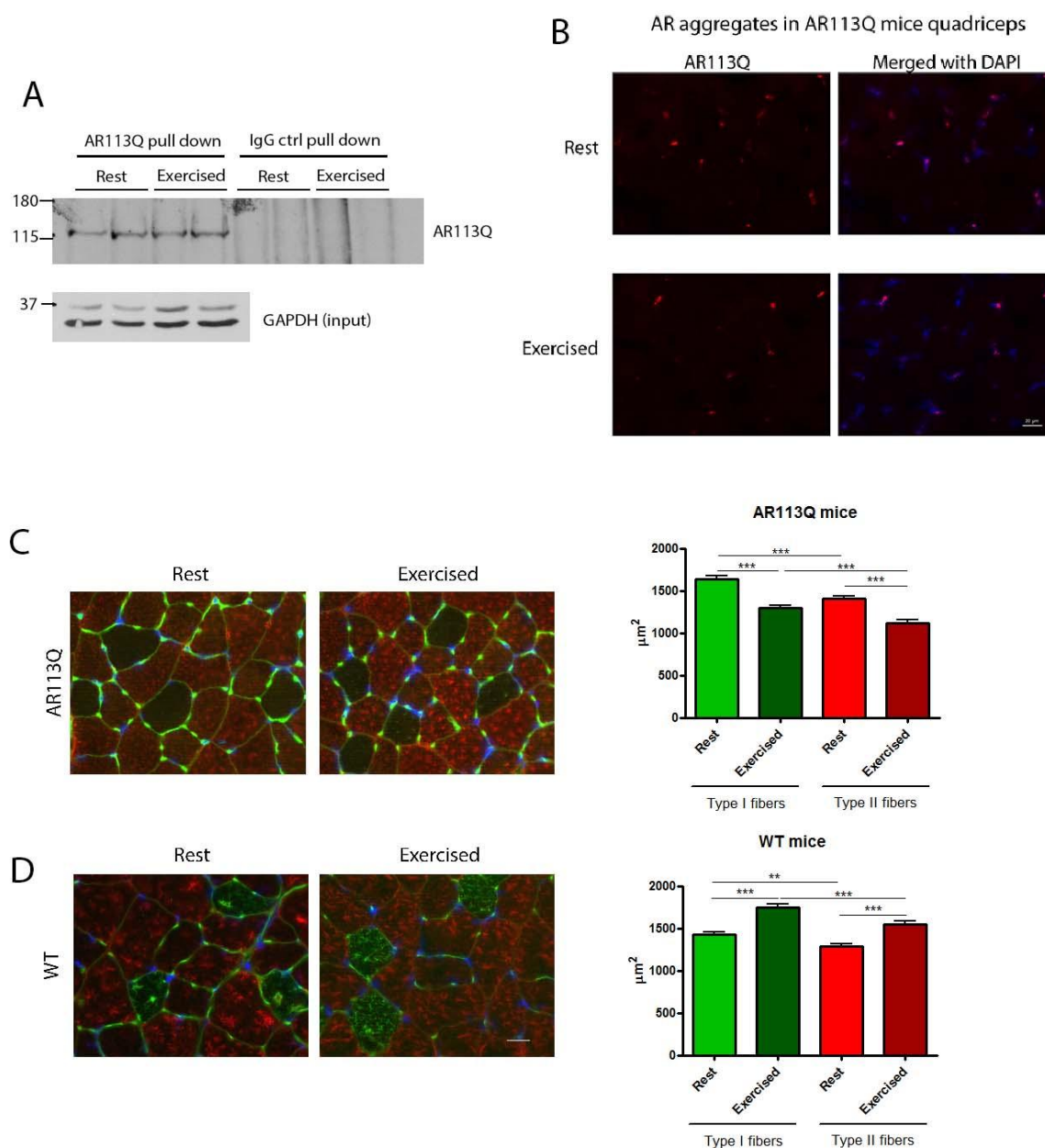
Given that AR protein levels did not change in quadriceps muscles, we sought to determine if exercise modulates other aspects of the muscle phenotype and therefore performed immunofluorescence analysis in soleus and gastrocnemius muscles. The soleus is considered

an oxidative muscle composed mainly of type I “slow” fibers, but also of type II “fast” fibers. We stained for both fiber types using antibodies against fiber type specific heavy chain myosins and for the basement membrane to label the outline of each fiber. As shown in Fig. 17C and relative quantifications of the sizes of the fibers, the average size of both type I and type II fibers is significantly reduced after exercise in AR113Q mice, providing unexpected data that needs further considerations. Therefore, we wondered if chronic exercise might induce similar effects in the soleus/gastrocnemius muscle of wt mice. We immunostained both type I and II fibers and measured fibers size. Surprisingly, fiber size in the exercised cohort of wt mice increased following chronic exercise, an opposite effect compared to that observed in the AR113Q mice (Fig. 17D and relative quantification).



**Figure 16**

Effects of chronic exercise on AR113Q and wild type mice. (A and B) Body weight (g) and grip strength (g) were measured every other week. No changes in body weight and grip strength were noticed in AR113Q whereas a significant increase in grip strength was detected in the exercised cohort of wt mice at the end of the study. Data are mean  $\pm$  SEM. \* $P < 0.05$  by ANOVA. (C, D) Six-weeks training improves running performances: distance run (C) and duration (D) of the exhausting exercise were recorded. Data are mean  $\pm$  SEM. \*\* $P < 0.01$ ; \*\*\* $P < 0.001$  by ANOVA. (E) Tibials weight measures (mg) in both groups revealed no changes after chronic exercise.

**Figure 17**

Muscle biochemical analysis following chronic exercise. (A) AR113Q protein was immunoprecipitated from quadriceps muscle of mutant mice and no changes in AR protein levels were observed between exercised and rest cohorts. (B) Immunofluorescence analysis performed on quadriceps to visualize AR aggregates nuclear accumulation (red). Nuclei were stained with DAPI. (C and D, left panels) Immunofluorescence analysis performed on soleus/gastrocnemius muscles: type I fibers and the basement membrane are in green, type II fibers are in red, nuclei were stained with DAPI. (C and D, right panels) Fibers area ( $\mu\text{m}^2$ ) was measured with ImageJ software. 25 fibers/mouse and 4 to 5 mice/group were analyzed. Data are mean  $\pm$  SEM. \*\*\* $P < 0.001$ .

## **Discussion**

Chronic exercise has a wide variety of effects, both in the periphery and in the central nervous system. Most of these effects are thought to be mediated by the reduction of inflammation, through the up-regulation of growth factors levels, and by the clearance of pro-inflammatory cytokines [151-153]. The mechanism of action through which exercise modulates various enzymatic cascades is still unclear and its complexity makes it difficult to describe completely. It seems that exercise has beneficial effects on many brain functions because it mobilizes growth factor cascades [143]: it restores IGF-1 and BDNF levels in inflammatory conditions [151, 152], and in a SCA1 mouse model a mild exercise regimen improved the survival and the levels of EGF in the brainstem [150]. Moreover, Chan and colleagues [157] recently reviewed the role of the transcriptional co-activator PGC-1 $\alpha$  as a key driver of metabolic programming in skeletal muscle and reported its up-regulation following exercise. PGC-1 $\alpha$  is strongly expressed in skeletal muscle, in particular "red" oxidative muscle like the soleus, and drives mitochondrial biogenesis [163]. Over-expression of PGC-1 $\alpha$  in transgenic mice protects from denervation atrophy, muscle dystrophy, aging-associated sarcopenia and other diseases (Reviewed in [157]).

Although many studies describe chronic exercise as beneficial by acting through the restoration of various pathways, it is even true that it might be detrimental in some pathological conditions. High-intensity endurance exercise training hastens a decrease in motor performance and death in an amyotrophic lateral sclerosis (ALS) mouse model [164]. In addition, exercise accelerates symptom onset in a mouse model of Huntington's disease (HD) suggesting that it might be detrimental to a vulnerable nervous system [165].

Given these considerations, we wondered if a mild exercise regimen might be beneficial in our AR113Q knock-in mouse model of SBMA. AR113Q mice are characterized by muscle atrophy [9], in part due to the reduced anabolic activity of the mutant receptor. Skeletal muscle has been recently proposed as an alternative contributor to disease pathogenesis next to motor neurons, and targeted reduction [18] or selective suppression [19] of mutant AR can ameliorate the functional defects in SBMA mice. We wondered whether exercise might have an anabolic effect on skeletal muscle by increasing IGF-1 levels to promote muscle hypertrophy through the activation of the phosphatidyl inositol 3-kinase (PI3K)/Akt pathway [166] and by restoring muscular sex steroid hormones levels [155].

Our results show that exercise does not exacerbate the disease phenotype, as observed in a mouse model of HD [165]. Moreover, exercise does not increase the survival of AR113Q mice, since the percentage of mutant mice that died during the training was similar in the rest and exercised cohorts. Although motor performance was greatly enhanced after six-weeks of exercise both in wt and mutant mice, only a slight improvement in grip strength measurements was observed in the wt exercised cohort at the end of the study (Fig. 16B). Biochemical analysis of AR113Q muscle tissues showed comparable levels of mutant androgen receptor in the rest and exercised cohorts (Fig. 17A and B). Unexpectedly, immunofluorescence analysis of soleus muscle revealed a reduction in the average size of both type I and II muscle fibers in exercised AR113Q mice, establishing that exercise does not counteract muscle atrophy in our mouse model of SBMA (Fig. 17C). While it is likely that the reduced size of type I/II fibers in soleus/gastrocnemius muscles is a negative consequence of exercise, it is also possible that it reflects a re-organization of muscle structure and a wider change in the expression of muscle-related genes. To begin to

distinguish between these possibilities, we examined type I/II fiber sizes in soleus/gastrocnemius muscles of wt mice (Fig. 17D). Surprisingly, fiber size in wt mice were significantly increased after the six-weeks training, an opposite situation compared to that observed with the mutant mice. These data suggest that chronic exercise might have anabolic and beneficial effects in non-pathological conditions but could be detrimental in the mutant mice. Future gene expression analysis will allow us to better understand the mechanisms involved in these muscle changes, both in wt and mutant mice, and to determine the extent to which fiber size reduction in AR113Q mice reflects their pathological condition.

It must be taken into account that our mice were trained on a treadmill for six weeks starting at 8 weeks of age and that we implemented a mild regimen of exercise. There is the possibility that a more intense and sustained exercise regimen with a longer daily duration and/or a longer total duration (more than six weeks) might be more effective. In any case, this study provides useful information about skeletal muscle responses to exercise in SBMA mice.



# Chapter 5

## *Conclusion*

## UPS and autophagy in SBMA

The link between UPS or autophagy and neurodegeneration has been extensively described: ubiquitinated substrates and UPS impairment have been shown in a variety of neurodegenerative disorders, including polyQ diseases [42, 135], but it is still debated if UPS impairment has a role in disease pathogenesis or is a consequence [167]. The involvement of autophagy in the initiation or progression of neurodegenerative diseases has also been proved with the observation that autophagic vacuoles accumulates in affected neurons [84, 168, 169]. Among neurodegenerative disorders, UPS and autophagy play a role also in SBMA pathogenesis. In fact, it has been extensively demonstrated that heat shock proteins (Hsps) overexpression increases UPS activity and ameliorates diseases phenotype in cellular and mouse models of SBMA [92, 93, 95, 96]. UPS-mediated polyQ AR degradation might be also enhanced by chemical Hsp90 inhibitors that facilitate client proteins dissociation from cytoplasmic chaperones and promote their degradation via the proteasome [99-102]. However, alternative evidence demonstrates that increased autophagic activity is beneficial in cellular models of SBMA since it facilitates cytoplasmic polyQ AR clearance and prevents nuclear accumulation [46, 105], whereas the role of autophagy in SBMA mice is still controversial [9, 109, 170], underlying the complexity of the autophagic pathway in the context of SBMA pathogenesis.

Both UPS and autophagy have an essential role in SBMA pathogenesis and therefore they might be a potential therapeutic target for the treatment of the disease.

### **Enhancing autophagic activity in SBMA.**

The nonsteroidal compound bicalutamide, a transcriptional antagonist of the androgen receptor (AR), is able to prevent ligand-dependent polyQ AR aggregation and toxicity in cellular models of SBMA by preventing the ability of AR to form an N/C interaction [51]. Secondly, the disaccharide trehalose, an mTOR-independent autophagy activator, has been shown to promote polyQ AR clearance [105], relieve the neurotoxicity of polyQ AR and rescue from ligand-dependent death in cellular models of SBMA [46].

Given that Bicalutamide and trehalose facilitate polyQ AR clearance with distinct mechanisms of action, we sought to determine whether the combined treatment might potentiate their individual effect. Biochemical analysis on cell lysates confirmed our hypothesis, showing a synergistic effect on polyQ AR removal mediated by the two compounds used together. We also proved the activation of the autophagic machinery by looking at two well-known autophagic markers, LC3-II and p62, that resulted increased after trehalose, but not bicalutamide, treatment.

Bicalutamide is widely used for the treatment of prostate cancer [171] and its good tolerability in patients makes it a valuable candidate for SBMA treatment. On the other hand, trehalose is a nontoxic and very well-tolerated disaccharide used as a natural preservative that has no restriction for oral intake. Therefore, the low toxicity and well tolerability of Bicalutamide and trehalose makes them potential candidates for SBMA therapy.

The analysis here reported have been conducted in cellular models of SBMA and further studies in animal models are required to verify the in vivo efficacy of the two compounds

used together. Bicalutamide has been extensively used in patients for the treatment of prostate cancer [171] whereas the beneficial effect of trehalose has been already demonstrated in animal models of other neurodegenerative diseases [122, 123]: in example, it has been recently shown that trehalose can reduce skeletal muscle denervation, protect mitochondria, and inhibit the proapoptotic pathway in a mouse model of ALS [127]. Moreover, the combined treatment with the antiandrogen bicalutamide and an autophagy activator, the mTOR inhibitor ridaforolimus, has been already proven effective in prostate cancer models [172], supporting our idea that bicalutamide and an autophagy enhancer, trehalose in our study, could act in combination.

#### **Promoting selective proteasomal degradation in SBMA.**

AR is known to be a client protein of the Hsp90/Hsp70 chaperone machinery and its stabilization or degradation is regulated by the interaction with Hsps. Therefore, targeting the chaperone machinery might be of therapeutic interest in SBMA. Two strategies can be pursued to promote clearance of the mutant AR: the inhibition of Hsp90 stabilizing activity or the enhancement of Hsp70 pro-degradative effect. The Hsp90 inhibitors geldanamycin [139] and the two less toxic derivatives 17-AAG [100, 101] and 17-DMAG [102], for example, are able to promote mutant AR degradation but, on the other hand, their effect is not specific and other client proteins might be degraded through the proteasome, thus causing a potential stress response. By contrast, Hsp70 binds only to already unfolded or damaged substrates without affecting the stability of proteins in their native conformation. The increase in Hsp70 activity mediated by the small molecule YM-1 results in enhanced mutant AR clearance and alleviation of SBMA phenotype in a *Drosophila* model [96] without

promoting the clearance of other client proteins. On the other hand, the extremely short half-life of the compound reduces its in vivo bioavailability.

Here we proposed a YM-1 derivative named JG98 with improved characteristic of in vivo bioavailability and we examined its efficacy in promoting mutant AR ubiquitination and UPS-mediated degradation in a cellular model of SBMA. Similarly to YM-1, JG98 binds to Hsp70 and stabilizes the chaperone in its active ADP-bound state, thus allowing increased interaction with unfolded proteins, such as mutant AR, and proteasomal degradation. YM-1 and JG98 mimic Hip protein activity: similarly to Hip, in fact, they bind and stabilize Hsp70, thus prolonging the interaction with the substrates. Therefore, similarly to Hip that was found able to favor the degradation of unfolded substrates, such as  $\alpha$ -synuclein [[142](#)], these compounds might be potentially therapeutic not only in SBMA but also in other degenerative diseases.

Moreover, the improved characteristic of in vivo bioavailability of JG98 will allow further studies in animal models of SBMA to verify the efficacy of the compound in a more complex biological system.

## **A non-pharmacological intervention: chronic exercise in SBMA.**

SBMA is a neuromuscular disorder characterized by muscle weakness and atrophy and many pharmacological interventions have been proposed to contrast muscle atrophy and counteract the disease. An example is leuprorelin, an analog of the gonadotropin-releasing hormone (GnRH) that reduces the release of testosterone in the anterior pituitary gland. Although beneficial effects of leuprorelin were found in patients, their quality of life worsened due to altered hormone levels [12, 173]. An alternative study did not show a significant effect of the 5 $\alpha$ -reductase inhibitor dutasteride on the progression of muscle weakness in SBMA [110]. The effectiveness of these pharmacological treatments can be limited and, moreover, side effects might not be well tolerated by patients.

Here we propose a potential non-pharmacological intervention for the treatment of SBMA: a mild regimen of chronic exercise. Wild type (wt) and mutant AR knock-in mice were trained on a treadmill for six weeks and then run to exhaustion. Our study showed that exercised mice run longer than the controls; however, no changes in body weight were observed whereas grip strength was increased only at the end of the study in the wt mice, but not in the mutants. Subsequent biochemical analysis on muscle samples revealed comparable levels of nuclear AR accumulation in the two groups. By contrast, both type I and type II fiber size resulted increased after exercise in wt mice and reduced in mutant mice, suggesting an abnormal response to exercise in the mutant mice. Future studies will point our attention on gene expression aimed to find possible muscle abnormalities that might explain the differences in fiber size. In fact, exercise has been described to modulate gene expression in several studies. It reduces inflammation by increasing the levels of growth factors and

reducing the amount of pro-inflammatory cytokines [[143](#), [150-152](#)], it stimulates steroidogenesis [[155](#)] and promotes the expression of mitochondrial-related genes like PGC-1 $\alpha$  in skeletal muscle [[157](#)]. Increased levels of IGF-1, also, has been shown to increase after exercise [[151](#)] and to have an anabolic effect on skeletal muscle [[174](#)]. Many genes might be modulated by exercise and we wonder whether exercise might differently modulate their levels in the muscles of wt and mutant mice. Future studies will examine the expression of these candidate mediators of beneficial or detrimental effects of exercise in wt and mutant mice.

# **Chapter 6**

## ***Materials and Methods***



## **Materials and Methods**

### **Compounds and chemicals**

The small molecules JG98 and YM-1 were kindly provided by J. Gestwicki (UCSF Medical Center, San Francisco, CA, USA). Chemicals, Lactacystin, MG-132, 3-MA and trehalose were from Sigma-Aldrich (St. Louis, MO, USA).

### **Plasmids**

The plasmids coding for AR.Q23 and AR.Q46, routinely used in our laboratory have been previously described [48]. The plasmid coding for the protein GFP-AR.Q48 was obtained by insertion of AR cDNA into the Green Fluorescent Protein (GFP) vector, expressing chimeric fluorescent fusion proteins.

The plasmids coding for human CHIP, HA-His-ubiquitin and 3xFLAG-Hip used in AR ubiquitination studies were kindly provided by Y. Osawa (University of Michigan Medical School, Ann Arbor, MI, USA). CHIP-myc-His plasmid expresses myc-tagged CHIP protein in CHIP/Hsp70 co-immunoprecipitation studies.

### **Cell cultures and transfections**

The immortalized motoneuronal cell line NSC34 [175, 176] is routinely used in our laboratory [48, 65, 100, 105, 129, 132, 177-180] and has been transfected with Lipofectamine (Life Technologies Corporation, Carlsbad, CA, USA)/transferrin (Sigma-Aldrich), as previously described [48, 65, 178], using 0.6 µg of plasmid DNA, 4 µl of transferrin solution and 2 µl of Lipofectamine.

Rat adrenal pheochromocytoma (PC12) cells stable transfected with the plasmid encoding AR.Q112 express AR under the control of a Tet-On promoter responsive to 1 µg/ml of doxycycline [produced (and kindly provided) by Professor D. Merry (TJU, Philadelphia, PA, USA)]. In the experiments involving steroid hormone treatments, the fetal bovine serum (FBS) was replaced with charcoal-stripped FBS and the horse serum (HS) with charcoal-stripped HS, to eliminate endogenous steroids [65, 177, 181]. PC12 cells has been transfected with plasmid DNA using Lipofectamine 2000 (Life Technologies).

The immortalized human HeLa cell line has been transiently transfected with CHIP-myc-His plasmid using Trans-IT LT1 transfection reagent (Mirus Bio LLC.).

### **Mouse studies**

Generation of knock-in mice with targeted AR allele containing 113 CAG repeats has been previously described [162, 182]. Mice were group housed in an SPF facility and provided with food and water *ad libitum*. Genotypes were confirmed by PCR of tail biopsy-derived DNA. AR knock-in mice were genotyped with forward primer 5'-CCAGAATCTGTTCCAGAGCGTG-3' and reverse primers 5'-TGTTCCCCTGGACTCAGATG-3' in a 1:1 ratio.

For exercise studies, a treadmill protocol was implemented as previously described [183]. Mice were trained 5 times/week 30 minutes/day on an Exer3/6 treadmill (Columbus Instruments) (Fig. 18) for six weeks from 8 to 14 weeks of age whereas control mice (rest group) were placed on the immobile apparatus for the same duration of time. At the end of the training, mice were acclimated to and trained on the treadmill for two days before the exhaustion exercise. On day 1, mice were run at 8 meters/minute for 5 minutes, and on day 2 mice were run at 8 meters/minute for 5 minutes then 10 meters/minute for 5 minutes.

Mice were run on day 3 for 40 minutes at 10 meters/min, then for 30 minutes with increasing speed 1 meter/minute every 10 minutes, and finally until exhaustion with increasing speed 1 meter/minute every 5 minutes. Mice were considered exhausted when they rested on the electric plate for at least 5 seconds without attempting to come back on the treadmill belt.

After two days of recovery, skeletal muscles were collected and flash frozen in liquid nitrogen for biochemical analysis or mounted in OCT compound and stored at -80°C for cryosectioning.



**Figure 18**

Pictures of an Exer3/6 treadmill apparatus (Columbus Instruments).

**mRNA expression analysis**

NSC34 cells were plated at 80000 cells/ml in six-well plates, transfected as described above and treated with 100 mM trehalose and/or 100 nM Bicalutamide and/or 10 nM testosterone for 48 h. Forty-eight hours after transfection, cells were harvested and centrifuged 5 min at 100 g at 4°C; the pellets were resuspended in 300 µl of TRI Reagent (Sigma-Aldrich) and RNA isolated according to manufacturer's instruction. RNA quantification was carried out by absorbance at 260 nm. Total RNA (1 µg) was treated with DNase (Sigma-Aldrich), and reverse transcribed into cDNA using the High-Capacity cDNA Archive Kit (Life Technologies Corporation) according to the manufacturer's protocol. Primers for real-time RT-PCR of the LC3-B, SQSTM1/p62 and GAPDH mRNAs were designed using the program Primer 3. The primers were synthesized by MWG Biotech (Ebersberg, Germany) with the following sequences: MAP-LC3b: 5' - CGT CCT GGA CAA GAC CA-3' (forward), 5' -CCA TTC ACC AGG AGG AA-3' (reverse); SQSTM1/p62: 5' -AGG GAA CAC AGC AAG CT-3' (forward), 5' -GCC AAA GTG TCC ATG TTT CA-3' (reverse); GAPDH: 5' -CCA GAA CAT CAT CCC TGC AT-3' (forward), 5' -CAG TGA GCT TCC CGT TCA-3' (reverse). The evaluated efficiency of each set of primers was close to 100% for both target and reference genes. Real-time PCR was performed using the CFX96 Real-Time System (Bio-Rad, Hercules, CA, USA) in a 10 µl total volume, using the iTaq SYBR Green Supermix (Bio-Rad), and with 500 nM primers. PCR cycling conditions were as follows: 94°C for 10 min, 40 cycles at 94°C for 15 s and 60°C for 1min. Melting curve analysis was performed at the end of each PCR assay as a control for specificity. Data were expressed as Ct values and used for the relative quantification of targets with the DDCT calculation. To exclude potential bias due to averaging data transformed through the equation  $2^{-DDCt}$  to give N-fold changes in gene expression, all

statistics were performed with D<sub>Ct</sub> values. Each experiment was carried out with four independent samples.

### ***Antibodies***

Primary antibodies used in Bicalutamide and trehalose co-treatment study (**Chapter 2**) were as follows: rabbit polyclonal AR-H280 to detect wt AR and polyQ AR; rabbit polyclonal anti-LC3 (Sigma-Aldrich) to detect LC3; rabbit polyclonal anti-SQSTM1/p62 (Abcam) to detect SQSTM1/p62; mouse monoclonal anti- $\alpha$ -tubulin (Sigma-Aldrich) to detect total  $\alpha$ -tubulin. Immunoreactivity was detected using the following secondary horseradish peroxidase-conjugated antibodies: goat anti-rabbit (Santa Cruz) was used to identify the anti-AR, the anti-LC3 and the anti-SQSTM1/p62 antibodies; goat anti-mouse (sc-2005, Santa Cruz) was used to identify the anti- $\alpha$ -tubulin antibody. Secondary antibodies used for IF studies were: Alexa 488 anti-rabbit and Alexa 594 anti-rabbit (Life Technologies).

Primary antibodies used in JG98 study (**Chapter 3**) for Western blotting and Filter Retardation analysis were against AR (N-20, Santa Cruz), HA (Covance), Hsp90 (Santa Cruz), Hsp70 (Enzo Life Sciences), Hsp40 (Enzo Life Sciences), Hsp25 (Enzo Life Sciences), AKT (Millipore), ERK 1/2 (Millipore), CHIP (Thermo Scientific), and GAPDH (Novus Biologicals). Primary antibodies for immunofluorescence were against AR (N-20, Santa Cruz). Horseradish peroxidase-conjugated secondary antibodies used for Western analysis were from Bio-Rad. AlexaFluor 594 conjugate secondary antibody used for immunofluorescence was from Invitrogen. For co-immunoprecipitation experiments, the anti-AR antibody PG-21 (Millipore) or the anti-myc antibody (Santa Cruz) were used, and pulldown was performed with Protein A-agarose beads or Protein A/G (Santa Cruz), respectively.

Primary antibodies used for IP analysis in the chronic exercise study (**Chapter 4**) were against AR (PG-21, Millipore) and GAPDH (Novus Biologicals). Primary antibodies for immunofluorescence were against AR (N-20, Santa Cruz), Type I/slow twitch heavy chain myosin (A4.840, DSHB, University of Iowa), and Type II/fast twitch heavy chain myosin (Ab-2, Thermo Scientific). Horseradish peroxidase-conjugated secondary antibodies used for Western analysis were from Bio-Rad. AlexaFluor 594, AlexaFluor 555, and wheat germ agglutinin AlexaFluor 488 conjugate antibodies used for immunofluorescence were from Invitrogen. FITC-conjugated donkey anti-mouse IgM was from Jackson ImmunoResearch.

#### ***Western blot (WB) analysis and Filter retardation Assay (FRA)***

In **Chapter 2**, NSC34 cells were plated in 12-well plates at 80000 cell/ml and transfected as previously described. For dose-dependent analysis, the cells were treated with 10 mM/100 mM/1 M trehalose. In the other experiments, the cells were treated with 100 mM trehalose and/or 100 nM Bicalutamide and/or 10 nM testosterone for 48 h. In experiments involving autophagy blockage, 10 mM 3-MA was added to the cells for the last 48 h. In experiments where proteasome was inhibited, the cells were treated with 10 mM MG132 for the last 16 h (overnight treatment). After 48 h, cells were harvested and centrifuged 5 min at 100 g at 4°C; the cell pellets were re-suspended in PBS (added of the protease inhibitors cocktail, Sigma-Aldrich) and homogenized using slight sonication as previously described [[181](#)]. Total proteins were determined with the bicinchoninic acid method (BCA assay, Euroclone).

PC12/AR112Q cells were plated in poly-D-lysine coated six-well plates at 2 mln cell/ml, induced with 1 µg/ml of doxycycline and treated with 100 mM trehalose and/or 100 nM Bicalutamide and/or 10 nM testosterone for 48 h. After 48 h, cells were harvested and

centrifuged 5 min at 100 g at 4°C; the cell pellets were re-suspended in RIPA buffer (added of the protease inhibitors cocktail, Sigma-Aldrich) and homogenized using slight sonication. The samples were centrifuged 15 min at 15 000 g at 4°C. The soluble fraction (supernatant) was separated from the insoluble one and the protein concentration was determined by the BCA assay. The pellet fraction was re-suspended in 20 µl of 4x sample buffer, and a relative amount was loaded into the gel, according to the protein assay on the soluble fraction.

WB was performed on 15% SDS–polyacrylamide gel electrophoresis loading 10–15 µg of total proteins. Samples were then electro-transferred to PVDF (polyscreen transfer membrane, PerkinElmer, Waltham, MA, USA) using a semi-dry transfer apparatus (Trans-Blotw Turbo™ Transfer System, Bio-Rad). The membranes were treated with a blocking solution containing 5% non-fat dried milk powder in Tris buffered saline with Tween for 1 h and then incubated with the primary antibodies.

FRA was performed by sample filtration through a 0.2 mm cellulose acetate membrane (Whatman, GE Healthcare) using a Bio-Dot SF Microfiltration Apparatus (Bio-Rad) and loading 9 µg (NSC34 cells) of the total proteins or 1.5 µg (PC12) of the supernatant fraction. Slot-blots were probed as described for WB to detect AR.Q46 or AR.Q112.

In **Chapter 3**, PC12/AR112Q cells were plated at 2 mln cell/ml in poly-D-lysine coated six-well plates, in the presence of 1 µg/ml doxycycline and 10 nM of the synthetic androgen R1881. In the 72 hrs experiment, doxycycline was washed out after 48 hrs of transgene expression and the cells were treated with 0.5 and 1 µM JG98 for the following 72 hrs. In the 48 hrs experiment and other western blotting (WB) analysis, cells were treated with the indicated amount of JG98 or 1 µM 17-AAG in the presence of doxycycline and R1881 for 48 hrs. 10 µM

Lactacystin (Sigma-Aldrich) was added for the last 16 hrs to inhibit proteasome activity. Cells were later harvested and centrifuged 5 min at 100 g at 4°C; the cell pellets were re-suspended in RIPA buffer (plus protease inhibitors cocktail, Roche) and sonicated. Samples were then centrifuged 15 min at 15000 g at 4°C to separate pellet and soluble fraction (supernatant). The pellet was re-suspended in 6X SDS sample buffer and loaded into the gel according to the BCA protein assay performed on the supernatant.

20 µg of protein lysates were resolved on 7.5% SDS–polyacrylamide gel electrophoresis and electro-transferred to a nitrocellulose membrane (Bio-Rad) using a semi-dry transfer apparatus (Trans-Blot® SD Semi Dry Transfer Cell, Bio-Rad).

To perform FRA analysis, PC12 cells were harvested, centrifuged 5 min at 100 g at 4°C and pellets were re-suspended in PBS. After slight sonication, protein concentration was determined by the BCA assay and then FRA was performed by sample filtration through a 0.2 µm cellulose acetate membrane (Whatman, GE Healthcare) using a Bio-Dot Apparatus (Bethesda Research Laboratories) and loading 5 µg of the total proteins. Slot-blots were probed as described for WB to detect AR112Q.

The immunoreactive regions were then visualized using the enhanced chemiluminescence detection kit reagents (ECL prime Western Blotting Substrate, GE Healthcare, Maidstone, UK). Optical intensity of samples assayed with WB or FRA was detected and analyzed using the Image Lab software (Bio-Rad).



***Co-immunoprecipitation (co-IP) studies***

For analysis of ubiquitination in **Chapter 3**, PC12 cells expressing AR112Q were plated at 2 mln cells/well in poly-D-lysine coated six-well plates (BD Falcon) and transiently transfected with plasmids encoding hCHIP (0.7 µg), HA-His-Ubiquitin (2.1 µg), 3xFLAG-Hip (1 µg) and CHIP-myc-His (3 µg) using Lipofectamine 2000 (Life Technologies). Cells were treated with 0.5 µg/ml doxycycline and 10nM R1881, and then with 0.5 µM or 1 µM YM-1 (last 24 hrs) and 10 µM MG132 to block the proteasome activity (last 16 hrs).

HeLa cells were plated at 400000 cells/well in six-well plates (BD Falcon), transiently transfected with 3 µg of human CHIP-myc-His plasmid and treated with 0.5 µM or 1 µM YM-1 for the last 24 hrs.

48 hrs after transfection, cell pellets were re-suspended in IP lysis/wash buffer (0.025M Tris, 0.15M NaCl, 0.001M EDTA, 1% NP-40, 5% glycerol; pH 7.4) containing 1 tablet/10ml of cOmplete mini protease inhibitor mix (Roche) and 5mM N-ethylmaleimide (Sigma-Aldrich). Samples were sonicated and centrifuged at 13000 x g for 10 minutes at 4°C. 400 µg of supernatant were incubated on a rotator for 2 hrs at 4°C with 2 µg of anti-AR or anti-myc antibody or the non-immune rabbit or mouse IgG. 20 µl of pre-washed protein A-agarose beads (Santa Cruz) was added and samples were incubated for 1 additional hour at 4°C. Protein-antibody-bead complexes were washed six times in IP lysis/wash buffer in filtered spin columns (Thermo Scientific), and proteins were eluted by boiling in SDS loading buffer for 5 minutes at 100°C.

**AR protein expression analysis in muscle tissues**

After collection, skeletal muscles were flash frozen in liquid nitrogen. At the time of the analysis, muscle tissues were re-suspended in RIPA buffer, minced with scissors and homogenized. Samples were then pre-cleared by centrifugation at 13,000 g for 10 minutes at +4°C and protein assay was performed on the supernatant fraction. For immunoprecipitation (IP) studies of AR, 500 µg of supernatant were incubated on a rotator over night at 4°C with 2 µg of anti-AR antibody or the non-immune rabbit or mouse IgG. 20 µl of pre-washed protein A-agarose beads (Santa Cruz) were added and samples were incubated for 1 additional hour at 4°C. Protein-antibody-bead complexes were washed six times RIPA buffer in filtered spin columns (Thermo Scientific), and proteins were eluted by boiling in SDS loading buffer for 5 minutes at 100°C. Samples were resolved on 7.5% SDS–polyacrylamide gel electrophoresis and electro-transferred to a nitrocellulose membrane (Bio-Rad) using a semi-dry transfer apparatus (Trans-Blot® SD Semi Dry Transfer Cell, Bio-Rad).

**Fluorescence, Immunofluorescence (IF) and Microscopy.**

In **Chapter 2**, NSC34 cells were plated in 12-well multiwell plates containing coverslips at 70000 cells/ml density, transiently transfected with the plasmid coding for GFP-ARQ48, as previously described, and treated with 100 mM trehalose and/or 100 nM Bicalutamide and/or 10 nM testosterone for 48 h. The cells were then fixed and processed as previously described [179]. Cells were probed with the indicated primary and fluorescent secondary antibodies and stained with DAPI to visualize the nuclei. An Axiovert 200 microscope (Zeiss Instr., Oberkochen, Germany) equipped with FITC/TRITC/DAPI and combined with a

Photometric Cool-Snap CCD camera (Ropper Scientific, Trenton, NJ, USA) was used. Images were processed using the Metamorph software (Universal Imaging, Downingtown, PA, USA).

In **Chapter 3**, PC12 cells were washed in PBS and fixed in 4% paraformaldehyde for 30 minutes at room temperature. Cells were incubated with blocking solution (5% donkey serum in PBS-T (Tween 0.1% in PBS)) 1 h at 37°C, then stained with the indicated primary antibody for 1 h at RT and the fluorescence secondary antibody for 30 min at 37°C, in 1.5% donkey serum in PBS-T. Slides were mounted using Vectashield medium plus DAPI for nuclei staining (Vector Laboratories), and sealed with nail polish.

In **Chapter 4**, quadriceps and soleus/gastrocnemius muscles were mounted in cryosection blocks with OCT Compound (Tissue-Tek) and stored at -80°C. Cryosections were then prepared using a Cryocut 1800 cryostat (Leica) at 10µm. Staining was performed using the indicated antibodies, mounted using Vectashield medium (Vector Laboratories), and sealed with nail polish. To distinguish between Type I and Type II fibers, FITC-conjugated donkey anti-mouse IgM was used against A4.840, and AlexaFluor 555 anti-mouse IgG was used against Ab-2. AlexaFluor 594 anti-rabbit IgG was used against ARN20. Fluorescence images were acquired using a Zeiss Axio Imager microscope. To calculate fiber type size, the cross-sectional area of each fiber within a 40X field was quantified using ImageJ, and fiber type was discriminated by antibody stain.

### ***Statistical analysis***

Statistical analysis has been performed using one-tailed Student's t-test for two groups comparisons and one- or two-way ANOVA for three or more group comparisons using the PRISM software (GraphPad Software, La Jolla, CA, USA).

## References

1. Kennedy, W., M. Alter, and J. Sung, *Progressive proximal spinal and bulbar muscular atrophy of late onset. A sex-linked recessive trait*. Neurology, 1968. **18**(7): p. 671-680.
2. La Spada, A.R., et al., *Androgen receptor gene mutations in X-linked spinal and bulbar muscular atrophy*. Nature, 1991. **352**(6330): p. 77-79.
3. Giorgetti, E., et al., *Synergic prodegradative activity of Bicalutamide and trehalose on the mutant androgen receptor responsible for spinal and bulbar muscular atrophy*. Hum Mol Genet. , 2014.
4. Orr, H.T. and H.Y. Zoghbi, *Trinucleotide Repeat Disorders*. Annual Review of Neuroscience, 2007. **30**: p. 575-621.
5. Kawahara, H., *A family of progressive bulbar palsy*. Aichi Medical School Journal, 1897. **16**: p. 3-4.
6. Schmidt, B.J., et al., *Expression of X-linked bulbospinal muscular atrophy (Kennedy disease) in two homozygous women*. Neurology, 2002. **59**(5): p. 770-772.
7. Katsuno, M., et al., *Testosterone reduction prevents phenotypic expression in a transgenic mouse model of spinal and bulbar muscular atrophy*. Neuron, 2002. **35**(5): p. 843-854.
8. Chevalier-Larsen, E.S., et al., *Castration restores function and neurofilament alterations of aged symptomatic males in a transgenic mouse model of spinal and bulbar muscular atrophy*. J Neurosci. , 2004. **24**(20): p. 4778-4786.
9. Yu, Z., et al., *Androgen-dependent pathology demonstrates myopathic contribution to the Kennedy disease phenotype in a mouse knock-in model*. J Clin Invest. , 2006. **116**(10): p. 2663-2672.
10. Harding, A.E., et al., *X-linked recessive bulbospinal neuronopathy: a report of ten cases*. J Neurol Neurosurg Psychiatry., 1982. **45**(11): p. 1012-9.
11. Sobue, G., et al., *X-linked recessive bulbospinal neuronopathy. A clinicopathological study*. Brain, 1989. **112**: p. 209-32.
12. Katsuno, M., et al., *Clinical features and molecular mechanisms of spinal and bulbar muscular atrophy (SBMA)*. Adv Exp Med Biol., 2010. **685**: p. 64-74.
13. Roselli, C., R. Handa, and J. Resko, *Quantitative distribution of nuclear androgen receptors in microdissected areas of the rat brain*. Neuroendocrinology, 1989. **49**(5): p. 449-53.
14. Simerly, R.B., et al., *Distribution of androgen and estrogen receptor mRNA-containing cells in the rat brain: an in situ hybridization study*. J Comp Neurol. , 1990. **294**(1): p. 76-95.
15. Rocchi, A. and M. Pennuto, *New Routes to Therapy for Spinal and Bulbar Muscular Atrophy*. Journal of Molecular Neuroscience, 2013. **50**(3): p. 514-523.
16. Nagashima, T., et al., *Familial bulbo-spinal muscular atrophy associated with testicular atrophy and sensory neuropathy (Kennedy-Alter-Sung syndrome). Autopsy case report of two brothers*. J Neurol Sci., 1988. **87**(2-3): p. 141-152.
17. Battaglia, F., et al., *Kennedy's Disease Initially Manifesting as an Endocrine Disorder*. J Clin Neuromuscul Dis. , 2003. **4**(4): p. 165-167.
18. Lieberman, A.P., et al., *Peripheral Androgen Receptor Gene Suppression Rescues Disease in Mouse Models of Spinal and Bulbar Muscular Atrophy*. Cell Reports, 2014. **7**(3): p. 774-784.
19. Cortes, C.J., et al., *Muscle Expression of Mutant Androgen Receptor Accounts for Systemic and Motor Neuron Disease Phenotypes in Spinal and Bulbar Muscular Atrophy*. Neuron, 2014. **82**(2): p. 295-307.
20. Sorarù, G., et al., *Spinal and bulbar muscular atrophy: skeletal muscle pathology in male patients and heterozygous females*. J Neurol Sci. , 2008. **264**(1-2): p. 100-105.
21. Palazzolo, I., et al., *Overexpression of IGF-1 in Muscle Attenuates Disease in a Mouse Model of Spinal and Bulbar Muscular Atrophy*. Neuron, 2009. **63**(3): p. 316-328.

22. Rinaldi, C., et al., *Insulinlike Growth Factor (IGF)-1 Administration Ameliorates Disease Manifestations in a Mouse Model of Spinal and Bulbar Muscular Atrophy*. Mol Med. , 2012. **18**(1): p. 1261-1268.
23. Mariotti, C., et al., *Phenotypic manifestations associated with CAG-repeat expansion in the androgen receptor gene in male patients and heterozygous females: a clinical and molecular study of 30 families*. Neuromuscul Disord., 2000. **10**(6): p. 391-397.
24. Lee, J.-H., et al., *Phenotypic variability in Kennedy's disease: implication of the early diagnostic features*. Acta Neurologica Scandinavica, 2005. **112**(1): p. 57-63.
25. Monks, D.A., et al., *Overexpression of wild-type androgen receptor in muscle recapitulates polyglutamine disease*. Proc Natl Acad Sci U S A. , 2007. **104**(46): p. 18259-64.
26. Funakoshi, H., et al., *Differential expression of mRNAs for neurotrophins and their receptors after axotomy of the sciatic nerve*. J Cell Biol. , 1993. **123**(2): p. 455-65.
27. Fischbeck, K., et al., *Localization of the gene for X-linked spinal muscular atrophy*. Neurology, 1986. **36**(12): p. 1595-8.
28. Chang, C., et al., *Androgen receptor: an overview*. Crit Rev Eukaryot Gene Expr., 1995. **5**(2): p. 97-125.
29. Rechsteiner, M. and S.W. Rogers, *PEST sequences and regulation by proteolysis*. Trends Biochem Sci., 1996. **21**(6): p. 267-71.
30. Katsuno, M., et al., *Pathogenesis and therapy of spinal and bulbar muscular atrophy (SBMA)*. Prog Neurobiol. , 2012. **99**(3): p. 246-256.
31. Parodi, S. and M. Pennuto, *Neurotoxic effects of androgens in spinal and bulbar muscular atrophy*. Front Neuroendocrinol., 2011. **32**(4): p. 416-25.
32. Clark, P., R. Irvine, and G. Coetzee, *The androgen receptor CAG repeat and prostate cancer risk*. Methods Mol Med., 2003. **81**: p. 255-66.
33. Davis-Dao, C., et al., *Shorter androgen receptor CAG repeat lengths associated with cryptorchidism risk among Hispanic white boys*. J Clin Endocrinol Metab. , 2012. **97**(3): p. E393-9.
34. Palazzolo, I., et al., *The role of the polyglutamine tract in androgen receptor*. J Steroid Biochem Mol Biol. , 2008. **108**(3-5): p. 245-53.
35. Kratter, I.H. and S. Finkbeiner, *PolyQ disease: too many Qs, too much function?* Neuron, 2010. **67**(6): p. 897-899.
36. Poletti, A., *The polyglutamine tract of androgen receptor: from functions to dysfunctions in motor neurons*. Front. Neuroendocrinol, 2004. **25**: p. 1-26.
37. Wyttenbach, A., *Role of heat shock proteins during polyglutamine neurodegeneration*. Journal of Molecular Neuroscience, 2004. **23**(1-2): p. 69-95.
38. Jochum, T., et al., *Toxic and non-toxic aggregates from the SBMA and normal forms of androgen receptor have distinct oligomeric structures*. Biochim Biophys Acta. , 2012. **1822**(6): p. 1070-1078.
39. Taylor, J.P., et al., *Aggresomes protect cells by enhancing the degradation of toxic polyglutamine-containing protein*. Hum Mol Genet., 2003. **12**(7): p. 749-757.
40. Muchowski, P.J. and J.L. Wacker, *Modulation of neurodegeneration by molecular chaperones*. Nat Rev Neurosci. , 2005. **6**(1): p. 11-22.
41. Li, M., et al., *Nonneural nuclear inclusions of androgen receptor protein in spinal and bulbar muscular atrophy*. The American Journal of Pathology, 1998. **153**(3): p. 695-701.
42. Rusmini, P., et al., *Aggregation and proteasome: The case of elongated polyglutamine aggregation in spinal and bulbar muscular atrophy*. Neurobiol Aging., 2007. **28**(7): p. 1099-1111.
43. Miller, J., et al., *Identifying polyglutamine protein species in situ that best predict neurodegeneration*. Nat Chem Biol., 2011. **7**(12): p. 925-934.
44. Adachi, H., et al., *Widespread nuclear and cytoplasmic accumulation of mutant androgen receptor in SBMA patients*. Brain, 2005. **128**(3): p. 659-70.
45. Suzuki, K., et al., *CAG repeat size correlates to electrophysiological motor and sensory phenotypes in SBMA*. Brain, 2008. **131**(1): p. 229-39.

46. Montie, H.L., et al., *Cytoplasmic retention of polyglutamine-expanded androgen receptor ameliorates disease via autophagy in a mouse model of spinal and bulbar muscular atrophy*. Human Molecular Genetics, 2009. **18**(11).
47. Takeyama, K.-i., et al., *Androgen-dependent neurodegeneration by polyglutamine-expanded human androgen receptor in Drosophila*. Neuron, 2002. **35**(5): p. 855-64.
48. Simeoni, S., et al., *Motoneuronal cell death is not correlated with aggregate formation of androgen receptors containing an elongated polyglutamine tract*. Hum. Mol. Genet. , 2000. **9**(1): p. 133-144.
49. Sambataro, F. and M. Pennuto, *Cell-autonomous and non-cell-autonomous toxicity in polyglutamine diseases*. Prog Neurobiol. , 2012. **97**(2): p. 152-72.
50. Nedelsky, N.B., et al., *Native functions of the androgen receptor are essential to pathogenesis in a Drosophila model of spinobulbar muscular atrophy*. Neuron, 2010. **67**(6): p. 936-52.
51. Orr, C.R., et al., *An interdomain interaction of the androgen receptor is required for its aggregation and toxicity in spinal and bulbar muscular atrophy*. J Biol Chem., 2010. **285**(46): p. 35567-77.
52. Lieberman, A.P., et al., *Altered transcriptional regulation in cells expressing the expanded polyglutamine androgen receptor*. Hum. Mol. Genet., 2002. **11**(17): p. 1967-1976.
53. Palazzolo, I., et al., *Akt blocks ligand binding and protects against expanded polyglutamine androgen receptor toxicity*. Hum Mol Genet. , 2007. **16**(13): p. 1593-603.
54. LaFevre-Bernt, M.A. and L.M. Ellerby, *Kennedy's disease. Phosphorylation of the polyglutamine-expanded form of androgen receptor regulates its cleavage by caspase-3 and enhances cell death*. J Biol Chem. , 2003. **278**(37): p. 34918-34924.
55. Montie, H.L., R.G. Pestell, and D.E. Merry, *SIRT1 Modulates Aggregation and Toxicity through Deacetylation of the Androgen Receptor in Cell Models of SBMA*. Neurobiology of Disease, 2011. **31**(48): p. 17425–17436.
56. Thomas, M., et al., *Androgen receptor acetylation site mutations cause trafficking defects, misfolding, and aggregation similar to expanded glutamine tracts*. J Biol Chem., 2004. **279**(9): p. 8389-95.
57. Mukherjee, S., et al., *Small ubiquitin-like modifier (SUMO) modification of the androgen receptor attenuates polyglutamine-mediated aggregation*. J Biol Chem., 2009. **284**(32): p. 21296-306.
58. Chua, J.P., et al., *Disrupting SUMOylation potentiates transactivation function and ameliorates polyglutamine AR-mediated disease*. J clin Invest., 2014.
59. Katsuno, M., et al., *Pharmacological induction of heat-shock proteins alleviates polyglutamine-mediated motor neuron disease*. PNAS, 2005. **102**(46): p. 16801–16806.
60. Hay, D.G., et al., *Progressive decrease in chaperone protein levels in a mouse model of Huntington's disease and induction of stress proteins as a therapeutic approach*. Hum Mol Genet. , 2004. **13**(13): p. 1389-405.
61. McCampbell, A., et al., *CREB-binding protein sequestration by expanded polyglutamine*. hum. Mol. Genet., 2000. **9**(4): p. 2197-2202.
62. Sopher, B., et al., *Androgen receptor YAC transgenic mice recapitulate SBMA motor neuronopathy and implicate VEGF164 in the motor neuron degeneration*. Neuron, 2004. **41**(5): p. 687-99.
63. Katsuno, M., et al., *Disrupted transforming growth factor-beta signaling in spinal and bulbar muscular atrophy*. J Neurosci., 2010. **30**(16): p. 5702-12.
64. Morfini, G., et al., *JNK mediates pathogenic effects of polyglutamine-expanded androgen receptor on fast axonal transport*. Nat Neurosci., 2006. **9**(7): p. 907-916.
65. Piccioni, F., et al., *Androgen receptor with elongated polyglutamine tract forms aggregates that alter axonal trafficking and mitochondrial distribution in motor neuronal processes*. The FASEB Journal, 2002.
66. Szebenyi, G., et al., *Neuropathogenic forms of huntingtin and androgen receptor inhibit fast axonal transport*. Neuron, 2003. **40**(1).
67. Katsuno, M., et al., *Reversible disruption of dynactin 1-mediated retrograde axonal transport in polyglutamine-induced motor neuron degeneration*. J Neurosci. , 2006. **26**(47): p. 12106-17.

68. Kemp, M.Q., et al., *Impaired motoneuronal retrograde transport in two models of SBMA implicates two sites of androgen action*. Hum Mol Genet., 2011. **20**(22): p. 4475-90.
69. Young, J.E., et al., *Polyglutamine-expanded androgen receptor truncation fragments activate a Bax-dependent apoptotic cascade mediated by DP5/Hrk*. J Neurosci., 2009. **29**(7): p. 1987-97.
70. Ranganathan, S., et al., *Mitochondrial abnormalities in spinal and bulbar muscular atrophy*. Hum Mol Genet., 2009. **18**(1): p. 27-42.
71. Pickart, C., *Back to the future with ubiquitin*. Cell, 2004. **116**(2): p. 181-90.
72. Hershko, A. and A. Ciechanover, *The ubiquitin system*. Annu Rev Biochem., 1998. **67**: p. 425-79.
73. Ciechanover, A., *Intracellular protein degradation: From a vague idea through the lysosome and the ubiquitin-proteasome system and onto human diseases and drug targeting*. Bioorganic & Medicinal Chemistry, 2013. **21**(12): p. 3400-3410.
74. Lin, H.K., et al., *Phosphorylation-dependent ubiquitylation and degradation of androgen receptor by Akt require Mdm2 E3 ligase*. The EMBO Journal, 2002. **21**(15): p. 4037-4048.
75. Chymkowitch, P., et al., *The phosphorylation of the androgen receptor by TFIIH directs the ubiquitin/proteasome process*. The EMBO Journal, 2011. **30**(3): p. 468-479.
76. Xu, K., et al., *Regulation of androgen receptor transcriptional activity and specificity by RNF6-induced ubiquitination*. Cancer Cell, 2009. **15**(4): p. 270-282.
77. Gottlieb, B., et al., *The androgen receptor gene mutations database: 2012 update*. Human Mutation, 2012. **33**(5): p. 887-894.
78. Ciechanover, A. and A. Stanhill, *The complexity of recognition of ubiquitinated substrates by the 26S proteasome*. Biochimica et Biophysica Acta (BBA) - Molecular Cell Research, 2014. **1843**(1): p. 86-96.
79. Pratt, W.B., et al., *Proposal for a role of the Hsp90/Hsp70-based chaperone machinery in making triage decisions when proteins undergo oxidative and toxic damage*. Exp Biol Med (Maywood), 2010.
80. Pratt, W.B., Y. Morishima, and Y. Osawa, *The Hsp90 chaperone machinery regulates signaling by modulating ligand binding clefts*. J Biol Chem., 2008. **283**(34): p. 22885-9.
81. Pratt, W.B. and D.O. Toft, *Regulation of Signaling Protein Function and Trafficking by the hsp90/hsp70-Based Chaperone Machinery*. Exp Biol Med (Maywood), 2003.
82. Pratt, W.B., et al., *A model in which heat shock protein 90 targets protein-folding clefts: Rationale for a new approach to neuroprotective treatment of protein folding diseases*. Experimental Biology and Medicine, 2014: p. 1-9.
83. Klionsky, D., *Autophagy revisited: a conversation with Christian de Duve*. Autophagy, 2008. **4**(6).
84. McCray, B.A. and J.P. Taylor, *The Role of Autophagy in Age-Related Neurodegeneration*. Neurosignals., 2008. **16**(1): p. 75-84.
85. Shaid, S., et al., *Ubiquitination and selective autophagy*. Cell Death Differ., 2013. **20**(1): p. 21-30.
86. Kabeya, Y., et al., *LC3, a mammalian homologue of yeast Apg8p, is localized in autophagosome membranes after processing*. EMBO J., 2000. **19**(21): p. 5720-8.
87. DJ Klionsky, et al., *Guidelines for the use and interpretation of assays for monitoring autophagy*. Autophagy, 2012. **8**(4): p. 445-544.
88. Lippai, M. and P. Lőw, *The role of the selective adaptor p62 and ubiquitin-like proteins in autophagy*. Biomed Res Int., 2014.
89. Petiot, A., et al., *Distinct classes of phosphatidylinositol 3'-kinases are involved in signaling pathways that control macroautophagy in HT-29 cells*. J Biol Chem., 2000. **275**(2): p. 992-8.
90. Tan, J.M.M., et al., *Lysine 63-linked ubiquitination promotes the formation and autophagic clearance of protein inclusions associated with neurodegenerative diseases*. Hum Mol Genet., 2008. **17**(3): p. 431-9.
91. Komander, D., et al., *Molecular discrimination of structurally equivalent Lys 63-linked and linear polyubiquitin chains*. EMBO Rep., 2009. **10**(5): p. 466-473.

92. Adachi, H., et al., *Heat shock protein 70 chaperone overexpression ameliorates phenotypes of the spinal and bulbar muscular atrophy transgenic mouse model by reducing nuclear-localized mutant androgen receptor protein*. J Neurosci, 2003. **23**(6).
93. Kobayashi, Y., et al., *Chaperones Hsp70 and Hsp40 suppress aggregate formation and apoptosis in cultured neuronal cells expressing truncated androgen receptor protein with expanded polyglutamine tract*. J Biol Chem., 2000. **275**: p. 8772-8778.
94. Bailey, C.K., et al., *Molecular chaperones enhance the degradation of expanded polyglutamine repeat androgen receptor in a cellular model of spinal and bulbar muscular atrophy*. Hum Mol Genet., 2002. **11**(2): p. 515-523.
95. Ishihara, K., et al., *Hsp105alpha suppresses the aggregation of truncated androgen receptor with expanded CAG repeats and cell toxicity*. J Biol Chem. , 2003. **278**(27): p. 25143-50.
96. Wang, A.M., et al., *Activation of Hsp70 reduces neurotoxicity by promoting polyglutamine protein degradation*. NATURE CHEMICAL BIOLOGY, 2013. **9**: p. 112-118.
97. Morishima, Y., et al., *CHIP deletion reveals functional redundancy of E3 ligases in promoting degradation of both signaling proteins and expanded glutamine proteins*. Hum. Mol. Genet., 2008. **17**(24): p. 3942-3952.
98. Adachi, H., et al., *CHIP overexpression reduces mutant androgen receptor protein and ameliorates phenotypes of the spinal and bulbar muscular atrophy transgenic mouse model*. Neurobiology of Disease, 2007. **27**(19): p. 5115-5126.
99. Thomas, M., et al., *Pharmacologic and genetic inhibition of hsp90-dependent trafficking reduces aggregation and promotes degradation of the expanded glutamine androgen receptor without stress protein induction*. Hum Mol Genet. , 2006. **15**(11): p. 1876-83.
100. Rusmini, P., et al., *17-AAG increases autophagic removal of mutant androgen receptor in spinal and bulbar muscular atrophy*. Neurobiology of Disease, 2011. **41**(1): p. 83–95.
101. Waza, M., et al., *17-AAG, an Hsp90 inhibitor, ameliorates polyglutamine-mediated motor neuron degeneration*. Nature Medicine, 2005. **11**: p. 1088-1095.
102. Tokui, K., et al., *17-DMAG ameliorates polyglutamine-mediated motor neuron degeneration through well-preserved proteasome function in an SBMA model mouse*. Hum. Mol. Genet., 2009. **18**(5): p. 898-910.
103. Pandey, U.B., et al., *HDAC6 rescues neurodegeneration and provides an essential link between autophagy and the UPS*. Nature, 2007. **447**(7146): p. 859-63.
104. Montie, H.L. and D. Merry, *Autophagy and access: understanding the role of androgen receptor subcellular localization in SBMA*. Autophagy, 2009. **5**(8): p. 1194 - 1197.
105. Rusmini, P., et al., *Clearance of the mutant androgen receptor in motoneuronal models of spinal and bulbar muscular atrophy*. Neurobiol Aging., 2013. **34**(11): p. 2585–2603.
106. Cortes, C.J., et al., *Polyglutamine-expanded androgen receptor interferes with TFEB to elicit autophagy defects in SBMA*. Nat Neurosci. , 2014. **17**(9): p. 1180-1189.
107. Tohnai, G., et al., *Paeoniflorin eliminates a mutant AR via NF-YA-dependent proteolysis in spinal and bulbar muscular atrophy*. Hum. Mol. Genet., 2014. **23**(13): p. 3552-3565.
108. Yu, Z., et al., *Macroautophagy is regulated by the UPR-mediator CHOP and accentuates the phenotype of SBMA mice*. PLoS Genet., 2011. **7**(10).
109. Chua, J.P., et al., *Transcriptional activation of TFEB/ZKSCAN3 target genes underlies enhanced autophagy in spinobulbar muscular atrophy*. Hum Mol Genet., 2014. **23**(5): p. 1376-86.
110. Fernández-Rhodes, L.E., et al., *Efficacy and safety of dutasteride in patients with spinal and bulbar muscular atrophy: a randomised placebo-controlled trial*. Lancet Neurol., 2011. **10**(2): p. 140-147.
111. Miyazaki, Y., et al., *Viral delivery of miR-196a ameliorates the SBMA phenotype via the silencing of CELF2*. Nat Med., 2012. **18**(7): p. 1136-1141.
112. Caplen, N.J., et al., *Rescue of polyglutamine-mediated cytotoxicity by double-stranded RNA-mediated RNA interference*. Hum Mol Genet., 2002. **11**(2): p. 175-184.



113. Minamiyama, M., et al., *Sodium butyrate ameliorates phenotypic expression in a transgenic mouse model of spinal and bulbar muscular atrophy*. Hum Mol Genet. , 2004. **13**(11): p. 1183-1192.
114. Yang, Z., et al., *ASC-J9 ameliorates spinal and bulbar muscular atrophy phenotype via degradation of androgen receptor*. Nature Medicine, 2007. **13**: p. 348 - 353.
115. Qiang, Q., et al., *Genistein, a natural product derived from soybeans, ameliorates polyglutamine-mediated motor neuron disease*. J Neurochem., 2013. **126**(1): p. 122-130.
116. Renier, K.J., et al., *Antiandrogen flutamide protects male mice from androgen-dependent toxicity in three models of spinal bulbar muscular atrophy*. Endocrinology, 2014. **155**(7): p. 2624-34.
117. Palazzolo, I., et al., *B2 attenuates polyglutamine-expanded androgen receptor toxicity in cell and fly models of spinal and bulbar muscular atrophy*. J Neurosci Res., 2010. **88**(10): p. 2207-2216.
118. Iida, M., et al., *Pioglitazone suppresses neuronal and muscular degeneration caused by polyglutamine-expanded androgen receptors*. Hum Mol Genet., 2014.
119. Minamiyama, M., et al., *Naratriptan mitigates CGRP1-associated motor neuron degeneration caused by an expanded polyglutamine repeat tract*. Nat Med. , 2012. **18**(10): p. 1531-1538.
120. Christopher R. Orr, et al., *An Interdomain Interaction of the Androgen Receptor Is Required for Its Aggregation and Toxicity in Spinal and Bulbar Muscular Atrophy*. J Biol Chem. , 2010. **285**(46): p. 35567–35577.
121. Castillo, K., et al., *Trehalose delays the progression of amyotrophic lateral sclerosis by enhancing autophagy in motoneurons*. Autophagy, 2013. **9**(9): p. 1308 - 1320.
122. Tanaka, M., et al., *Trehalose alleviates polyglutamine-mediated pathology in a mouse model of Huntington disease*. Nature Medicine, 2004. **10**: p. 148 - 154.
123. Sarkar, S., et al., *Trehalose, a novel mTOR-independent autophagy enhancer, accelerates the clearance of mutant huntingtin and alpha-synuclein*. The Journal of Biological Chemistry, 2007: p. 5641-5652.
124. Davies, J.E., S. Sarkar, and D.C. Rubinsztein, *Trehalose reduces aggregate formation and delays pathology in a transgenic mouse model of oculopharyngeal muscular dystrophy*. Hum. Mol. Genet., 2006. **15**(1): p. 23-31.
125. Aguib, Y., et al., *Autophagy induction by trehalose counteracts cellular prion infection*. Autophagy, 2009. **5**(3): p. 361-369.
126. Lan, D.-M., et al., *Effect of trehalose on PC12 cells overexpressing wild-type or A53T mutant  $\alpha$ -synuclein*. Neurochemical Research, 2012. **37**(9): p. 2025-2032.
127. Zhang, X., et al., *MTOR-independent, autophagic enhancer trehalose prolongs motor neuron survival and ameliorates the autophagic flux defect in a mouse model of amyotrophic lateral sclerosis*. Autophagy, 2014. **10**(4): p. 588–602.
128. Barmada, S.J., et al., *Autophagy induction enhances TDP43 turnover and survival in neuronal ALS models*. Nat. Chem. Biol., 2014. **10**: p. 677–685.
129. Rusmini, P., et al., *Proteasomal and autophagic degradative activities in spinal and bulbar muscular atrophy*. Neurobiology of Disease, 2010. **40**(2): p. 361–369.
130. Carra, S., et al., *Different anti-aggregation and pro-degradative functions of the members of the mammalian sHSP family in neurological disorders*. Phil. Trans. R. Soc. B 2013. **368**(1617).
131. Crippa, V., et al., *A role of small heat shock protein B8 (HspB8) in the autophagic removal of misfolded proteins responsible for neurodegenerative diseases*. Autophagy, 2010. **6**(7): p. 958 - 960.
132. Crippa, V., et al., *The small heat shock protein B8 (HspB8) promotes autophagic removal of misfolded proteins involved in amyotrophic lateral sclerosis (ALS)*. Hum. Mol. Genet., 2010. **19**(17): p. 3440-3456.
133. Liu, R., et al., *Trehalose differentially inhibits aggregation and neurotoxicity of beta-amyloid 40 and 42*. Neurobiology of Disease, 2005. **20**(1): p. 74-81.
134. Xiaoju Wang, et al., *Degradation of TDP-43 and its pathogenic form by autophagy and the ubiquitin-proteasome system*. Neuroscience Letters, 2010. **469**(1): p. 112–116.

135. Ciechanover, A. and P. Brundin, *The ubiquitin proteasome system in neurodegenerative diseases: sometimes the chicken, sometimes the egg*. *Neuron*, 2003. **40**(2): p. 427–446.
136. Wang, A.M., et al., *Inhibition of hsp70 by methylene blue affects signaling protein function and ubiquitination and modulates polyglutamine protein degradation*. *J Biol Chem.*, 2010. **285**(21): p. 15714-15723.
137. Malik, B., et al., *Co-induction of the heat shock response ameliorates disease progression in a mouse model of human spinal and bulbar muscular atrophy: implications for therapy*. *Brain*, 2013. **136**(3): p. 926-943.
138. Li, Z., F.U. Hartl, and A. Bracher, *Structure and function of Hip, an attenuator of the Hsp70 chaperone cycle*. *Nature Structural & Molecular Biology*, 2013. **20**: p. 929-935.
139. Gorska, M., et al., *Geldanamycin and its derivatives as Hsp90 inhibitors*. *Frontiers in Bioscience*, 2012. **17**: p. 2269-2277.
140. Li, Z., et al., *Discovery of diamine-linked 17-arylamido-17-demethoxygeldanamycins as potent Hsp90 inhibitors*. *Eur J Med Chem.*, 2014. **87C**: p. 346-363.
141. Howarth, J.L., C.P.J. Glover, and J.B. Uney, *HSP70 interacting protein prevents the accumulation of inclusions in polyglutamine disease*. *J Neurochem*, 2009. **108**(4): p. 945–951.
142. Roodveldt, C., et al., *Chaperone proteostasis in Parkinson's disease: stabilization of the Hsp70/alpha-synuclein complex by Hip*. *The EMBO Journal*, 2009. **28**: p. 3758-3770.
143. Cotman, C.W., N.C. Berchtold, and L.-A. Christie, *Exercise builds brain health: key roles of growth factor cascades and inflammation*. *Trends Neurosci.*, 2007. **30**(9).
144. Rovio, S., et al., *Leisure-time physical activity at midlife and the risk of dementia and Alzheimer's disease*. *The Lancet Neurology*, 2014. **4**(11): p. 705 - 711.
145. Lautenschlager, N., K. Anstey, and A. Kurz, *Non-pharmacological strategies to delay cognitive decline*. *Maturitas*, 2014. **79**(2): p. 170-173.
146. Busse, M., et al., *A randomized feasibility study of a 12-week community-based exercise program for people with Huntington's disease*. *J Neurol Phys Ther.*, 2013. **37**(4).
147. Tuon, T., et al., *Physical training prevents depressive symptoms and a decrease in brain-derived neurotrophic factor in Parkinson's disease*. *Brain Res Bull*, 2014. **108**: p. 106-112.
148. Oguh, O., et al., *Back to the basics: Regular exercise matters in Parkinson's disease: Results from the National Parkinson Foundation QII Registry study*. *Parkinsonism Relat Disord.*, 2014.
149. Harrison, D.J., et al., *Exercise attenuates neuropathology and has greater benefit on cognitive than motor deficits in the R6/1 Huntington's disease mouse model*. *Experimental Neurology*, 2013. **248**: p. 457–469.
150. Fryer, J.D., et al., *Exercise and Genetic Rescue of SCA1 via the Transcriptional Repressor Capicua*. *Science*, 2011. **334**(690).
151. Gill, J., *Physical activity, cardiorespiratory fitness and insulin resistance: a short update*. *Curr Opin Lipidol.*, 2007. **18**(1): p. 47-52.
152. Tong, L., et al., *Brain-derived neurotrophic factor-dependent synaptic plasticity is suppressed by interleukin-1 $\beta$  via p38 mitogen-activated protein kinase*. *J Neurosci.*, 2012. **32**(49): p. 17714-24.
153. Kathryn E Nichol, et al., *Exercise alters the immune profile in Tg2576 Alzheimer mice toward a response coincident with improved cognitive performance and decreased amyloid*. *J Neuroinflammation.*, 2006. **5**(13).
154. Sato, K. and M. Iemitsu, *Exercise and sex steroid hormones in skeletal muscle*. *J Steroid Biochem Mol Biol*, 2014.
155. Sato, K., et al., *Resistance training restores muscle sex steroid hormone steroidogenesis in older men*. *FASEB J*, 2014. **28**(4): p. 1891-1897.
156. Broskey, N.T., et al., *Skeletal muscle mitochondria in the elderly: effects of physical fitness and exercise training*. *J Clin Endocrinol Metab.*, 2014. **99**(5).
157. Chan, M.C. and Z. Arany, *The many roles of PGC-1 $\alpha$  in muscle — recent developments*. *Metabolism*, 2014. **63**(4): p. 441–451.

158. Pilegaard, H., B. Saltin, and P.D. Neuffer, *Exercise induces transient transcriptional activation of the PGC-1alpha gene in human skeletal muscle*. J Physiol., 2003. **546**: p. 851-858.
159. Akimoto, T., et al., *Exercise stimulates Pgc-1alpha transcription in skeletal muscle through activation of the p38 MAPK pathway*. J Biol Chem., 2005. **280**.
160. Olesen, J., et al., *Role of PGC-1α in exercise training- and resveratrol-induced prevention of age-associated inflammation*. Experimental Gerontology, 2013. **48**(11): p. 1274–1284.
161. Rinaldi, C., L.C. Bott, and K.H. Fischbeck, *Muscle Matters in Kennedy's Disease*. Neuron, 2014.
162. Yu, Z., et al., *Abnormalities of Germ Cell Maturation and Sertoli Cell Cytoskeleton in Androgen Receptor 113 CAG Knock-In Mice Reveal Toxic Effects of the Mutant Protein*. Am J Pathol., 2006. **168**(1): p. 195–204.
163. Lin, J., et al., *Transcriptional co-activator PGC-1 alpha drives the formation of slow-twitch muscle fibres*. Nature, 2002. **418**: p. 797-801.
164. Mahoney, D.J., et al., *Effects of high-intensity endurance exercise training in the G93A mouse model of amyotrophic lateral sclerosis*. Muscle Nerve, 2004. **29**(5): p. 656–662.
165. Potter, M.C., et al., *Exercise is not beneficial and may accelerate symptom onset in a mouse model of Huntington's disease*. PLoS Curr. , 2010.
166. Rommel, C., et al., *Mediation of IGF-1-induced skeletal myotube hypertrophy by PI(3)K/Akt/mTOR and PI(3)K/Akt/GSK3 pathways*. Nature Cell Biology 2001. **3**: p. 1009 - 1013.
167. Nedelsky, N., P.K. Todd, and J.P. Taylor, *Autophagy and the ubiquitin-proteasome system: collaborators in neuroprotection*. Biochim Biophys Acta., 2008. **1782**(12): p. 691-699.
168. Nixon, R.A., et al., *Extensive involvement of autophagy in Alzheimer disease: an immuno-electron microscopy study*. J Neuropathol Exp Neurol., 2005. **64**(2): p. 113-122.
169. Anglade, P., et al., *Apoptosis and autophagy in nigral neurons of patients with Parkinson's disease*. Histol Histopathol. , 1997. **12**(1).
170. Doi, H., et al., *p62/SQSTM1 differentially removes the toxic mutant androgen receptor via autophagy and inclusion formation in a spinal and bulbar muscular atrophy mouse model*. J Neurosci., 2013. **33**(18): p. 7710-27.
171. Kolvenbag, G., G. Blackledge, and K. Gotting-Smith, *Bicalutamide (Casodex) in the treatment of prostate cancer: history of clinical development*. Prostate., 1998. **34**(1): p. 61-72.
172. Squillace, R.M., et al., *Synergistic activity of the mTOR inhibitor ridaforolimus and the antiandrogen bicalutamide in prostate cancer models*. Int J Oncol., 2012. **41**(2): p. 425-432.
173. Banno, H., et al., *Phase 2 trial of leuprorelin in patients with spinal and bulbar muscular atrophy*. Ann Neurol., 2009. **65**(2): p. 140-150.
174. Sandri, M., *Signaling in muscle atrophy and hypertrophy*. Physiology (Bethesda), 2008. **23**(3): p. 160-170.
175. Cashman, N.R., et al., *Neuroblastoma x spinal cord (NSC) hybrid cell lines resemble developing motor neurons*. Developmental Dynamics, 1992. **194**(3): p. 209–221.
176. Durham, H.D., S. Dahrouge, and N.R. Cashman, *Evaluation of the spinal cord neuron X neuroblastoma hybrid cell line NSC-34 as a model for neurotoxicity testing*. Neurotoxicology, 1993. **14**(4): p. 387-395.
177. Pozzi, P., et al., *Androgen 5-alpha-reductase type 2 is highly expressed and active in rat spinal cord motor neurones*. Journal of Neuroendocrinology, 2003. **15**(9): p. 882–887.
178. Marron, T.U., et al., *Androgen-induced neurite outgrowth is mediated by neuritin in motor neurones*. Journal of Neurochemistry, 2005. **92**(1): p. 10-20.
179. Sau, D., et al., *Mutation of SOD1 in ALS: a gain of a loss of function*. Hum. Mol. Genet., 2007. **16**(13): p. 1604-1618.
180. Onesto, E., et al., *Muscle cells and motoneurons differentially remove mutant SOD1 causing familial amyotrophic lateral sclerosis*. Journal of Neurochemistry, 2011. **118**(2): p. 266–280.
181. Poletti, A., et al., *5Alpha-reductase type 2 and androgen receptor expression in gonadotropin releasing hormone GT1-1 cells*. Journal of Neuroendocrinology, 2001. **13**(4): p. 353–357.

182. Albertelli, M.A., et al., *Glutamine tract length of human androgen receptors affects hormone-dependent and -independent prostate cancer in mice*. Hum Mol Genet. , 2008. **17**(1): p. 98-110.
183. He, C., et al., *Exercise-induced BCL2-regulated autophagy is required for muscle glucose homeostasis*. Nature., 2012. **481**(7382): p. 511–515.